# Effect of Composition on the Drug Release Behaviour and Properties of Hydrogels for Contact Lenses

**Magda Proença Falcão Carrilho**

Thesis to obtain the Master of Science Degree in

## Biomedical Engineering

Supervisors:

Doctor Benilde de Jesus Vieira Saramago

Doctor Ana Paula Valagão Amadeu do Serro

## Examination Committee

Chairperson: Doctor João Pedro Estrela Rodrigues Conde

Supervisor: Doctor Benilde de Jesus Vieira Saramago

Members of the Committee: Doctor Anabela Catarino Fernandes

**June 2016**

# Acknowledgements

The present thesis allows the conclusion of an important cycle of my life and it could not have been possible without the support of some important people.

I would first like to thank to my supervisors, Doctor Benilde Saramago and Doctor Ana Paula Serro, for their extraordinary support, commitment, patience and kindness throughout this journey. For the endless reunions discussing the better approaches and solving problems. I am also deeply grateful to them for the carefully reading and commenting on the revisions of my thesis. Thank you for having me in your research group, I have learned a lot. I could not have asked for better supervisors.

Second, I would like to thank to Doctor Anabela Fernandes for all the support and patience explaining me everything about the measurements with the DSC. To Doctor Vitor Alves from Instituto Superior de Agronomia, whose help was crucial in the measurements of the mechanical properties.

To my laboratory colleagues: Ana Topete, Andreia Pimenta, Diana Silva, Raquel Galante, and Sofia Oliveira for their kindly reception when I was new in the research group and for all your help. Many months were spent working hard in that laboratory but when you have great colleagues working near you, everything is better.

To my friends: Diana Oliveira, Joana Santos, Marta Pinheiro, Rita Soares, and Sofia Amaral, for their friendship and for giving me motivation to achieve my goals. To my Erasmus friend Sylvia Hoogenboom that despite the distance has always supported me in this journey.

I cannot fail to thank to one of my sources of strength, my dear family, especially to my parents, for their love, support and for always believing in me and in my abilities. Thank you for all your efforts so I had always the best conditions.

My last thanks goes to another important person in my life, my boyfriend Manuel Mateus. Thank you for your love, loyalty, friendship and huge support. I am also deeply thankful to you for being such a good listener and always giving me the best advices. Thank you for being always by my side, especially in this important moment of my life.

# Abstract

Many efforts have been done in order to overcome the problems of conventional ocular treatments. Therapeutic soft contact lenses have gained special attention and different strategies to obtain controlled drug release profiles have been followed.

In this work, the effect of changing the composition of hydrogels for contact lenses, on their properties, especially the drug release behaviour, was evaluated. The hydrogels produced were based on the following components: monomethacryloxypropyl-terminated Polydimethylsiloxane (mPDMS) and 3-[tris(trimethylsiloxy)silyl]propyl methacrylate (TRIS) (hydrophobic silicone compounds); N,N-Dimethylacrylamide (DMA) and 2-hydroxyethyl methacrylate (HEMA) (hydrophilic compounds); N-vinylpyrrolidone (NVP), 3-methacryloxy-2-Hydroxypropoxy(propylbis(trimethylsilyloxy)methylsilane (SiGMA), and ethylene glycol dimethacrylate (EGDMA) (crosslinker). The release profiles of diclofenac and dexamethasone from hydrogels were investigated. Some properties, relevant for the contact lenses performance, such as, transmittance, ionic permeability, swelling capacity, wettability, surface energy, surface morphology, mechanical properties, water states in hydrogels and porosity were determined.

Hydrogels with higher amounts of EGDMA showed smaller pores, which in turn decreased the cumulative diclofenac release, ionic permeability and swelling, and increased the Young's modulus and tension at break. NVP increases the water content, leading to higher amounts of drug released, in contrast with SiGMA which decreases swelling and drug release. Unexpectedly, the substitution of TRIS by mPDMS (super hydrophobic) lead to an increase in the swelling and drug release. DMA proved to be more hydrophilic than HEMA, and seems to be an excellent hydrophilic component, increasing the swelling and diclofenac release, while keeping adequate mechanical properties and ionic permeability. Dexamethasone was released in much lower amounts than diclofenac, for all hydrogels.



**Key words:** ophthalmic drug delivery, hydrogels, hydrophilic and hydrophobic materials, drugs, properties, soft contact lenses.

# Resumo

Têm sido feitos esforços para contornar os problemas dos tratamentos oculares convencionais. As lentes de contacto têm ganho especial atenção e têm sido adotadas estratégias de carregamento de fármacos para obter perfis de libertação controlada.

Neste trabalho, foi estudado o efeito da alteração da composição dos hidrogéis para lentes de contacto nas suas propriedades, nomeadamente no perfil de libertação de fármacos. Na produção dos hidrogéis utilizaram-se os materiais: monomethacryloxypropyl-terminated Polydimethylsiloxane (mPDMS) e 3-[tris(trimethylsiloxy)silyl]propyl methacrylate (TRIS) (componentes hidrofóbicos de silicone); N,N- Dimethylacrylamide (DMA) e 2-hydroxyethyl methacrylate (HEMA) (componentes hidrofílicos); N-vinylpyrrolidone (NVP), 3-methacryloxy-2-Hydroxypropoxy(propylbis(trimethylsilyloxy)methylsilane (SiGMA) e ethylene glycol dimethacrylate (EGDMA) (agente reticulante). Os perfis de libertação de diclofenac e dexametasona foram investigados. Algumas propriedades: transmitância, permeabilidade iónica, intumescimento, molhabilidade, energia de superfície, morfologia, propriedades mecânicas, tipos de água e porosidade foram avaliadas.

Hidrogéis com quantidades elevadas de EGDMA mostraram menores dimensões de poros, diminuição da libertação de diclofenac, permeabilidade iónica e intumescimento e aumento do módulo de Young e tensão na rutura. O NVP fez aumentar o teor de água, levando ao aumento de fármaco libertado, ao contrário do SiGMA que fez diminuir o intumescimento e a quantidade de diclofenac libertada. A substituição de TRIS por mPDMS (super-hidrofóbico) levou ao aumento do intumescimento e da libertação de diclofenac. O DMA provou ser mais hidrofílico que o HEMA e parece ser um excelente componente hidrofílico, aumentando o intumescimento e a libertação de diclofenac, mantendo as propriedades mecânicas apropriadas e permeabilidade iónica. A quantidade de dexametasona libertada dos hidrogéis foi menor que a de diclofenac.

**Palavras-chave:** entrega ocular de fármacos, hidrogéis, materiais hidrofílicos e hidrofóbicos, fármacos, propriedades, lentes de contacto.

# Contents

# Figures List

# Tables List

# Abbreviations List

| | |
|---|---|
| **AIBN** | 2,2′-Azobis(2-methylpropionitrile) |
| **AMD** | Age-related macular degeneration |
| **$CL_s$** | Contact lenses |
| **COX** | Cyclooxygenase pathway |
| **DD water** | Distilled and deionized water |
| **$D_{ion}$** | Ionoflux diffusion coefficient |
| **DMA** | N,N-Dimethylacrylamide |
| **DSC** | Differential scanning calorimetry |
| **EGDMA** | Ethylene glycol dimethacrylate |
| **EGF** | Epidermal growth factor |
| **HEMA** | 2-hydroxyethyl methacrylate |
| **IR** | Infrared |
| **MAA** | Methacrylic acid |
| **MMA** | Methyl methacrylate |
| **mPDMS** | Monomethacryloxypropyl terminated Polydimethylsiloxane |
| **NMR** | Nuclear magnetic resonance |
| **NSAIDs** | Nonsteroidal anti-inflammatory drugs |
| **NVP** | N-Vinylpyrrolidone |
| **OH** | Hydroxyl group |
| **PDMS** | Poly(dimethylsiloxane) |
| **pHEMA** | Poly(2-hydroxyethyl methacrylate) |
| **PMMA** | Poly(methyl methacrylate) |
| **PVP** | Poly(vinylpyrrolidone) |
| **RGP** | Rigid gas-permeable |
| **SC** | Swelling capacity |
| **SEM** | Scanning electron microscopy |
| **SiGMA** | 3-methacryloxy-2-Hydroxypropoxy(propylbis(trimethylsilyloxy)methylsilane |
| **TEGDMA** | Tetraethyleneglycoldimethacrylate |
| **TGA** | Thermogravimetric analysis |
| **TRIS** | 3-[Tris(trimethylsiloxy)silyl]propyl methacrylate |
| **UV** | Ultraviolet |
| **UVA** | Ultraviolet A |
| **UVB** | Ultraviolet B |
| **UVC** | Ultraviolet C |
| **UV-Vis** | Ultraviolet-Visible |
| **Vis** | Visible |
| **WC** | Water content |

# 1 Introduction

## 1.1 Objective and Description of the Thesis

The main goal of the presented master thesis is to study the effect of the composition of hydrogels, which can be used in the manufacture of therapeutic drug loaded soft contact lenses, on their properties, in particular, the drug release behaviour. Typically, this type of hydrogels results from the combination of hydrophilic monomers, which lead to high ion permeability and wettability, with hydrophobic monomers that ensure high oxygen permeability and mechanical strength. Usually, a macromer has to be added to ensure solubilisation of these two components. Changing the composition of the hydrogels is one of the strategies that has been adopted with the objective of controlling the drug release. However, few systematic studies in this area exist in the literature, hence the importance of the present work. It is of great interest to understand the role that each hydrogel component plays in order to achieve optimised compositions for controlled drug release while keeping adequate characteristics as contact lens materials.

This master thesis is divided into 5 chapters: introduction, materials and methods, results and discussion, conclusions and future work, and bibliography.

In the first chapter, it is presented a theoretical overview which explains the main subjects that will be addressed throughout the work and will help to understand the results obtained. It starts with a short explanation of the eye anatomy and eye related pathologies. Then, the conventional methods used to treat the ocular diseases and the problems associated with them are briefly described. Knowing the drawbacks of conventional treatments for ocular therapy, the possibility of using contact lenses as vehicles for drug release in the treatment of eye pathologies is raised. The different methods of loading drugs in contact lenses, specifying from the earliest methods until the latest ones, are described. Afterwards, the contact lenses history is introduced briefly and an overview of the materials that are commonly used to produce hydrogel contact lenses is made, with particular attention to those used in this work. Finally, the main properties that hydrogels need to have in order to be used as contact lenses for ocular drug delivery are described.

Chapter 2 presents all the materials used in this work as well as the different experimental techniques. The first subchapter includes the materials used for the hydrogels preparation, the drugs chosen for the drug loading/release experiments and other materials required for other techniques. In the subchapter about the methods, all the steps taken in the hydrogels preparation, drug loading and release are described, as well as the techniques used in the characterisation of hydrogels' properties.

Chapter 3 is divided into 8 subchapters, which describe all the results obtained in this work and a discussion for each of them. The first 5 subchapters start with the presentation of the results of the drug release experiments using diclofenac as the model drug, and then some of the hydrogels' properties are presented. A correlation between the drug release results and the hydrogels' properties is attempted, to see whether or not they are directly related. In the subchapter 6, the results of further characterisation

of the most relevant hydrogel formulations, according to the results obtained in the previous subchapters, are shown. These properties include: diclofenac release at different loading temperatures, swelling capacity at different temperatures and media, wettability, surface energy, surface morphology, mechanical properties, states of water inside the hydrogels, and pore-size dimensions. Drug release tests were also done with other drug (dexamethasone) to check whether or not there are significant differences in using a hydrophilic drug (diclofenac) or a hydrophobic one (dexamethasone). At subchapter 7, the release profiles of both drugs are compared with the respective therapeutic windows to get an idea of the possible *in vivo* efficacy. The last subchapter, presents a global discussion of all the results obtained.

In chapter 4, the main conclusions of this work are presented, after making a brief analysis of the results obtained for the different types of hydrogels. Future work that could be of interest to deepen the conclusions obtained in this thesis is also referred.

Finally, chapter 5 presents all the references quoted in the master thesis.

## 1.2 Context

### 1.2.1 Drug Delivery in the Eye

#### 1.2.1.1 The Eye and its Pathologies

The eye is a complex structure and, because of being in direct contact with the external environment, it is considered one of the most vulnerable organs in the body. A normal adult eye is a spherical ball and has a diameter of approximately 2.5 centimetres. The eyes receive the input from the outside and then send this information as a signal to the brain, which processes it in order to get the final output as an image. The vision system also includes accessory structures which have the role of protection, lubrication and movement. In the accessory structures are included the eyelids, eyebrows, conjunctiva, lacrimal apparatus and extrinsic eye muscles [1–3].

The eye has two important segments: the anterior and the posterior segment (Figure 1). The anterior segment represents one-third of the front eye and includes the cornea, conjunctiva, aqueous humour, iris, ciliary body and crystalline lens. The posterior segment comprises the sclera, choroid, Bruch's membrane, retina and vitreous humour [1].

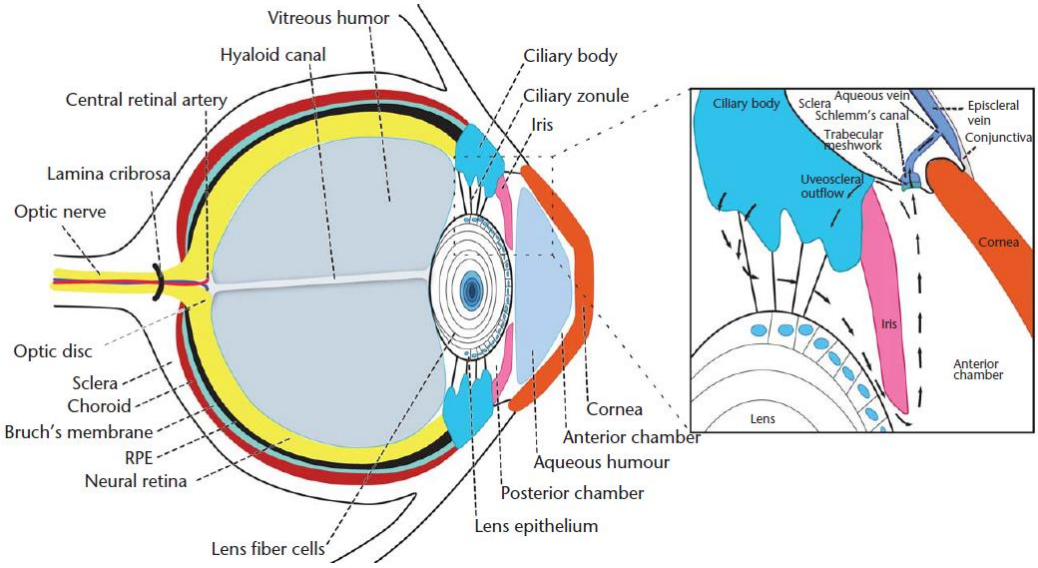


**Figure 1 -** Schematic representation of the human eye. Adapted from [2].

Despite the vision impairments associated mostly to the failure of the cornea and lens, there are other lesions/diseases that can affect the eye. Glaucoma, allergic conjunctivitis, dry eye, anterior uveitis and cataract are examples of diseases that can have a bad impact on the anterior segment, whereas diabetic retinopathy and age-related macular degeneration (AMD) can affect the posterior segment [4,5].

#### 1.2.1.2 Conventional Treatments

A variety of options are available to treat eye diseases, including drugs administration, laser procedures, and surgery. The most used is drug administration. Due to the eye complexity, all drug delivery strategies should meet some key requirements, such as biocompatibility, ease of use, comfort, do not

affect the vision or produce side effects. In order to achieve all these requisites, over the years, drug ocular therapy has been considered a major challenge for scientists. Nowadays, topical administration in the form of solutions, emulsions, suspensions and ointments is the most common therapy for the treatment of ocular diseases located in the anterior segment. These forms of administration have the great advantage of being essentially non-invasive [4–7].

A human tear film contains approximately 7 μL of fluid. After eye drops instillation, the drug is dispersed in the entire tear volume increasing it up to 30 μL. Due to the limited capacity of the eye (approximately 10 μL), part of the drug is pulled out of the eyes whereas another fraction of the drug goes to the drainage pathway into the nasal cavity, being absorbed later by the systemic circulation. Despite these pathways where the drug is lost, it is important to refer that the drug molecules can diffuse also to the conjunctiva, which has 17 fold larger area compared to cornea, limiting the portion of the administered dose that is adequately absorbed through the cornea to about 5% [7,8].

The rapid clearance of drug is not the only drawback in applying eye drops. There are other disadvantages, such as:

- Ocular and systemic toxicity problems caused by the larger drug concentrations that are needed in order to have a high bioavailability of drug in the eye;
- Ocular inflammation and irritation, redness and vision problems;
- Patient compliance problems, mainly in elderly people, when a higher frequency of instillation (for example hourly instillations) is needed or when multiple medications are required to be administered, like in glaucoma patients [5,7,8].

Additives, such as viscosity and permeation enhancers, have been studied to fight the drawbacks of eye drops. Viscosity enhancers have the role of increasing the residence time of drug and at the same time the bioavailability, whereas the permeation enhancers are intended to improve the corneal uptake by modifying its integrity [5].

#### 1.2.1.3 Contact Lenses as a New Drug Carrier

During the past decades, studies have been made in order to overcome the limitations of conventional topical administration. While researchers are trying to improve the performance of the treatments, new areas of interest are arising for the treatment of both anterior and posterior segment diseases [5].

Since 1965, the well-known contact lenses ($CL_s$) have been increasing their importance as a new revolutionizing drug delivery vehicle. At the present, they no longer have only the goal of correction of ametropia problems, but they are also starting to gain importance as new drug carriers. $CL_s$ are being study to get around some drawbacks presented by the conventional treatments. This possible medical device can provide higher drug bioavailability, comfort, mechanical support and protection, maintenance of corneal epithelial hydration, safety and higher patient compliance. Another benefit is the improvement of the pharmacokinetics. In the case of eye drops, the drug concentration increases after instillation, and then a rapid clearance of the drug occurs. In contrast, $CL_s$ can deliver the drug at a more controlled rate and prevent the achievement of toxicity levels, as shown in Figure 2. The major drawbacks of these new

drug carriers are: the low affinity of silicone CLs with some drugs, and the regulatory, processing and storage issues that lead to barriers to their commercialization [4,7,9,10].

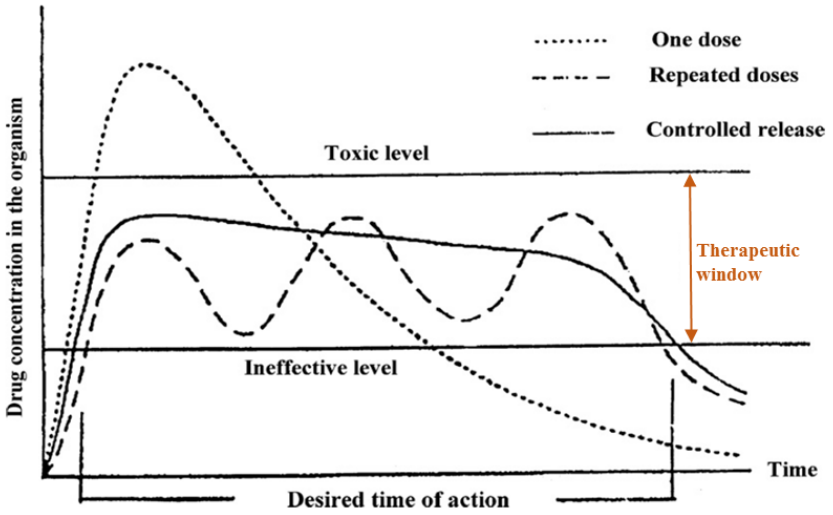


**Figure 2 -** Schematic representation of the pharmacokinetics depending on the treatment used. Adapted from [11].

When the loaded contact lens is placed in the eye, the drug can diffuse through the post-lens tear film, the thin layer located between the cornea and the contact lens, and through the pre-lens tear film, the thin layer that separates the contact lens from the air. The drug that reaches the interface between the post-lens tear film and cornea can stay there for a long period of time, improving the residence time of the drug in the eye compared to the conventional treatments (Figure 3) [4,7].

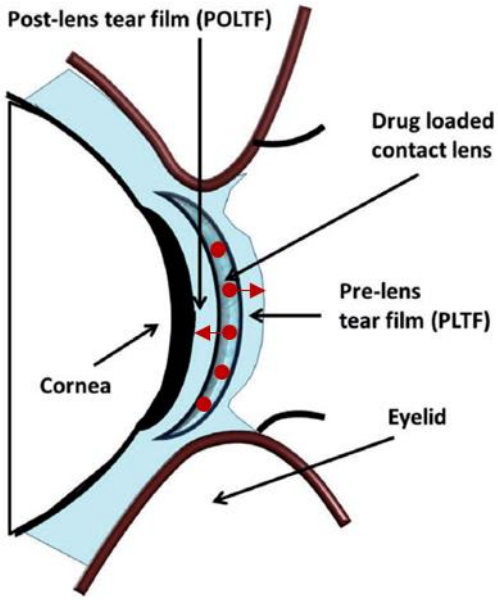


**Figure 3 -** Drug delivery mechanism of loaded CLs. Note: the arrows indicate the direction of the exit of the drug. Adapted from [7].

An optimal drug delivery system is the one that releases the medication at a controlled rate to the cornea, with minimal side effects. An example of a device that meets this requirement are CLs, which are placed directly on the cornea. Over the years, different strategies have been followed to achieve the desired control of the drug release (Figure 4). The first approach used and the most well-known is the immersion

of contact lens in aqueous solutions with high drug concentrations and subsequent insertion of the lens into the eye of the patient. This strategy is also called drug soaking method and it is used for the delivery of a varied number of drugs, such as antibiotics and non-steroidal anti-inflammatory drugs. Despite the higher bioavailability of the drug compared with eye drops, this strategy presents some disadvantages. The first one is the low drug loading that depends on some issues, such as the water content and thickness of the lens, solubility of the drug in the gel matrix and its molecular weight. Another limitation of this method is the low residence time of the drug, leading to a fast release within a few hours. Even so, and since drug loaded contact lenses still do not exist in the market, ophthalmologists often prescribe the application of eye drops on the surface of the $CL_s$ after its insertion and/or the placement of the drug solution in the concavity of the $CL_s$ before putting them in the eye to increase the time of residence of the drug [4,8,9,12,13].

Recently, more advanced strategies of drug delivery through $CL_s$ have been studied in order to overcome the flaws of the approaches mentioned above (Figure 4). Some of the new strategies are presented below:

- Incorporation of functional monomers into the hydrogel, that interact with the drug molecules [8];
- Incorporation of molecular diffusion barriers, whose main goal is to hamper the path of diffusion of the drug. It is considered a diffusion barrier any solid or liquid material that is impermeable to the drug and does not interfere with the transparency of the lens. An example of a diffusion barrier is vitamin E. Recent studies showed a more controlled drug release through $CL_s$ with incorporated vitamin E [8,14];
- Molecular imprinting, which involves the formation of a complex between functional monomers (from the lens composition) and drug template molecules. The functional monomers present in the mixture arrange themselves around the drug, according to their affinity. After the polymerization process, the drug and the unreacted monomers are removed from the contact lens. At this time, the polymer network contains active sites with the size and the appropriate chemical groups to interact again with the drug, when loaded again. This strategy increases the drug loading capacity as well as the release duration. However, the major drawback is the change in properties like water content, oxygen permeability and Young's modulus [7,8,12,15];
- Supercritical solvent impregnation/deposition method in which the drug is dissolved into compressed high-volatile fluids (for example carbon dioxide) at subcritical or supercritical conditions and then, the resulting mixture contacts with the polymeric matrix. This method has proven to be effective many times since it does not affect the physical, mechanical or chemical properties of the polymers. Nevertheless, supercritical solvent impregnation have problems in controlling the release rate and in loading high molecular weight drugs [8,9];
- Nanotechnology-based ocular formulations, such as nanomicelles, nanoparticles, nanosuspensions, liposomes. These formulations are loaded with a compatible drug and, then they are incorporated in the hydrogel matrix before or after the polymerization process. With this approach, the extended drug release is achieved because of the improved specificity of the

nanocarriers leading to a decrease in the levels of toxicity in the body. The main disadvantage of this process is the possible loss of the transparency of the lens [4,8,9,16].

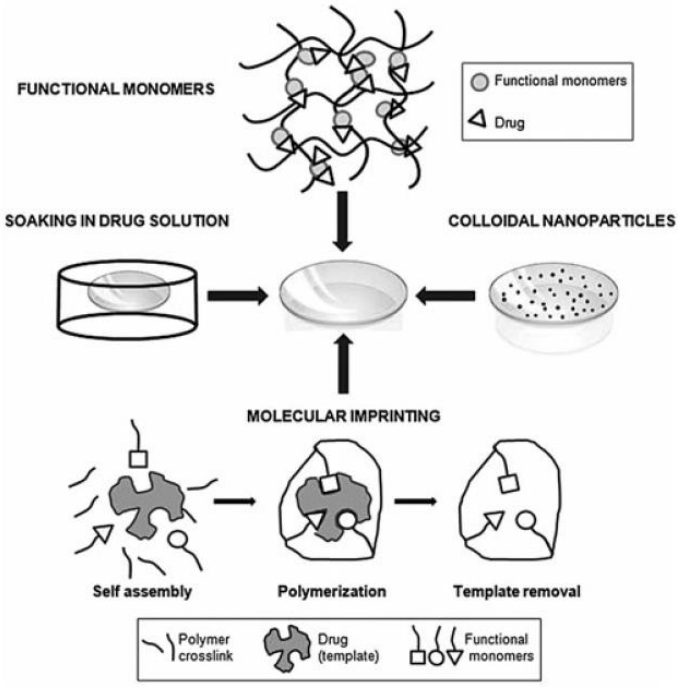


**Figure 4 -** Schematic representation of some recent strategies adopted for the drug release through $CL_s$. Adapted from [8].

Numerous studies have been done with different ophthalmic drugs loaded into $CL_s$ to treat effectively several eye problems. Eye infections, like conjunctivitis, keratitis and endophthalmitis, require a frequent application of an antibiotic, so the use of $CL_s$ can be an alternative to the conventional eye drops, giving rise to a more controlled drug release with less toxicity risks. One of the most used drugs to treat these infections is ciprofloxacin. The first mechanism studied for loading ciprofloxacin was the soaking method in silicone hydrogel $CL_s$; however, their release was so quick that other strategies had to be investigated [17]. Nanosphere-encapsulation showed promising results [8,18].

Another disorder that can be treated with drug loaded $CL_s$ are the corneal injuries, for example, corneal wounds, ocular trauma, corneal erosions, etc. In these cases, $CL_s$ can be used as a drug carrier for the delivery of the epidermal growth factor (EGF) to accelerate the wound healing process [19]. On the other hand, studies have shown that silicone $CL_s$ can be also used as a bandage for corneal healing and pain relief, leading to a fast recovery [8,20].

Allergic conjunctivitis is an inflammation of the conjunctiva that leads to symptoms like ocular itching, mucus discharge and redness [21]. It can be treated using antihistamines, such as ketotifen fumarate, that are applied in the form of eye drops many times a day. In this type of inflammation, it is important to keep a stable concentration of the drug in the eye for a long period of time. An interesting option could be imprinted $CL_s$, loaded with ketotifen fumarate, that showed, in some tests, high bioavailability and drug release up to 26 hours [22].

The dry eye is a syndrome that affects the tears and the ocular surface leading to visual disturbance and tear film instability. For the treatment of this syndrome, re-wetting agents are usually used, such as lubricants or artificial tears applied as eye drops. Release studies have been made with hydrogel $CL_s$ loaded with hyaluronic acid and good results were obtained, especially the improvement of the pharmacokinetics [8,23].

Glaucoma is a progressive disease that leads to a high intraocular pressure, causing damage in the optic nerve, fibre layer and ganglion cells that in severe cases can lead to vision loss. After cataract, glaucoma is considered the second largest cause of blindness worldwide. Currently, the therapy for this type of disease is the drug administration via eye drops, one or more times a day. Several studies have been done with $CL_s$ for the extended delivery of timolol, the most commonly used drug to treat glaucoma. One example of success was the study of Hsu and co-workers [24], who proved that vitamin E diffusion barriers can lead to extended release of timolol [8,25].

Ocular inflammations occur mainly during the recovery of surgeries, such as cataract surgery. These inflammations are associated with redness, swelling, and/or pain in the eye. In these situations, the arachidonic acid cascade is initiated, which in turn produces prostaglandins by activation of cyclooxygenase pathway (COX-1 and COX-2). The most common used treatment is the topical administration of corticosteroids or nonsteroidal anti-inflammatory drugs (NSAIDs), which may block parts of the ocular inflammation pathway. Corticosteroids inhibit the release of arachidonic acid and prostaglandins, whereas NSAIDs inhibit the COX pathway. Dexamethasone is an example of a corticosteroid that can be used for several ocular inflammations. However, it leads to various systemic side effects, such as cataract formation, immune system problems and increase in intraocular pressure [26,27]. An alternative and safer option is the use of NSAIDs, such as diclofenac, ketorolac, bromfenac and nepafenac [27,28].

In this work, two drugs were chosen for the drug release studies: diclofenac, as diclofenac sodium salt, and dexamethasone. The main characteristics of each drug are presented in Table 1.

**Table 1 -** Characteristics of the drugs used in this work [29–32].

| **Drug Name** | **Diclofenac Sodium Salt** | **Dexamethasone** |
|---|---|---|
| **Classification** | Nonsteroidal anti-inflammatory | Anti-inflammatory 9-fluoro-glucocorticoid |
| **Action** | Anti-inflammatory, analgesic and antipyretic | Anti-inflammatory |
| **Mechanism of Action** | Standard NSAID and competitive inhibitor of cyclooxygenase (COX) | Corticosteroid hormone receptor agonist |
| **Molecular Formula** | $C_{14}H_{10}Cl_2NNaO_2$ | $C_{22}H_{29}FO_5$ |

| | | |
|---|---|---|
| **Chemical Name** | 2-[(2,6-Dichlorophenyl)amino]benzeneacetic acid sodium salt | (11β,16α)-9-Fluoro-11,17,21-trihydroxy-16-methylpregna-1,4-diene-3,20-dione |
| **Chemical Structure** | 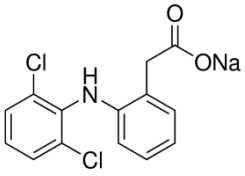 | 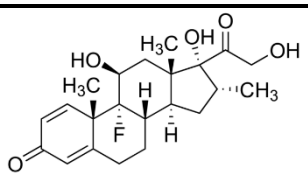 |
| **Molecular Weight (g mol$^{-1}$)** | 318, 13 | 392,46 |

## 1.2.2 Hydrogel Contact Lenses

### 1.2.2.1 Historical Overview

The history of CLs reports to the 1500s, when Leonardo da Vinci, in 1508, had the first idea of placing a water-filled glass into the eye to improve the refractive power of the cornea and the clarity of the image. More than a century later, René Descartes proposed a lens with a water-filled tube attached, to place only on the cornea. However, this method was unfeasible because of the difficulty in blinking [33,34].

Later on, in 1801, Thomas Young made the first set of CLs using the model of Descartes, but he reduced the dimensions of the water-filled tube. Young used wax to fix the CLs in the eye and as Descartes, his idea was not viable. In the 1820s, Sir John Herschel (English astronomer) suggested to make a mould of the eye in order to get an accurate curvature of the cornea for vision correction purposes. Later in the 1800s, the first true CLs were created by A.E. Fick, a Swiss physician. These CLs were made of glass and were intended to correct refractive errors. Due to its rigidity, these CLs were not comfortable to wear except in conditions like keratoconus, where pressure may help, or in cases where the cornea needed protection from infections [33–35].

In addition to the comfort issues, another problem of CLs made of glass was the permeability to oxygen. Until new ideas emerge, the researchers managed this situation with the introduction of small holes in the periphery of glass to ease the oxygen transference to the cornea. These problems have led researchers to discover a new era of CLs. In 1938, poly(methyl methacrylate) (PMMA) was presented as a new material to produce lenses in the form of plastic to cover the cornea and sclera. Although these CLs continued to be impermeable to oxygen, they showed to be simpler to manufacture, more resistant and less fragile. In 1958, the chemist Otto Wichterle discovered a new plastic material, poly(2-hydroxyethyl methacrylate) (pHEMA), which due to its hydrophilicity (high affinity for water) and high capacity of water absorption allowed the production of more comfortable lenses. Early in the 1970s, these CLs were licensed and commercialized [33,34,36].

Still in the 1970's, the first silicone hydrogel CLs appeared. These highly oxygen-permeable lenses were created to allow people to wear soft CLs for long periods of time. However, they only gained importance

in the market in the 1990's. Due to the hydrophobic nature (low affinity for water) of silicone, different generations of silicone hydrogel CLs came out over the years, each one combining different properties, and surface treatments to allow comfortable wear [33,34,36]. This evolution of the materials used in the CLs field comes from the need of improving the oxygen permeability, patient comfort, optical transparency, and biocompatibility with the ocular surface.

At the moment, there are two main types of CLs in the market: rigid gas-permeable (RGP) and soft. RGPs are more resistant and they allow the cornea to receive the adequate amount of oxygen. Its rigidity makes these lenses a good option for people who have the cornea with an unusual shape (astigmatism) since, in these cases, soft lenses will not provide an accurate vision. Soft CLs are more comfortable than RGPs and they are made of soft plastics that provide an easy adjustment to the eye and, at the same time, contribute to the correct oxygen transmission through the cornea. This type of CLs has diverse categories concerning the way of use such as, daily-wear lenses (for daily use only, being removed at night), extended-wear lenses (worn day and night and replaced weekly), and disposable-wear lenses (used for a long period of time and removed at night). They can also be used with different purposes: toric (to correct astigmatism), bifocal or multifocal (to correct different types of vision problems) and coloured lenses (for aesthetic reasons) [37,38].

The market of soft CLs is increasing from year to year. This type of lenses is the most used in Europe (about 95%) [39]. In the 2015 activity report of Euromcontact, 33 European countries were analysed in terms of number of soft CLs sold and their market value. According to this report, in 2014, Sweden was the European country that had the highest percentage of 15-64 years old population wearing soft CLs (14.09%) [40]. In this report, it was also shown the split of market of the different types of soft CLs during 2014 (Figure 5).

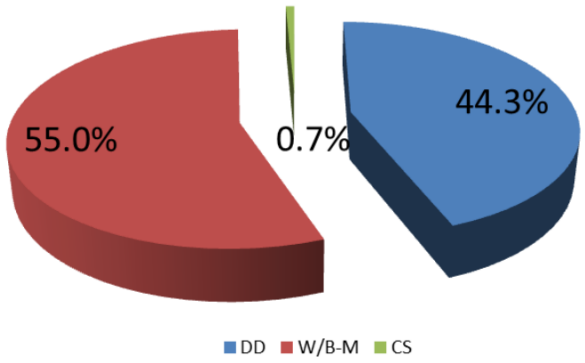


**Figure 5 -** Split of the market (in %) of the total of 33 European countries analysed in 2014. DD - daily disposable; W/B&M - weekly/bi-weekly and monthly lenses; CS - conventional soft lenses (quarterly, half-yearly and yearly). Note: silicone hydrogel lenses are included in the DD and W/B&M group. Adapted from [40].

### 1.2.2.2 Hydrogel Lens Materials

Currently, CLs are generally made of hydrogels. Hydrogel's materials are composed of chains of several monomers linked among them, which form a polymer network with a high capacity to absorb water [41]. The monomers used in CLs polymers can be hydrophilic, when containing parts that interact with water,

or hydrophobic, which have no affinity for water but increase the mechanical strength. Cross-linking agents can be used to increase both mechanical strength and thermal stability [42].

In the hydrogel $CL_s$' field, there are two important groups: conventional hydrogel $CL_s$ and silicone hydrogel $CL_s$. Conventional hydrogel lenses have addressed the physiological problem of corneal hypoxia (lack of oxygen supply to the cornea), in two possible ways: the development of super thin lenses, and the incorporation of monomers such as, 2-hydroxyethyl methacrylate (HEMA) copolymerized with other hydrophilic monomers, such as N-vinylpyrrolidone (NVP) and methacrylic acid (MAA) [43–45]. HEMA is the most used hydrophilic monomer in conventional hydrogel $CL_s$ and it is responsible for the ion and fluid transport. Its hydrophilic nature can be justified by the presence of the hydroxyl group (OH) at the end of the monomer, which contributes for the hydrogen bonding with water molecules [43,46]. NVP is a highly hydrophilic and a non-ionic monomer and it is frequently used in $CL_s$, essentially, to increase the water content. NVP also allows a minimal deposition of proteins and lipids from tear film on the surface of the lens. This feature is important to prevent blurred vision, eye inflammation and discomfort to the patient [47–49]. Studies proved that hydrogels containing HEMA and NVP reduce the protein adsorption [49]. MAA is also hydrophilic and an ionic monomer, and when it is in contact with a saline environment (for example, tear film) increases the water content of the hydrogel [50]. However, studies showed that hydrogels containing HEMA and MAA adsorbed considerable quantities of proteins, such as lysozyme [49].

To overcome the issue of the oxygen permeability, scientists also introduced new materials, such as silicone rubber [43]. Silicone rubber materials, e.g. poly(dimethylsiloxane) (PDMS), are transparent and have a great permeability to oxygen and carbon dioxide, providing a better gas exchange to the cornea [36]. However, one of the major limitations of the use of silicone rubber materials in $CL_s$ field is their hydrophobic nature. This characteristic of silicone can origin protein and lipid surface deposition, poor surface wettability and discomfort for the patient, decreasing the performance of $CL_s$ when in contact with eye. [45,51]

To deal with the limitations of silicone rubber lenses, the researchers start to develop new silicone hybrid lenses, so called silicone hydrogel $CL_s$. These new hybrid lenses combine the best characteristics of silicone, high oxygen permeability, and the properties of hydrophilic materials, such as the ease of the fluid transport and high wetting capacity. Despite the good characteristics of this type of lenses, there is still a problem. Silicone materials, like PDMS or 3-[tris(trimethylsiloxy)silyl]propyl methacrylate (TRIS), are hydrophobic and have low miscibility with hydrophilic monomers, such as HEMA or NVP, so the combination of these two materials results in a phase-separation, making the resulting polymers opaque and unsuitable for the use in $CL_s$. However, there are two different ways to overcome this issue. The first method implies the insertion of polar groups in certain sections of the silicon monomers, in order to help the miscibility with hydrophilic monomers. The second approach is the addition to the mixture of macromers that are intended to ensure the solubilization of the silicone with the hydrophilic monomer [36,41,46,52]. In the work of Kim et al.[53], the macromer 3-methacryloxy-2-Hydroxypropoxy(propylbis(trimethylsilyloxy)methylsilane (SiGMA) whose structure is shown in Figure 6, was used to prevent the problem of phase separation that can occur in silicone $CL_s$. This macromer has

a hydrophilic part and a hydrophobic part, which can link, respectively, to the hydrophilic monomer and the silicone (Figure 6).

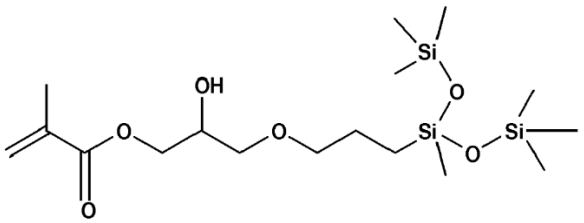


**Figure 6 -** Structural formula of SiGMA.

In Table 2, the monomers used in this work for $CL_s$ preparation as well as their structural formulas are shown.

**Table 2 -** Monomers used in this work and their structural formulas [54–58].

| Material Name | Structural Formula |
|---|---|
| 3-[Tris(trimethylsiloxy)silyl]propyl methacrylate (TRIS) * | 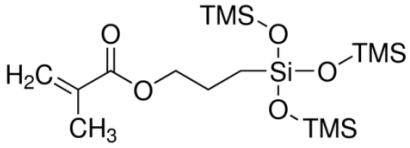 |
| Monomethacryloxypropyl terminated Polydimethylsiloxane (mPDMS) | 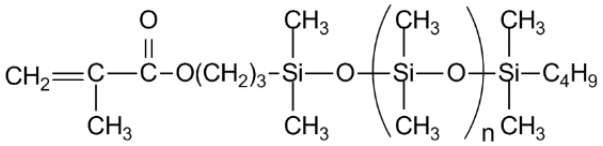 |
| 2-Hydroxyethyl methacrylate (HEMA) | 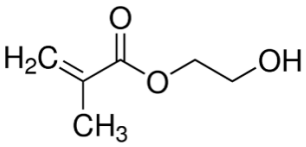 |
| N,N-Dimethylacrylamide (DMA) | 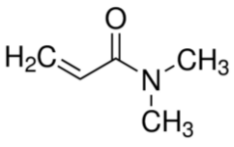 |
| N-Vinylpyrrolidone (NVP) | 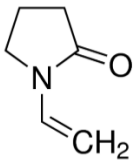 |

* TMS: tetramethylsilane

### 1.2.2.3 Main Properties

#### 1.2.2.3.1 Oxygen Permeability

Among the variety of properties that characterize $CL_s$, the oxygen permeability is one of the most important ones to maintain the corneal integrity. It is usually measured by the parameter Dk (expressed in barrers), which represents the ability of a material to carry oxygen through its bulk and depends on the lens thickness [41,47]. Relatively to silicone $CL_s$, the parameter Dk is mostly dependent on the amount of silicone contained inside the base material, whereas in conventional hydrogel $CL_s$, it only depends on the water content [59]. Conventional hydrogel $CL_s$ present low oxygen permeability since the diffusion of oxygen through water is limited: a conventional hydrogel with 100% water has a Dk of only 80 barrers (Figure 7). On the other hand, silicone $CL_s$ have high oxygen permeability, due to the silicone-oxygen bonds in the polymer side chains. Thus, the hypoxia problems caused by lens wear are diminished, contributing to the physiological integrity of the cornea. This property is of great importance in $CL_s$ and it is considered crucial for new developments in this area [41,60,61].

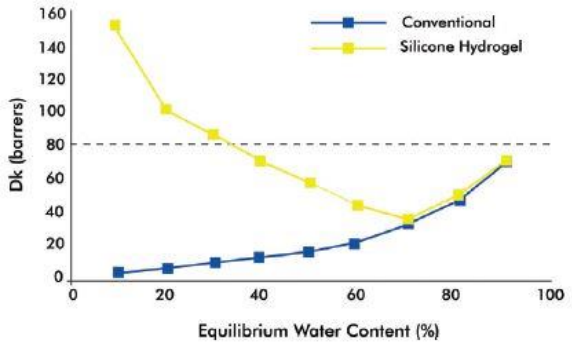


**Figure 7 -** Relationship between oxygen permeability (Dk) and the equilibrium water content (%) for conventional hydrogel CL's and silicone hydrogel CL's. Adapted from [45].

#### 1.2.2.3.2 Optical Transparency

The electromagnetic spectrum is composed of different types of waves: radio, microwaves, infrared (IR), visible (Vis), ultraviolet (UV), X-rays and gamma-rays. The visible light, which is the part of the electromagnetic spectrum that the human eyes can detect, is situated between infrared and ultraviolet and covers the wavelengths between 400 to 700 nm. The ultraviolet radiation emitted from the sun can damage the eye. UV is divided into three bands: UVC (100-280 nm), UVB (280-315 nm), and UVA (315-400 nm) [62].

Optical transparency is an important pre-requisite that hydrogels used in $CL_s$ need to fulfil, in order to provide a clear vision for the wearer. It is expressed as the percentage of light that can be transmitted. Hydrogels are suitable for use as $CL_s$ when the visible light transmittance is above 90%. On the other hand, the hydrogels must have a low transmittance in the range of UV light to avoid ocular problems [43,62].

The transmittance of $CL_s$ is normally assessed with the help of a UV-Vis spectrophotometer [62]. The lens is placed on one side of the cuvette, as shown in Figure 8. The spectrophotometer determines the

transmittance (T) of the light at a specific wavelength from the intensity of the incident light ($I_0$) and transmitted light (I), through the following ratio:

$$T = \frac{I}{I_0} \quad \textbf{(1)}$$

which is often expressed in terms of percentage.

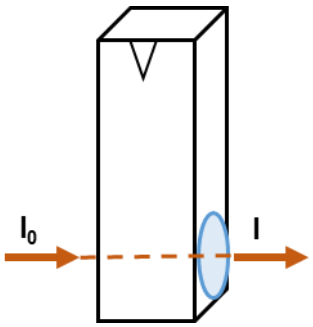


**Figure 8 -** Schematic representation of the transmittance measurement using the UV-Vis spectrophotometer.

The absorbance of the light relates with the transmittance and may be calculated by Equation 2:

$$A = -\log_{10}(T) \quad \textbf{(2)}$$

#### 1.2.2.3.3 Ionic Permeability

The ionic permeability is another key property of $CL_s$ because it is responsible for the lens motion, preventing $CL_s$ from adhering permanently to the cornea. This property depends on the diffusion of ions (mainly $Na^+$ and $Cl^-$) through the lens matrix [63].

For the measurement of this property, it is usually used a diffusion cell that has a donor and a receiver compartment [63,64]. The ionic permeability through a contact lens corresponds to the ionoflux diffusion coefficient ($D_{ion}$) which can be estimated applying the Fick's law [53,63]:

$$\frac{F.V}{A} = D_{ion}\left(\frac{dC}{dx}\right) \quad \textbf{(3)}$$

where $F$ = rate of the ion transport, $V$ = volume of the receiver solution, $A$ = area of the silicone hydrogel lens, and $\left(\frac{dC}{dx}\right)$ = initial NaCl concentration gradient across the lens [53,63]. According to a US patent [65], Nicolson et al. claimed that the value of $D_{ion}$ should be at least $1.5\times10^{-6}$ $mm^2$ $min^{-1}$ in order to have an adequate on-eye movement of the lens.

#### 1.2.2.3.4 Swelling

The capability of hydrogels of retaining aqueous solvents, such as water, makes these materials a good medium for the diffusion of drugs. Swelling is the capacity of hydrogels to retain large amounts of solvent between the polymer chains. When a hydrogel is in contact with the solvent, the polymer starts to expand, allowing more solvent molecules to enter into the network (Figure 9). At this time, two opposing forces are competing: the osmotic forces (from the solvent) and the elasticity forces (from the polymer network). When the equilibrium is reached these two forces are balanced and no more solvent enters

into the polymer network. The equilibrium swelling, dimensional modification of hydrogels and the drug release behaviour can be determined by many factors such as, the degree of cross-linking, the hydrophilic/hydrophobic proportion of the hydrogels and the degree of ionization [66,67].

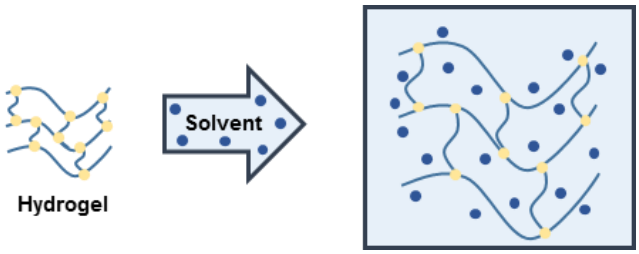


**Figure 9 -** Schematic representation of a hydrogel swelling when in contact with a solvent.

The rate at which the solvents enter the hydrogel depends on some physicochemical parameters, such as the affinity between the solvent molecules and the hydrogel's matrix, the size of the solvent molecules and the porosity of the structure (higher pore dimensions, faster swelling rate) [67].

The swelling capacity (SC) of a hydrogel can be estimated by the following equation:

$$SC = \frac{W_t - W_0}{W_0} \times 100 \quad \textbf{(4)}$$

where $W_0$ is the weight of the dry hydrogel and $W_t$ is the weight at time $t$ [64]. When the equilibrium swelling is reached, the water content (WC) can be calculated by the Equation 5:

$$WC = \frac{W_\infty - W_0}{W_\infty} \times 100 \quad \textbf{(5)}$$

where $W_\infty$ is the weight of the hydrogel at the equilibrium [64].

#### 1.2.2.3.4.1 States of Water in Hydrogels

The determination of the different states of water in a hydrogel is very important in order to understand the interactions between the polymer network and water, and the drug diffusion mechanism through the hydrogel. Also, the study of the states of water is important to understand the physical properties of hydrogels [68,69].

Hydrogels have three different types of water in their network (Figure 10) which may be classified based on the interactions that the water molecules establish with the polymeric network [69]. The free (or bulk) water is composed by water molecules that do not directly interact with the polymer matrix, freezing at 273 K. Loosely bound water interacts weekly with the polar groups of the polymer matrix through hydrogen bonding, freezing between 180 and 273 K. Finally, the tightly bound water (freezable below 180 K) is strongly bonded to the polar groups of the polymer matrix by hydrogen bonding or is linked to the ionic residues of the network [69]. Due to the strong bonding of these water molecules to the pore walls of the hydrogel's network, the phase transition of the tightly bound water does not appear in calorimetric analysis [70]. Different techniques can be used for the quantification of the water states in hydrogels including: differential scanning calorimetry (DSC), thermogravimetric analysis (TGA), and nuclear magnetic resonance (NMR) [69]. In this work, it was used the DSC technique, being the samples analysed in their swollen state. Typically, DSC measures the heat flow difference between the sample

and an inert reference. The obtained curve depicts the relationship between the heat flow and the temperature and from that, it is possible to calculate the sample's melting and freezing temperatures and the respective heats of fusion and freezing [71]. The quantity of the two types of water (free water and loosely bound water) that can be measured in the DSC analysis are determined by the integration of the melting/crystallization peak and the pore water melting peak corresponding to the freezing point depression [72].

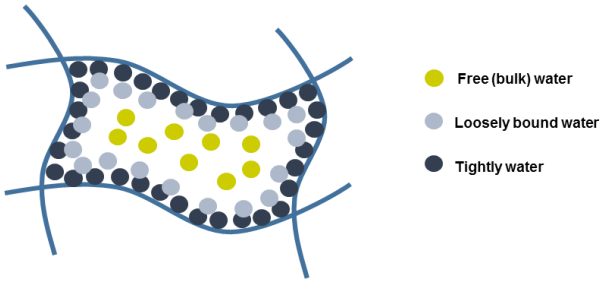


**Figure 10 -** Schematic representation of the states of water in a hydrogel pore.

The crosslinking degree of the hydrogel affects the relative amounts of free and bound water. Higher crosslinking decreases the pores diameter, leading to a more rigid and tight hydrogel structure, and, in consequence, reduces the mobility of free water [69].

Apart from the states of water, the DSC can also be used for the determination of the pore shape, pore volume and pore-size distribution of hydrogel's network. The study of these features is of extreme importance, since they affect the swelling capability and the mechanical properties of hydrogels as well as the diffusion of an eventual solute through the matrix [72].

Thermoporometry is a calorimetric method that allows to infer the pore shape and size distribution of the materials based on the melting or crystallization temperature depression of a liquid confined in their pores. DSC is an adequate technique because of its precision in measuring the temperature shifts. Usually, water is the liquid chosen due to its well-known melting point at 273.15 K, and its specific heat of fusion (333.6 J $g^{-1}$), which is higher than the majority of the other liquids, enhancing the sensitivity of the DSC when small volumes of liquid are used [73,74].

The pores can be characterized with respect to their shape as cylindrical, spherical, conical or both spherical and cylindrical. However, in this work the pores were considered cylindrical for simplicity reasons. Through the use of the Gibbs-Thomson equation, it is possible to determine the dimensions of the pores because it relates the temperature shift and the pore radius, $r_p$ [70]:

$$r_p(nm) = \frac{2T_m\gamma_{sl}cos\theta}{\Delta T\rho H_f} \quad \textbf{(6)}$$

where $T_m$ is the water melting temperature (273.15 K), $\gamma_{sl}$ is the ice-water interfacial tension, $\theta$ is the contact angle of water in the hydrogel, $\Delta T$ is the melting temperature depression, $\rho$ is the water density ($10^6$ g $m^{-3}$), and $H_f$ is the specific heat of fusion of water (333.6 J $g^{-1}$) [70].

The melting temperature depression in DSC can be calculated using three methods (Figure 11): $\Delta T_{pk}$ (difference between the maximum of each peak), $\Delta T_{on}$ (difference between extrapolated onsets), and $\Delta T_{on-pk}$ (difference between the peak corresponding to the loosely bound water and the extrapolated onset of the free water). In view of the results obtained in this work, for the pore-size calculations, it was used $\Delta T_{pk}$ [73].

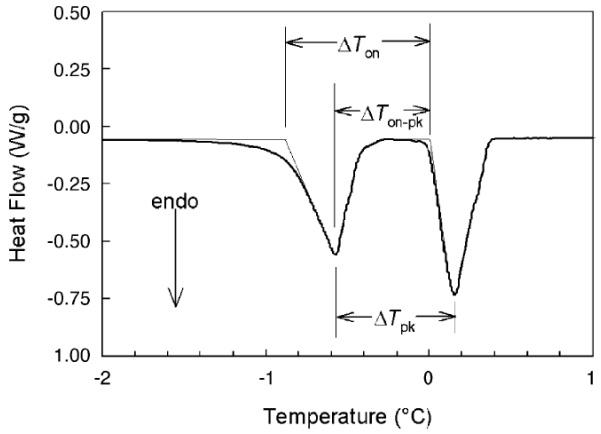


**Figure 11 -** Comparison between the three possible methods of determining the melting temperature depression in DSC. Adapted from [73].

The use of Equation 6 has some disadvantages because the values of the interfacial tension ice-water ($\gamma_{sl}$) on the triple point temperature, and the contact angle ($\theta$) are difficult to obtain experimentally and the values reported in the literature vary widely [75]. To overcome these difficulties, many authors tried a different approach [73], by using reference materials (for example, porous silica) that have been precisely quantified by other methods. This allowed to have a calibration for pore-size determination. This approach relies on the adjustment of Equation 6 to the experimental data [73]. Brun et al. arrived at the following expressions by factoring the experimental temperature dependence of specific heat capacity, heat of fusion, specific volume, and interfacial tension in the Kelvin equation [73,75]:

$$r_p(nm) = -\frac{32{,}33}{\Delta T(K)} + 0{,}68\ (melting) \quad \textbf{(7)}$$

$$r_p(nm) = -\frac{64{,}67}{\Delta T(K)} + 0{,}57\ (freezing) \quad \textbf{(8)}$$

Equations 7 and 8 are valid for the shifts of melting and freezing temperature of water, considering hypothetical cylindrical pores. Later on, Landry tried another approach, but still used data from a porous glass to calibrate for pore-size determination, and reached the following equations for the determination of the pore radius [73]:

$$r_p(nm) = -\frac{19{,}082}{\Delta T(K) + 0{,}1207} + 1{,}12\ (melting) \quad \textbf{(9)}$$

$$r_p(nm) = -\frac{38{,}558}{\Delta T(K) - 0{,}1719} + 0{,}04\ (freezing) \quad \textbf{(10)}$$

Fitting the equations to the melting data was reported to yield better results than to the freezing data. In this work, it was decided to use Brun and Landry "melting" equations and then compare the results obtained with both methods.

#### 1.2.2.3.5 Wettability

Wettability is described as the capability of a liquid to spread on a solid surface. This property is determined by the cohesion between liquid molecules and also by the adhesion between liquid and solid molecules. This property is very important, especially for hydrogels used in $CL_s$, because it is related to their ability to support a stable tear layer; otherwise, it can affect the visual performance giving rise to the increase of debris accumulation and discomfort for the patient [43,76,77].

The study of wettability is usually performed by measuring the contact angle between the liquid and the solid, which is the angle formed between the tangent to liquid-vapour interface at the triple line and the solid-liquid interface. The contact angle, $\theta$, can be correlated with the interfacial tension between solid and vapour, $\gamma_{SV,}$, the interfacial tension between solid and liquid, $\gamma_{SL}$, and the interfacial tension between liquid and vapour, $\gamma_{LV}$, by the Young's equation [78]:

$$\cos\theta = \frac{\gamma_{SV} - \gamma_{SL}}{\gamma_{LV}} \quad \textbf{(11)}$$

When the value of the contact angle is small, the interaction between the liquid and the solid is great, and the liquid spreads on the surface. In this case, the surface has high wettability and it is called hydrophilic if the liquid is water (Figure 12). On the other hand, when the contact angle is high, the interaction between the liquid and the solid is small and the liquid does not spread on the surface. In this case, the surface has low wettability and it is called hydrophobic, again if the liquid is water (Figure 12) [76,77].

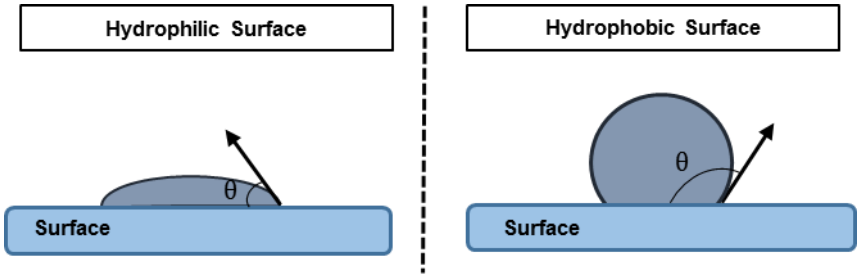


**Figure 12 -** Schematic representation of a hydrophilic and a hydrophobic surface.

The contact angle can be measured by different methods being the sessile drop and the captive bubble methods two of the most used. In the sessile drop method, a liquid drop is deposited on the surface using a syringe and then, with the help of a goniometer and software data analysis, the contact angle is measured (Figure 13). One of the major disadvantages of this technique is the possible evaporation of the liquid during the measurements. To avoid this problem, the measurement should be made inside an ambient chamber saturated with water vapour. In the captive bubble approach, the surface is immersed in the liquid inside a glass cell and a gas bubble from a syringe is inserted on the bottom of the surface (Figure 13). The contact angle may be determined in the same way, as referred previously, with the help of a goniometer and software data analysis. From the experimental point of view, this method is more

complex than the sessile drop method, being necessary to fix the sample in an inverted position inside the liquid and to ensure its strict horizontality. The water contact angles measured with the captive bubble technique on hydrated surfaces are generally lower compared to those obtained by the sessile drop technique on dry samples. This may be due to changes in the surface properties, together with the fact that in sessile drop the angles are may be seen as advancing whereas in captive bubble they are receding angles [43,76,77,79,80].

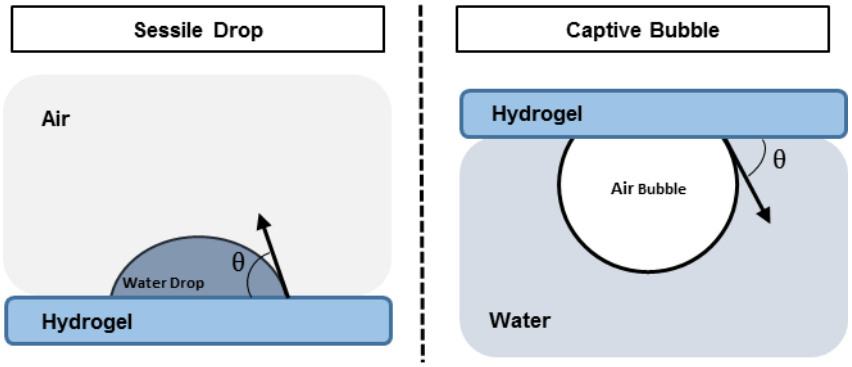


**Figure 13 -** Schematic representation of two methods that are used to determine the contact angle.

#### 1.2.2.3.5.1 Effect of Surface Roughness on the Wettability

Surface roughness is an important parameter that controls the wettability. Sometimes the contact angles obtained in the hydrogels do not express the intrinsic values of the material and one of the reasons can be the roughness of the surface. There are different models that can explain the effect of roughness on contact angles, being the Wenzel and Cassie-Baxter models the most well-known. In the Wenzel model, it is considered that the water droplet is in contact with the entire rough surface, filling all the depressions (Figure 14) [81]. According to Wenzel, the equilibrium contact angle between the liquid and a rough surface, $\theta^W$, is given by the following equation:

$$cos\theta^W = rcos\theta \quad \textbf{(12)}$$

where $r$ is the surface roughness factor that corresponds to the ratio between the actual and apparent surface areas and $\theta$ is the contact angle measured on an ideal (smooth) surface. Considering that the surface roughness is greater than 1, this model predicts that the contact angle observed when the liquid wets the surface ($\theta$<90º) will decrease with the surface roughness ($\theta^W < \theta$). In the same way, the contact angle when the liquid does not wet the surface ($\theta$>90º) will increase with the surface roughness ($\theta^W > \theta$) [82].

On the other hand, the Cassie-Baxter model applies to the situation where the water droplet does not cover the entire rough surface due to the air that is trapped inside the depressions (Figure 14) [81]. In this model, the contact angle measured on a rough surface is given by the following equation [82]:

$$cos\theta^{CB} = -1 + f_s(cos\theta + 1) \quad \textbf{(13)}$$

where $f_s$ is the fraction of solid that is in contact with the liquid, and $\theta$ is the contact angle measured on an ideal (smooth) surface. Analysing the Equation 13, the decrease in the $f_s$ value leads to higher contact angles because the contact area between the solid and liquid is lower.


**Figure 14 -** Two models applied to rough surfaces. Left: Wenzel model; Right: Cassie-Baxter model. Adapted from [83]

#### 1.2.2.3.5.2 Surface Energy

In order to understand the surface energy determination, it is necessary to introduce some important concepts. When a liquid drop relies on a solid, there are three different phases and three interfacial tensions that need to be considered: solid-liquid, liquid-gas, and solid-gas [84]. These interactions can be related using the Young's equation referred above (Equation 11). Observing the Equation 11, the variable $\gamma_{SL}$ cannot be measured directly and in order to determine it, more relationships between $\gamma_{SV}$, $\gamma_{SL}$ and $\gamma_{LV}$ need to be achieved [84]. Firstly, the work of adhesion is introduced as the work necessary to separate an interface into two new surfaces. When it comes to a solid and a liquid phase, the work of adhesion, $W_{SL}$, is given by the following equation [85]:

$$W_{SL} = \gamma_{LV} + \gamma_{SV} - \gamma_{SL} \quad \textbf{(14)}$$

Then, combining the Equation 11 and 14, it is possible to arrive to the Young-Dupré equation [85]:

$$W_{SL} = \gamma_{LV}(1 + cos\theta) \quad \textbf{(15)}$$

The work of adhesion between the solid and liquid is also assumed as the geometric mean of the cohesion work of a solid and the cohesion work of the liquid and it is given by the following equation [85]:

$$W_{SL} = \sqrt{2\gamma_{SV}2\gamma_{LV}} \quad \textbf{(16)}$$

The surface energy can be calculated by measuring the contact angle of two liquids with different polarities. For example, water (high polarity) and diiodomethane (low polarity) can be used as testing liquids. Over the years, several models were used to determine the surface energy, being the Fowkes the one with the pioneer idea [86]. According to Fowkes, the surface free energy can be divided into two components [84]:

$$\gamma_S = \gamma_S^d + \gamma_S^{nd} \quad \textbf{(17)}$$

where $\gamma_S^d$ stands for the dispersive interactions contributions and $\gamma_S^{nd}$ corresponds to the polar interactions. Fowkes also assumed that the interactions which contribute to the work of adhesion operate only across the interface and that only the dispersion interactions are important. Considering this characteristics, the interfacial surface energy can be determined as follows [85]:

$$\gamma_{SL} = \gamma_{SV} + \gamma_{LV} - 2\sqrt{\gamma_{SV}^d \gamma_{LV}^d} \quad \textbf{(18)}$$

where $\gamma_{SV}^d$ and $\gamma_{LV}^d$ are the dispersion components of the solid and the liquid surface tensions, respectively. However, Owens and Wendt went further and assumed that, when both liquid and solid are polar substances, both dispersive and polar interactions contribute to the work of adhesion according to the following equation[85]:

$$W_{SL} = 2\sqrt{\gamma_{SV}^{d}\gamma_{LV}^{d}} + 2\sqrt{\gamma_{SV}^{p}\gamma_{LV}^{p}} \quad \textbf{(19)}$$

where the subscripts $d$ and $p$ are related to the dispersive and polar components, respectively. From Equations 15 and 19, it is possible to obtain the dispersive and polar components of a surface by measuring the contact angles of two liquids with different polarities and with known dispersive and polar components. In this work, it was used water and diiodomethane and the surface components were obtained solving the following system of equations:

$$\begin{cases} \gamma_{L_1V}(cos\theta^1 + 1) = 2\left(\sqrt{\gamma_{SV}^{d}\gamma_{LV_1}^{d}} + \sqrt{\gamma_{SV}^{p}\gamma_{LV_1}^{p}}\right) \\ \gamma_{L_2V}(cos\theta^2 + 1) = 2\left(\sqrt{\gamma_{SV}^{d}\gamma_{LV_2}^{d}} + \sqrt{\gamma_{SV}^{p}\gamma_{LV_2}^{p}}\right) \end{cases} \quad \textbf{(20)}$$

where 1 and 2 represents the water and diiodomethane liquids, respectively. The determination of the dispersive and polar components was done by solving the system of Equations 20, and taking the polar and dispersive components of the water and diiodomethane from the literature [87] (Table 3).

**Table 3 -** Surface free energy and respective components for water and diiodomethane [87].

| Liquid | Surface Free Energy (mJ m$^{-2}$) | Dispersive Component, $\gamma^d$ (mJ m$^{-2}$) | Polar Component, $\gamma^p$ (mJ m$^{-2}$) |
|---|---|---|---|
| Water | 72.8 | 21.8 | 51.0 |
| Diiodomethane | 50.8 | 49.5 | 1.3 |

#### 1.2.2.3.6 Morphology

One of the techniques that is widely used for the study of morphology is the scanning electron microscopy (SEM), which is a method that allows the analysis of very small features in the surface due to its high-resolution and magnification [88,89].

SEM involves the emission of a beam of accelerated electrons from an electron gun through a column. Then, the electron beam passes through a series of lenses that will narrow the beam into the desired shape for analysing the sample. With the help of scanning coils at the end of the column, the electron beam travels through the surface in a raster scan pattern. The interactions of the electrons with the surface of the sample produce a variety of signals, including secondary electrons, backscattered electrons, diffracted backscattered electrons, characteristic X-rays, visible light and heat. Some of them may be identified by a detector. However, there are two signals that are most used in SEM imaging: the secondary electrons, and the backscattered electrons. The secondary electrons result from the interaction between the beam and the atoms of the surface and present a low energy. This signal gives information, in the form of grey scale images, about the morphology and topography of the samples. On the other hand, backscattered electrons are of high energy and result from interactions between the beam and the nucleus of the sample atoms. The image obtained in the backscattered electron mode

can reveal the density of the surface since the atoms can have different atomic numbers, leading to different levels of scattering [89–92].

In order to make a good characterization, if the material is not conductive, it is necessary to cover the surface with a thin conductive layer with several nanometres (e.g. gold). Since the SEM analysis is made under vacuum (≈$10^{-4}$ Pa), this technique only allows to characterize dry hydrogel's samples

#### 1.2.2.3.7 Mechanical Properties

Over the years, mechanical properties of CLs have gained attention, especially due to the complications that the stiffer lenses present. Comfort and visual performance are the key requirements from the CLs wearer's perspective. Comfort can be achieved with flexible lenses. However, they cannot be too soft because they need to have the capacity to resist to forces, such as those involved in the eye movement, blinking and handling. Additionally, CLs must have the ability to maintain their shape when placed in liquids , like the conservation and/or cleaning liquids [93 94].

Several mechanical tests can be made to the hydrogels in order to study their behaviour and to prevent the decrease in optical performance. In this work, it was used the tensile test in which the sample was subjected to a constant load causing the elongation of the material until its failure. In this type of test, a stress-strain curve (Figure 15) is drawn, which relates load with elongation measurements made on the sample. In the stress-strain curve, the stress (σ) is the force applied (F) per unit of cross-sectional area of the sample (A) [93]:

$$\sigma = \frac{F}{A} \quad \textbf{(21)}$$

On the other hand, strain is described as the deformation that the sample suffers during the test in the direction of the force. When the tensile properties of materials, like hydrogels, are being analysed, the amount of deformation that a material suffers is called elongation (ε). This parameter is characterized by the change in length of the sample compared to its original length, and it is given by the Equation 22 [93]:

$$\varepsilon = \frac{(L - L_0)}{L_0} \quad \textbf{(22)}$$

where, $L$ is the length of the sample, and $L_0$ is the initial length of the sample. The elastic elongation corresponds to the maximum elongation that is recoverable, when the load is released. In contrast, elongation at break is the change in length at the point at which the material breaks [93].

Tensile tests allow to calculate the modulus of elasticity, *E*, (also called Young's modulus), which represents the resistance of the sample to a deformation, in Pascal (Pa) [93]:

$$E = \frac{\sigma}{\varepsilon} \quad \textbf{(23)}$$

When tensile tests are performed with an elastic material, the Young's modulus can be calculated directly from the slope of the stress-strain curve due to its linearity. In the case of viscoelastic materials, like CLs, it is different because the Young's modulus changes with the amount of stress. In this case, the stress-strain curve of these materials starts with a linear region, called elastic region, where the

sample can still return to its original shape if the load is removed (Figure 15). The slope of this part of the curve, is the one that is used to calculate the Young's modulus. Then, when the material continues to suffer a stress that passes the elastic limit, this point is called yield strength. From that moment on, the deformation of the sample is permanent, entering into the plastic region, like is depicted in Figure 15. In this region, the sample continues to suffer a stress until reaches its limit (ultimate strength) and, after that, the break/failure occurs. Ultimate strength is also called tensile strength and it is related to the ultimate load that the sample can support before the break/failure. It also provides the measure of the strength of the material and can be numerically calculated by the following equation [42,93]:

$$Tensile\ strength = \frac{Maximum\ load\ applied}{Cross - sectional\ area} \quad \textbf{(24)}$$

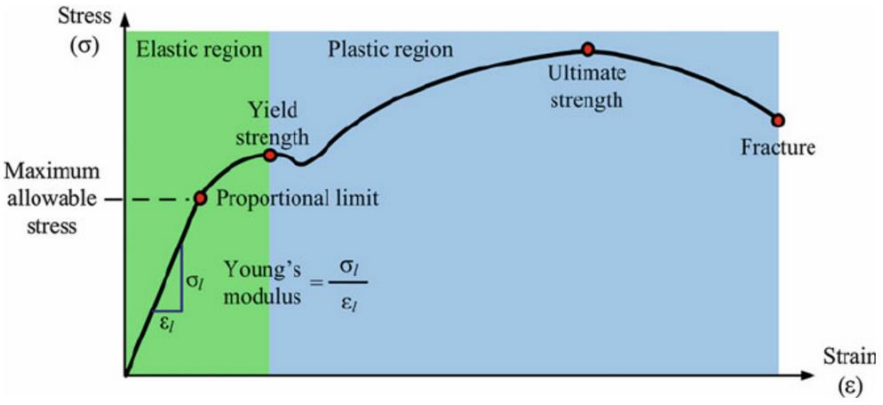


**Figure 15-** Example of a stress-strain curve for a viscoelastic material. Adapted from [95].

Toughness is the amount of energy that a sample can absorb before it breaks, and corresponds to the area under the stress-strain curve (Figure 16). Materials can be brittle and in this case, the fracture occurs in the elastic region, with a low energy absorption. Alternatively, the materials can be ductile and higher amounts of energy are absorbed before the failure in the plastic region. It is important to refer that strength and toughness are not directly related because a material can be strong but not tough. For example, if a material needs high levels of stress to break/fail, but it undergoes a little deformation, it would be a strong but not tough material [93].

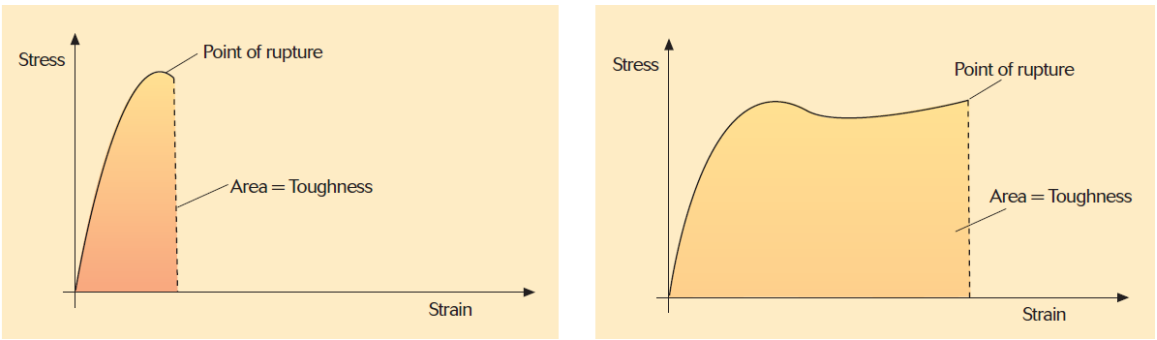


**Figure 16 -** Stress-strain curve of two different materials: brittle (left), and ductile (right). Adapted from [93].

As referred above, Young's modulus can affect the comfort and the visual performance. Over the years, studies have been made in order to improve the mechanical properties of hydrogels. The researchers made several attempts with monomer combinations and tried different amounts of cross-link to reach a composition with the desired mechanical properties. Table 4 presents the Young's modulus of different commercial silicone $CL_s$ [93].

**Table 4 -** Young's modulus of different types of silicone $CL_s$ [94,96].

| Lens Type | Principal Monomers* | Young's Modulus (MPa) |
|---|---|---|
| Lotrafilcon A (Focus NIGHT & DAY®) | DMA + TRIS + siloxane monomer | 1,5 |
| Lotrafilcon B ($O_2$ OPTIX™) | DMA + TRIS + siloxane monomer | 1,0 |
| Senofilcon A (ACUVUE® OASYS®) | mPDMS + DMA + HEMA + siloxane monomer + TEGDMA + PVP | 0,72 |
| Galyfilcon A (ACUVUE® ADVANCE®) | mPDMS + DMA + EGDMA + HEMA + siloxane monomer + PVP | 0,43 |

* DMA: N,N-Dimethylacrylamide; EGDMA: ethylene glycol dimethacrylate; HEMA: 2-Hydroxyethyl methacrylate; mPDMS: monofunctional methacryloxypropyl terminated polydimethylsiloxane; PVP: poly(vinylpyrrolidone); TEGDMA: tetraethyleneglycoldimethacrylate; TRIS: trimethylsiloxy silane.

Mechanical properties can be related to some other features of $CL_s$, such as:

- Water content: lenses with higher water content, usually show a low Young's modulus and are less stiff;
- Silicone content: higher amounts of silicone lead to a lower water content and subsequently to a higher modulus;
- Oxygen permeability: lenses with greater Dk are more stiff;
- Amount of cross-link: the higher the quantity of cross-link in the polymeric network, the higher the modulus [94,97].

# 2 Materials and Methods

## 2.1 Materials

### 2.1.1 Hydrogel Materials

For the hydrogels' production, the following reagents were used:

- 3-[Tris(trimethylsiloxy)silyl]propyl methacrylate (TRIS), 98%, from Sigma-Aldrich®;
- Monomethacryloxypropyl terminated Polydimethylsiloxane (mPDMS) (Bisomer® Bu-PDMS), from GEO Specialty Chemicals®;
- N-Vinylpyrrolidone (NVP), ≥ 98%, from Merck®;
- 3-Methacryloxy-2-Hydroxypropoxy(propylbis(trimethylsilyloxy)methylsilane (Bisomer® SiGMA), 96.9%, from GEO Specialty Chemicals®;
- 2-Hydroxyethyl methacrylate (HEMA), ≥ 98%, from Sigma-Aldrich®;
- N,N-Dimethylacrylamide (DMA), ≥ 99.5% (GC), from Sigma-Aldrich®;
- Ethylene glycol dimethacrylate (EGDMA), 98%, from Sigma-Aldrich®;
- 2,2′-Azobis(2-methylpropionitrile) (AIBN), 98%, from Sigma-Aldrich®.

### 2.1.2 Drugs

For the release studies two different drugs were used:

- Diclofenac sodium salt, > 99%, from Sigma-Aldrich®;
- Dexamethasone, >96%, from Carbosynth®.

### 2.1.3 Other Materials

The reagents used for the silanization process of the glasses used in the hydrogels' production are presented below:

- Dichlorodimethylsilane, 99.5% (GC), from Fluka®;
- Carbon tetrachloride, 99.9%, from Sigma-Aldrich®;
- Dichloromethane, from Sigma-Aldrich®;

The contact angles determination was done using:

- Diiodomethane, 99%, from Sigma-Aldrich®;
- Distilled and deionized (DD) water.

## 2.2 Methods

### 2.2.1 Hydrogel Preparation

For the hydrogels preparation different methods were used, depending on the type of hydrogels. Below, it will be described the protocol for the different types of hydrogels:

- TRIS/NVP/HEMA hydrogels: 5 mL solutions containing TRIS, NVP and HEMA in the volume percentages presented in Table 6 from the results section, and a fixed concentration of the

crosslinker EGDMA (4.7 mM) were prepared. Then, the solutions were degassed by ultra-sounds for 5 minutes and after that, they were bubbled with a gentle stream of nitrogen for 15 minutes. Afterwards, a fixed quantity (6.7 mM) of the polymerization initiator, AIBN, was added and then, the resulting mixtures were magnetically stirred for about 10 minutes, in order to obtain homogeneous solutions. The mixtures were then injected into a mould composed by two silanized glasses (preparation protocol referred below) (5x10 cm) separated by a Teflon spacer, with a thickness of approximately 0.3-0.6 mm. The mould was placed in the oven and the polymerization reaction occurred at 60ºC for 24 hours.

The preparation of other hydrogels differing only in the amount of crosslinker, followed the same protocol outlined above.

- TRIS/NVP/SiGMA/DMA/HEMA hydrogels: the preparation of this type of samples followed the same protocol as above; the only difference was the polymerization process, which occurred through ultraviolet radiation for 120 minutes. A UV lamp (UV-Exposure box 2; with a wavelength of 350 nm and a power of 15 W) was used and the moulds were placed approximately 10 cm from the lamp. In this type of hydrogels, it was performed the polymerization reaction by ultraviolet radiation because in the first attempts, it was used the oven (at 60ºC for 24 hours) and they became opaque.
- TRIS/mPDMS/NVP/SiGMA/HEMA and mPDMS/NVP/SiGMA/DMA hydrogels: depending on the type of hydrogel, TRIS, mPDMS, NVP, HEMA or DMA were added in the volume percentages shown in Table 7 and Table 9 from the results section, one at a time, to prepare 5 mL solution. Degassing by ultra-sounds for 5 minutes was carried out between the adding of each material. After that, the mixtures were bubbled with gentle stream of nitrogen, for 15 minutes, and, at the same time, magnetically stirred at 50ºC. This step was needed in order to eliminate all the air bubbles and to prevent the phase separation. EGDMA (4.7 mM) and AIBN (6.7 mM) were added after cooling the solutions because these agents can precipitate with the heat [98]. After that, the mixtures were magnetically stirred (10 minutes) and then, they were injected into the mould described above. In this case, the polymerization process occurred through ultraviolet radiation for 120 minutes.

After the polymerization reaction, all hydrogels referred above were washed by immersion for 5 days, in DD water which was renewed 3 times a day. This procedure is needed to easily remove the glasses attached to the hydrogel and to remove the unreacted monomers [99]. After that, the hydrogels were dried at 36ºC in the oven, for 24 hours, and then, they were stored in a dry place and protected from the light before further use. In Figure 17, it is possible to observe the different protocols adopted for the preparation of the different types of hydrogels.

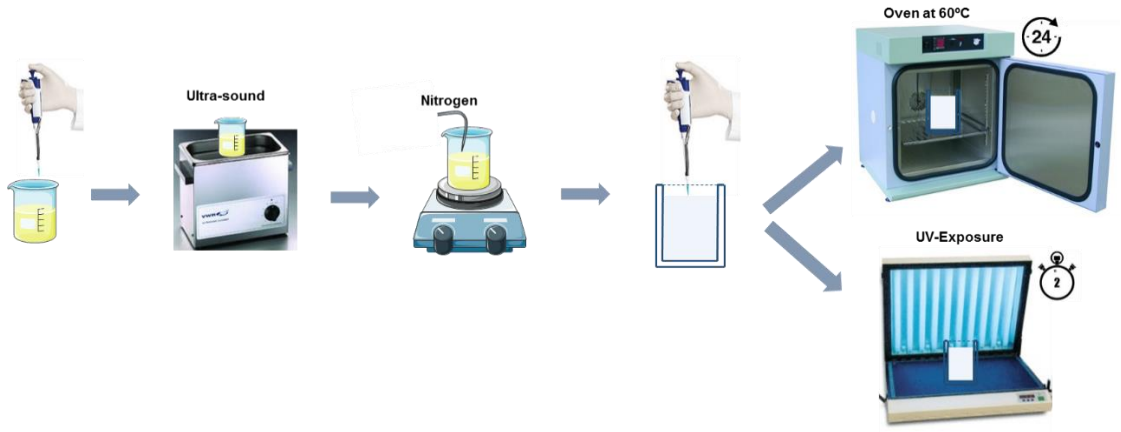


**Figure 17 -** Schematic representation of the different protocols used for the hydrogels preparation used in this work.

The glasses that were used as a mould to put the hydrogel mixture need to be hydrophobic, in order to be possible the removal of the hydrogel after the polymerization reaction. To meet this requirement, the silanization protocol was done according to the procedure described by Vazquez et al. [100], where the glasses were immersed in a 2% solution of dichlorodimethylsilane in carbon tetrachloride, for 1 hour. After that, the glasses were rinsed with dichloromethane and dried with nitrogen.

### 2.2.2 Drug Loading/Release

For the drug release tests, the hydrated hydrogels were cut with 10 mm diameter and then they were dried at 36ºC for 24 hours. After that, the weight of hydrogels was measured for further calculations.

The drug loading was performed using the drug soaking method, where the hydrogels were immersed in 3 mL of drug solution for 38 hours at 4ºC. In some cases, the loading was also carried out at 60ºC for comparison purposes. For the drug release tests using diclofenac, the loading was performed in a NaCl solution (130 mM) with a drug concentration of 1 mg $mL^{-1}$. For dexamethasone release experiments, the hydrogels were loaded in NaCl solution with a drug concentration of 0.08 mg $mL^{-1}$ or in an ethanol solution with a drug concentration of 1 mg $mL^{-1}$. It was necessary to test this drug in two loading solutions because the dexamethasone is slightly soluble in aqueous solvents [101].

After the drug incorporation, the drug release experiments were performed. The loaded hydrogels were removed from the drug solution, dipped in DD water and blotted with dry absorbent paper. This procedure is important to remove the excess of drug that is on the surface of the hydrogel. Then, the hydrogels were immersed in 3 mL of NaCl solution (to mimic the lacrimal fluid) and placed in a shaker (Incubating Mini Shaker from VWR) at 36ºC and 180 rpm.

As sketched in Figure 18, aliquots of 0.2 mL were collected during the release experiments and replaced with 0.2 mL of fresh NaCl solution (130 mM). This procedure was done each hour, in the first 8 hours, and then each 24 hours until the plateau is reached, point at which no more drug is released from the hydrogels. The absorbance of each aliquot was determined by a UV-Vis spectrophotometer (Multiskan™ GO Microplate Spectrophotometer of Thermo™ Scientific), using the appropriate wavelength for each drug. For diclofenac, it was used a wavelength of 276 nm, whereas for

dexamethasone it was used a wavelength of 240 nm. The drug concentration was then determined by converting the absorbance into concentration of drug, using Beer's Law. For this purpose, it was necessary to make a calibration curve for each drug, by measuring the absorbance of several solutions with different drug concentrations.

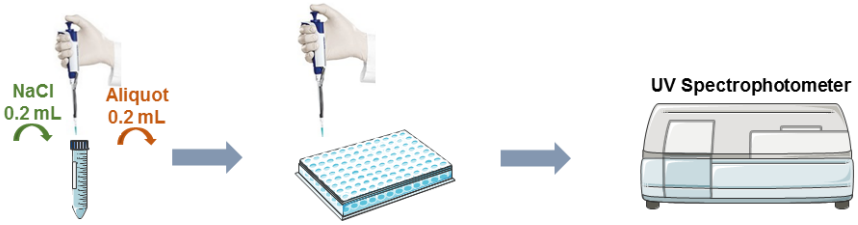


**Figure 18 -** Schematic representation of the drug release protocol used in this work.

## 2.2.3 Characterisation of Hydrogels

### 2.2.3.1 Optical Transparency

For the optical transparency analysis hydrogel samples with 10 mm of diameter were used in their swollen state. The absorbance, in the range of the visible light (400 to 700 nm), was measured using the UV-Vis spectrophotometer (Multiskan™ GO Microplate Spectrophotometer from Thermo™ Scientific). Firstly, the calibration was made using an empty quartz cuvette, in order to have a standard zero in the spectrophotometer. Then, fully hydrated hydrogels were mounted on one side of the outer surface of the cuvette, according to Figure 19. The cuvette was then placed in the UV-Vis spectrophotometer and the absorbance values were obtained. This procedure was held, at least, in triplicate for each type of hydrogel and in different regions of the hydrogel. The percent of transmittance was calculated using Equation 2 from the last section.

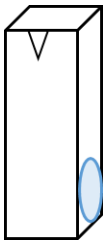

**Figure 19 -** Schematic representation of the hydrogels' assembly in the cuvette.

### 2.2.3.2 Ionic Permeability

For the ionic permeability studies, a home-made PMMA horizontal diffusion cell, with two compartments, the donor and the receiver chamber, was used. The hydrogel, hydrated in DD water, was mounted between the two compartments, and 24 mL of NaCl solution (130 mM) and 32 mL of DD water were inserted into the donor and receiver compartment, respectively (Figure 20). This experiment was held in triplicate for each type of hydrogel at 36ºC. For these measurements, hydrogels were cut in discs with 12 mm of diameter in order to seal the aperture between both compartments of the cell. The conductivity, in $\mu S\ cm^{-1}$, was measured hour by hour for at least ten hours using a conductivity meter (Handheld meter Cond 340i from WTW).

In the beginning of the experience the $Na^+$ and $Cl^-$ ions are in the donor compartment. As time passes, the ions pass through the lens matrix towards the receiver compartment, which has DD water and where the conductivity is measured (Figure 20).

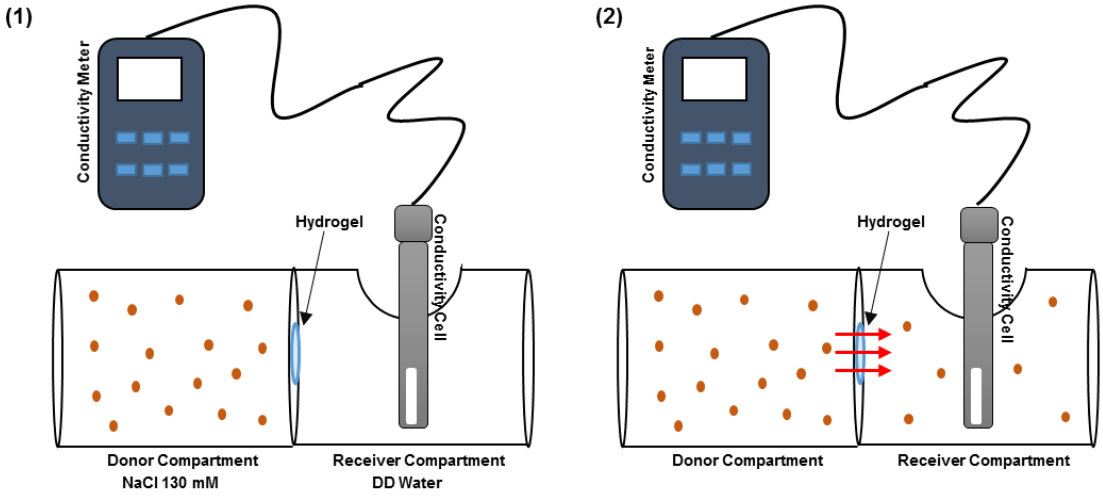


**Figure 20 -** Schematic representation of the ionic permeability experiment. (1) – The beginning of the experience; (2) - During the experience the ions pass through the hydrogel matrix.

The conductivity data acquired were then converted into NaCl concentration (in mg $mL^{-1}$) through a calibration curve previously obtained. The NaCl concentration in the receiver compartment was plotted as a function of time and the rate of ion transport (F) was obtained from the slope of the linear regression. The ionic permeability was then calculated using Equation 3 from the previous section.

### 2.2.3.3 Swelling

This experiment was made in order to study the hydrogels' capability of absorbing water. Firstly, the hydrogels, with 10 mm diameter, were dried for in the oven for 24 hours. Then, the hydrogels were weighted, and immersed in 3 mL of DD water at 4ºC. This temperature was chosen because the drug loading of the hydrogels was held at 4ºC too. During the assay, the hydrogels were taken out of the solution, gently blotted with absorbent paper, weighted and then immersed in the same DD water solution at 4ºC. This procedure was done at 2, 4, 6, 8, 24, 48, and 72 hours. The last measurement varied according to the time needed for the sample to achieve the equilibrium swelling. The swelling capacity was then calculated using the Equation 4 from the previous section.

Further swelling experiments were done with hydrogels of specific compositions using a salt solution (NaCl) as the immersion medium. These assays were held at 4ºC and 60ºC to evaluate the effect of the temperature.

#### 2.2.3.3.1 States of Water in Hydrogels and Thermoporometry

For the study of the states of water present in the hydrogels and the determination of the pore-size dimensions, it was used a differential scanning calorimeter, DSC 200 F3 Maia from NETZSCH, and the Proteus® Software for the data analysis. In this experiment, the samples were disks of hydrogels

hydrated in DD water with 2 mm of diameter, in order to fit the crucible. Before the experiment, it was necessary to calibrate the DSC using two substances with known melting points (DD water and Indium) which were subjected to heating and cooling cycles at the desired rate for these studies (2ºC/min).

For the experiments, the samples were taken out of DD water and carefully blotted with wet absorbent paper to prevent the hydrogel from losing water. After that, it was registered the weight of the crucible + lid (pan) and then the weight of pan + sample. The set pan + sample was then hermetically sealed with a sealing press and placed in the heating block of the equipment (Figure 21). With this technique, it is necessary to have a reference, which is an empty pan, to determine the heat flow differences between the reference and the sample during the test. Inside the heating block, both sample and reference were in a closed environment and in a dry atmosphere provided by a nitrogen gas flow. Underneath the pans there are supports that are responsible for the temperature control by the power compensation control circuit during the tests.

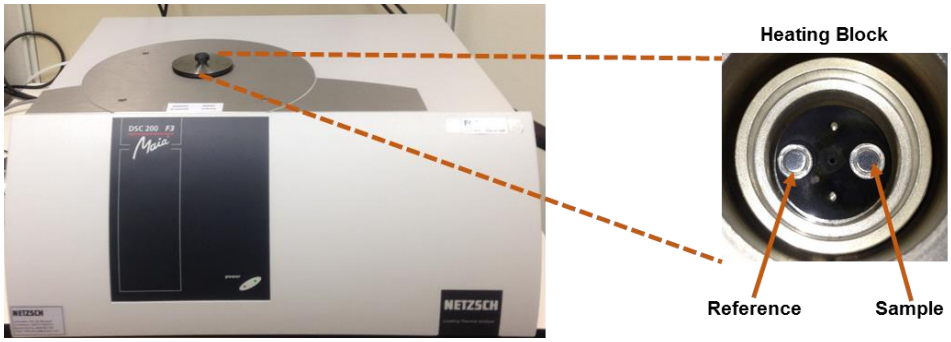


**Figure 21 -** DSC equipment used in this work and its respective assembly.

The samples were subjected to heating and cooling cycles. The samples were initially kept at 20ºC for 10 minutes in order to stabilize the temperature inside the heating block. After that, the samples were subjected to a cooling step where the temperature decreased at the rate of 2ºC/min until -60ºC and then, another isothermal step occurred for 10 minutes. Afterwards, the heating step started at a rate of 2ºC/min until 20ºC. Then, an isothermal step occurred and the experiment ended. In Figure 22, it is depicted the cooling and heating steps that each sample suffered during the whole experiment. These tests were done in triplicate for each type of hydrogel analysed. This range of temperatures was chosen in order to ensure the crystallization of the free and loosely bound water inside the hydrogel, and then a clear phase transition of the two water states when the heating step occurs.

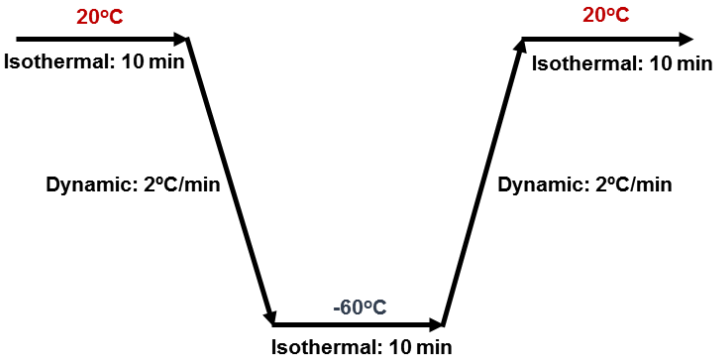


**Figure 22 -** Cycle used in DSC experiments.

The obtained data were then analysed with the Proteus® Software, which displayed a graphic, for each sample, relating the heat flow (rate at which thermal energy is supplied to reference and to the sample) with the temperature. With this software it was possible to access the onset and peak temperatures of the peaks corresponding to both free and loosely bound water, which are important for the calculations of the pore-size of hydrogels. Also, the software gave the values for enthalpy of both free and loosely bound water, by the integration of each peak, which were used for further calculations of the states of water in each type of hydrogel.

In order to have an idea of the quantity of tightly bound water present in the hydrogel, a little hole was made with a needle in the lid, after the DSC measurements, and then the pans were placed in the vacuum oven at 50ºC for 24 hours to remove as much as possible the free and loosely bound water of the hydrogel's matrix. After that, the sample was weighted. From the difference between the weight of the dried sample and that of the fully hydrated sample, the amount of tightly bound water was estimated.

#### 2.2.3.4 Wettability

For the wettability studies, the contact angle was measured, at room temperature, using two methods: sessile drop and captive bubble. For the sessile drop method, dry hydrogel disks with 10-12 mm diameter were used. The hydrogels were carefully dried in the oven at 50ºC for 72 hours, in order to remove as much quantity of water as possible. After that, the contact angle was measured, placing drops of 3-5 µL of DD water with a micrometric syringe, on the surface of the hydrogel (Figure 23). For further calculations of hydrogels' surface energy, it was necessary to measure the contact angle of a non-polar liquid. Diiodomethane was the chosen liquid and it was followed the same procedure referred above. After placing the drop on the hydrogel's surface, a set of images was recorded. A video camera (JAI CV-A50) attached to a microscope (Wild M3Z) was used for the image acquisition and the video signal was transmitted to a frame grabber (Data Translation DT3155). For each type of hydrogel analysed, at least 10 drops were monitored for 1 minute, being obtained 14 images along the time for each drop. This time was chosen because, according to preliminary tests, the volume and radius of drops did not vary much over time.

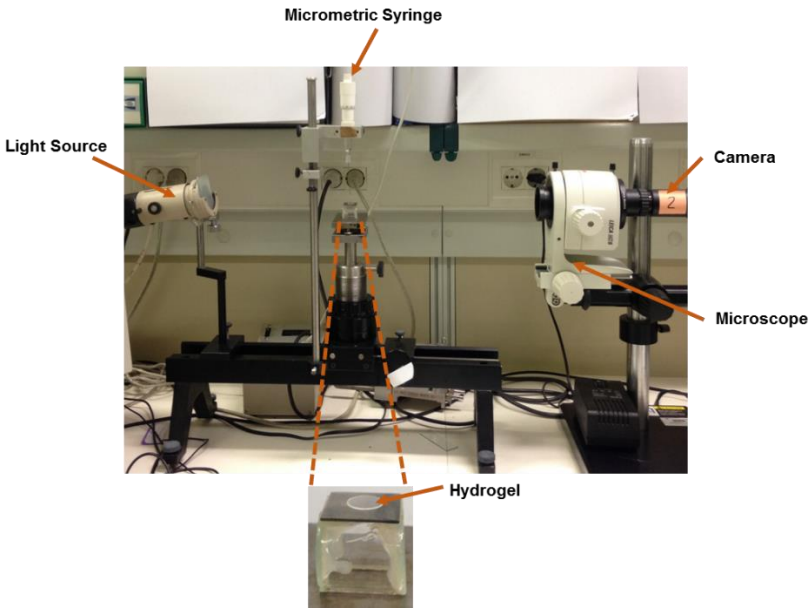


**Figure 23 -** Apparatus for the sessile drop method.

For the contact angle determination using the captive bubble, hydrogels in their swollen state were glued to a plastic support and then placed downwards in a liquid cell with quartz windows, which was full of DD water (Figure 24). Then, with the help of a micrometric syringe with an inverted needle, an air bubble of approximately 3-5 μL was placed on the hydrogel's inferior surface. In this experiment at least 10 air bubbles were recorded for 1 minute. Again, 14 images were obtained along the time for each bubble.

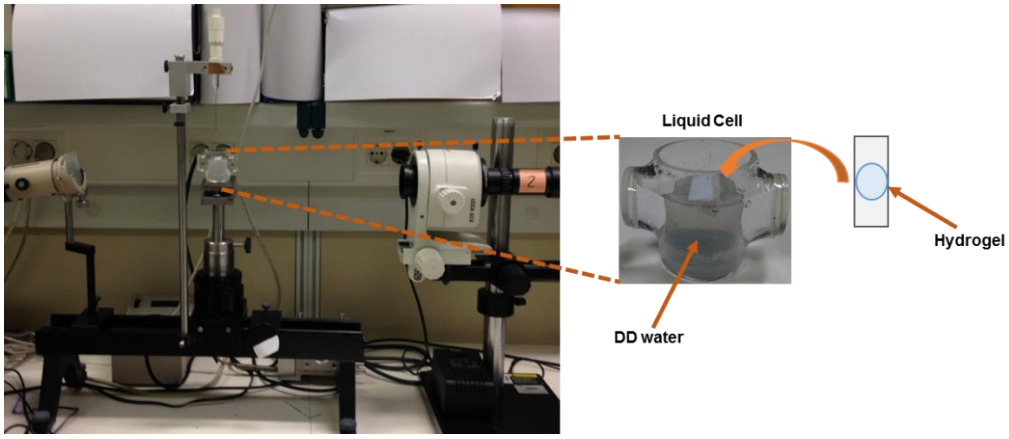


**Figure 24 -** Apparatus for the captive bubble method.

The image analysis was then performed, using the ADSA-P software (Axisymmetric Drop Shape Analysis Profile), which relates the Laplace's capillary equation (Equation 25) with the profile of the bubble:

$$\Delta P = \gamma \left( \frac{1}{R_1} + \frac{1}{R_2} \right) \quad \textbf{(25)}$$

where ΔP is the difference of pressure in the interface air/liquid, γ is the surface tension of the liquid, $R_1$ and $R_2$ is the main curvature radius of the bubble which are related with the contact angle by geometrical relations [102].

#### 2.2.3.5 Morphology

To access the hydrogels' surface morphology, SEM images were taken. Initially, the samples were hydrated in DD water and then carefully cleaned with an absorbent paper. Then, the samples were dried at 36ºC for 3 days, to take out the water of the hydrogel as much as possible. After drying the samples, they were coated with a thin gold layer using the equipment Q150T ES from Quarum Technologies. The samples were then analysed using a Field Emission Gun (FEG) SEM JEOL JSM-7001, and images from the different types of hydrogels were obtained with various magnifications: 3 000x, 10 000x, and 20 000x. Both, gold coating and SEM analysis, were done in the MicroLab, Electron Microscopy Laboratory of Instituto Superior Técnico.

#### 2.2.3.6 Mechanical Properties

Various tests can be done in order to study the mechanical properties of hydrogels. In this work, tensile tests were performed, according to what was described in the previous section. Through this type of test, it is possible to easily estimate the Young's modulus of hydrogels and other mechanical properties. The mechanical tests were done in Physics of Food Laboratory at Instituto Superior de Agronomia, using a TA.XT*plus* Texture Analyser equipment and the software *Exponent* for data collection.

For this experiment, the hydrogels were cut in strips with the following dimensions:

- Width: 5 mm
- Gauge length: ≈10 mm
- Thickness: 0.4-0.6 mm

These strips were previously hydrated in DD water and maintained in their swollen state during the whole experiment. Before the tests, it was necessary to calibrate the equipment in order to ensure the accuracy of the measurements. The calibration was made using weights adequate to the load cell used. The load cell is attached to the equipment (Figure 25) and measures the force in tension during the tensile tests. For this experiment, a load cell of 5 kg was used and for the calibration it was used a 1 kg weight that was placed in the calibration plate.

For the measurements, each strip was fixed between two clamps in the sample testing area, at the top and at the bottom (Figure 25). Sandpaper was used to prevent the hydrogel from slipping during the test. After placing the hydrogel in the equipment, an adjustment was made to maintain the hydrogel stretched at the beginning of the test, with the help of the control panel. The test conditions were introduced in the software *Exponent*. The test speed used was 0.3 mm $s^{-1}$ and the trigger force was 0.005 N. Then, the test started and the data were collected until the hydrogel broke. These experiments were performed at room temperature (≈20ºC). Six strips of each type of hydrogel were tested.

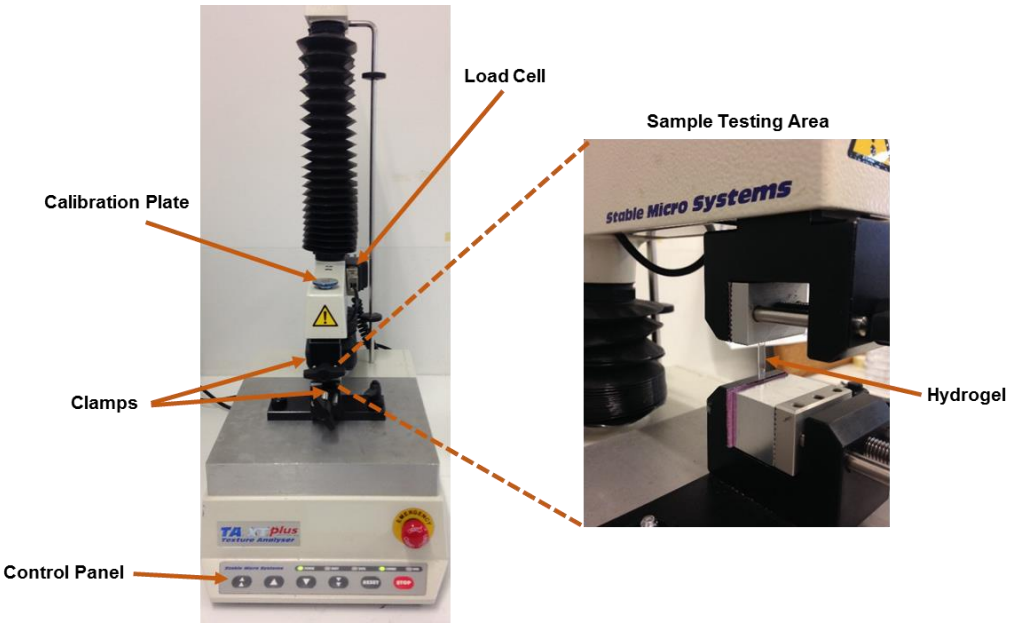


**Figure 25 -** Schematic representation of a tensile test apparatus.

From *Exponent,* it was exported the following data:

- Force applied in the hydrogel, in N, at every 5 milliseconds;
- The length variation of the sample, in mm, at every 5 milliseconds.

The data analysis was done using the software *Excel*. A stress-strain graphic was drawn, using the data from *Exponent* and the dimensions of each hydrogel (width, gauge length and thickness). For the determination of stress, it was used the Equation 21 (last section) taking into account the measured force, F, in N, and the values of width and thickness of the hydrogels to calculate the initial area, $A_0$. For the determination of the strain (Equation 22 from last section), it was used the gauge length, $L_0$, of each hydrogel and the length variation of the sample at each instant, from the *Exponent*. Then, from the first part of the graphic (elastic region) it was taken the slope of the curve, which corresponds to the Young's modulus. The average of the values obtained for the different samples of each type of hydrogel was calculated.

From this experiment, it was also possible to obtain other information about the hydrogels' mechanical properties, such as, tension at break, elongation at break and toughness. To obtain the values of tension and elongation at break, it was necessary to identify the last point before the break in the stress-strain plot. The x coordinate of that point corresponds to the elongation at break and the y coordinates corresponds to the tension at break. From the values obtained in independent experiments, the average tension at break and elongation at break for each type of hydrogel studied was calculated. For the determination of the toughness, which corresponds to the area under the stress-strain graphic, the software *TableCurve 2D 5.0* was used. With this software it was possible to adjust an appropriate equation to each curve and then to integrate this equation. Again, the average toughness for each type of hydrogel was calculated.

# 3 Results and Discussion

## 3.1 The Effect of the Amount of the Crosslinker

In the first set of experiments, it was studied the role of the crosslinker EGDMA on the hydrogels' properties. TRIS-based hydrogels with the composition TRIS/NVP/HEMA (36.8/41.8/21.5, V/V/V %), were prepared varying only the quantity of the crosslinker in the mixture. Initially, it was prepared one hydrogel with the normal quantity of the crosslinker (1x EGDMA) and then another three hydrogels were made increasing twofold, fourfold and eightfold the amount of the crosslinker. Table 5 presents the four hydrogels produced. The last column is in color red to show what was varied in this study. The nomenclature adopted for these hydrogels was based in the amounts of EGDMA that were added in each hydrogel.

**Table 5 –** Compositions, in V/V %, of the TRIS-based hydrogels with different amounts of EGDMA.

| Material / Name | TRIS | NVP | HEMA | EGDMA |
|---|---|---|---|---|
| **1x EGDMA** | 36.8 | 41.8 | 21.5 | 0.64 |
| **2x EGDMA** | 36.8 | 41.8 | 21.5 | 1.28 |
| **4x EGDMA** | 36.8 | 41.8 | 21.5 | 2.56 |
| **8x EGDMA** | 36.8 | 41.8 | 21.5 | 5.13 |

### 3.1.1 Drug Release

Drug release tests were performed in order to understand the effect of increasing EGDMA in the release kinetics. In these tests the drug chosen was diclofenac. The experimental conditions for drug loading and release were referred in section 2.2.2. Figure 26 shows the cumulative diclofenac release profiles. The increase of the amount of EGDMA in the hydrogel leads to a decrease in the cumulative diclofenac release. This is an expected result because with the increase of the amount of crosslinker, the hydrogels' mesh becomes tighter, making more difficult the entry and exit of the drug [103]. Despite the increased amount of crosslinker in the hydrogels 2x EGDMA and 4x EGDMA, no significant differences are seen between the two cumulative diclofenac releases. However, in 8x EGDMA the hydrogel's mesh was so tight that the loading and the release were much reduced. All hydrogels showed an initial burst in the first 24 hours and the kinetics of release was not improved.

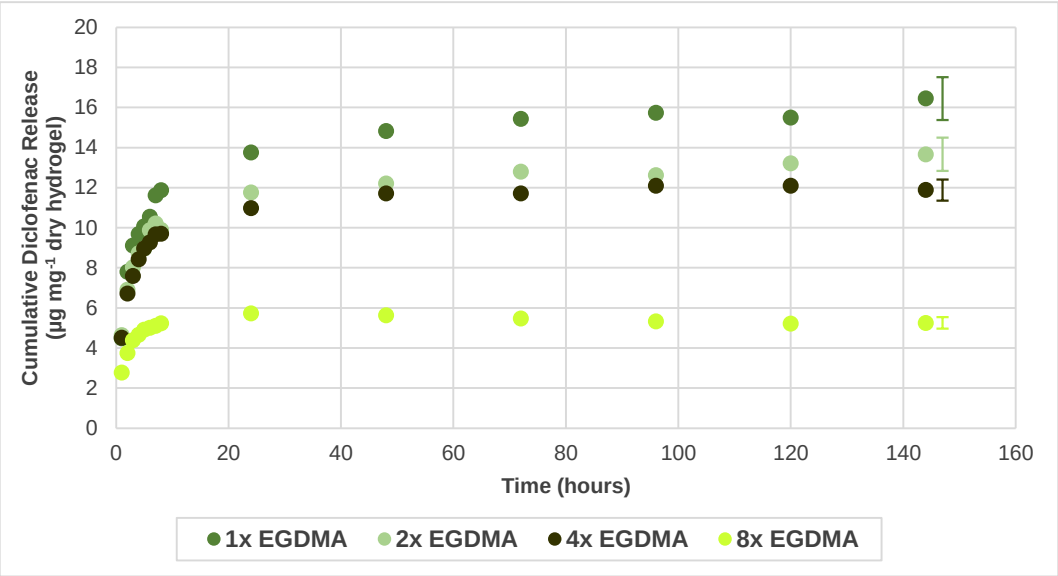


**Figure 26 -** Cumulative diclofenac release from TRIS-based hydrogels with different amounts of crosslinker (EGDMA). The error bars correspond to the mean standard deviation.

### 3.1.2 Transmittance

Hydrogels to be used as $CL_s$ need to be transparent in order to ensure that wearers' vision is not affected. Transmittance measurements were performed in the range of the visible light (400-700 nm). Hydrogels are suitable for the use as $CL_s$ when the transmittance is above 90% [43]. Observing Figure 27, all the transmittance values are above the minimum accepted value.

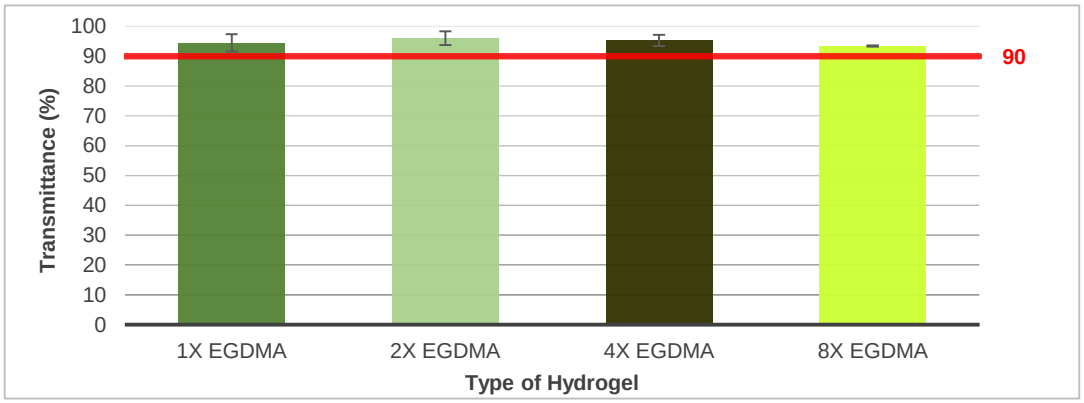


**Figure 27 -** Transmittances of the TRIS-based hydrogels with different amounts of the crosslinker (EGDMA). The error bars correspond to the standard deviation.

### 3.1.3 Ionic Permeability

Ionic permeability is an important parameter which determines the lens motion as well as its adherence to the cornea. It is expressed as $D_{ion}$ and according to Nicolson et al., the minimum value accepted to have an adequate on-eye movement is $1.5\times10^{-6}$ $mm^2$ $min^{-1}$ [65]. In Figure 28 the ionic permeability values for the different hydrogels compositions are presented. When the amount of EGDMA increases, the value of $D_{ion}$ decreases. Since the hydrogels' mesh size decreases, the ions have more difficulty to pass through the matrix, leading to lower $D_{ion}$ values. This tendency is in agreement with the previous results of the drug release experiments. Also, all the values are above the minimum accepted value.

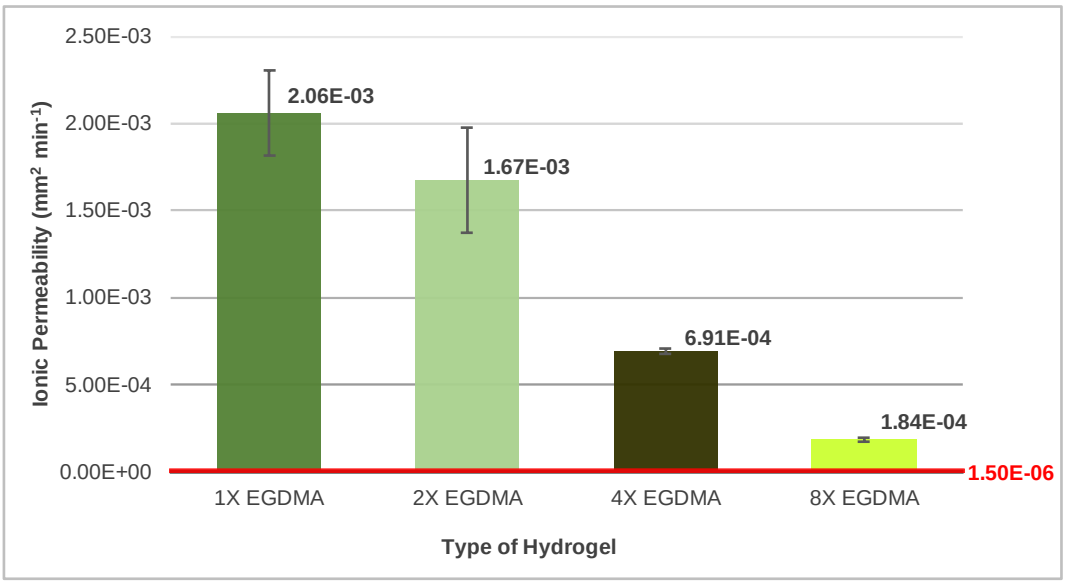


**Figure 28 -** Ionic permeability of the TRIS-based hydrogels with different amounts of crosslinker (EGDMA). The error bars correspond to the standard deviation.

### 3.1.4 Swelling

The swelling capacity of hydrogels depends on the crosslinking ratio and is usually related to the drug loading and release capacity of the hydrogels' matrix [104]. Hydrogels' structures with higher amounts of crosslinker tend to swell less because the mesh is tighter [104]. Observing Figure 29, one may conclude that the increase of the amount of EGDMA led to a decrease in the swelling percentage of the hydrogels, as expected.

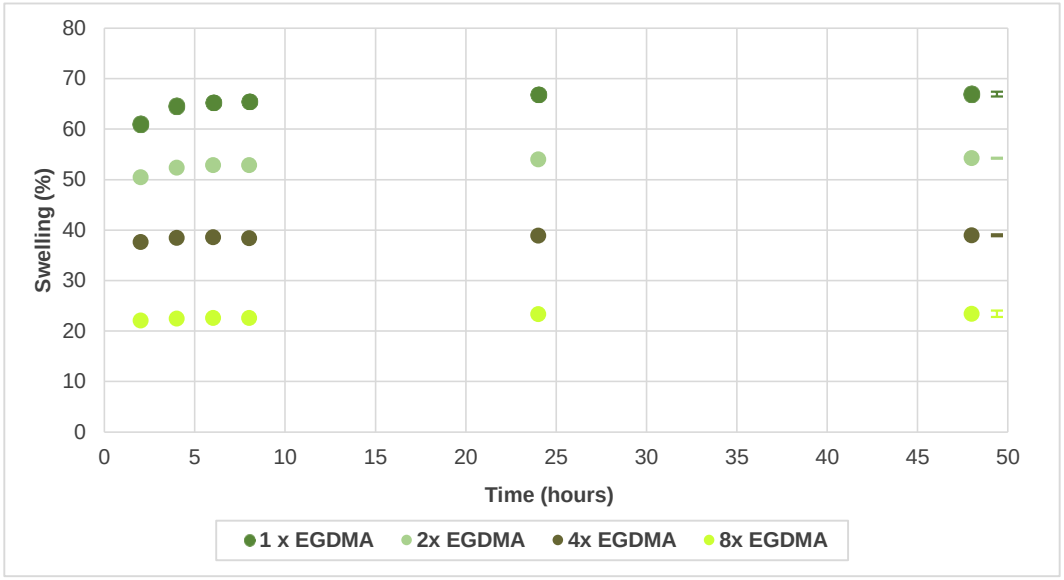


**Figure 29 –** Swelling results of TRIS-based hydrogels with different amounts of crosslinker (EGDMA). The error bars correspond to the mean standard deviation.

It is possible to conclude from the above results that the drug release behaviour, ionic permeability and swelling are directly related: when the amount of crosslinker increases, the cumulative diclofenac release, the ionic permeability as well as the swelling percentage decrease.

## 3.2 Study of Different Compositions of TRIS-based Hydrogels

In this part of the work, the goal was to try different compositions of TRIS-based silicone hydrogels in order to understand better the role of each component. In order to achieve that, several hydrogels were prepared by varying the amount of the components TRIS, HEMA, and NVP, while keeping a fixed quantity of EGDMA (4.7 mM, the same as in 1x EGDMA) and AIBN (6.7 mM). In Table 6, the compositions of the different hydrogels produced in this stage are presented. The nomenclature adopted to identify these hydrogels was TRIS (from TRIS-based hydrogels) followed by the used volumes (in percentage) of TRIS, NVP and HEMA.

**Table 6 –** Compositions, in V/V %, of the TRIS-based hydrogels and the respective visual transparency after the polymerization reaction.

| Material / Name | TRIS | NVP | HEMA | Transparency |
|---|---|---|---|---|
| **TRIS 34 50 16** | 34 | 50 | 16 | Transparent |
| **TRIS 37 45 16** | 37 | 45 | 18 | Transparent |
| **TRIS 38 43 19** | 38 | 43 | 19 | Transparent |
| **TRIS 36.8 41.8 21.5** | 36.8 | 41.8 | 21.5 | Transparent |
| **TRIS 50 40 10** | 50 | 40 | 10 | Transparent |
| **TRIS 43.3 35 21.7** | 43.3 | 35 | 21.7 | Opaque |
| **TRIS 50 30 20** | 50 | 30 | 20 | Opaque |
| **TRIS 50 20 30** | 50 | 20 | 30 | Opaque |
| **TRIS 60 10 30** | 60 | 10 | 30 | Opaque |

As can be seen in Table 6, some hydrogels became opaque, after the polymerization reaction, suggesting that phase separation had occurred (Figure 30). The phase separation happens when cohesive interactions between chemically related molecules are stronger than adhesive interactions between chemically distinctive molecules [47]. Looking at Table 6, it is concluded that it is necessary to have a minimum amount of NVP to have transparent hydrogels, which is 40 (V/V %). For the drug release tests and further properties studies, only the transparent hydrogels (first five compositions in the Table 6) were considered because they are the ones that can ensure, a good optical performance.

**Figure 30 -** Example of a hydrogel that became opaque after the polymerization reaction.

### 3.2.1 Drug Release

Drug release tests were performed with the transparent TRIS-based hydrogels to see if the changes in the amount of each material cause alterations in their behaviour. Figure 31 shows that the cumulative diclofenac release increases with the amount of NVP. An explanation for this result is the fact that NVP is a super water absorbent material, leading to high quantities of drug loaded into the hydrogel [105]. An initial burst occurred in the first 24 hours and then, a plateau is achieved.

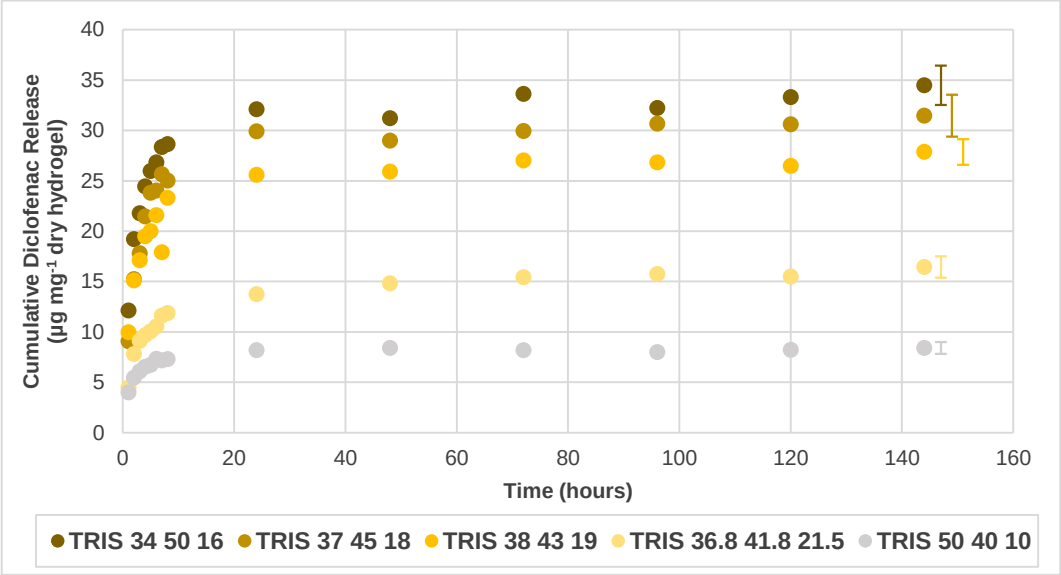


**Figure 31 -** Cumulative diclofenac release of the TRIS-based hydrogels. The error bars correspond to the mean standard deviation.

### 3.2.2 Transmittance

Even for the transparent hydrogels, it was necessary to determine their transmittance to see if they are suitable for the use as $CL_s$. Observing Figure 32, it can be seen that all transmittance values are above 90%.

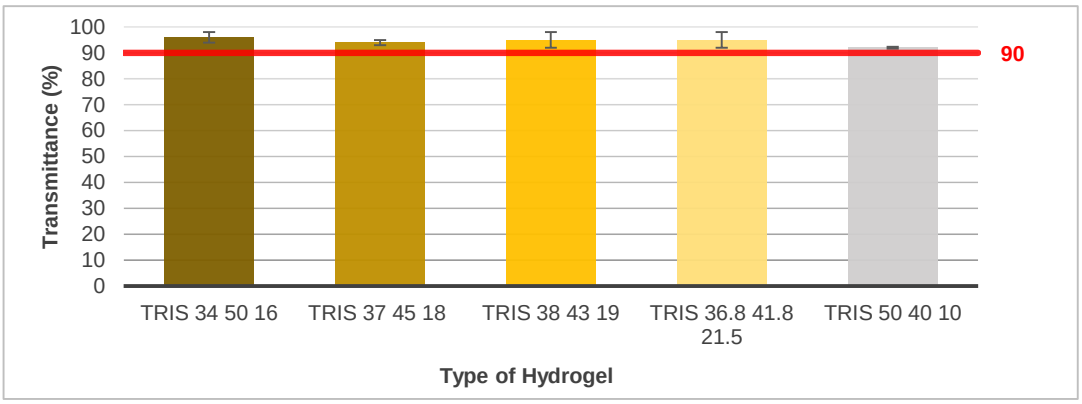


**Figure 32 -** Transmittance of the TRIS-based hydrogels. The error bars correspond to the standard deviation.

### 3.2.3 Ionic Permeability

Observing Figure 33, it was concluded that the ionic permeability values of the TRIS-based hydrogels increase with the amount of NVP and are all above the minimum accepted value.

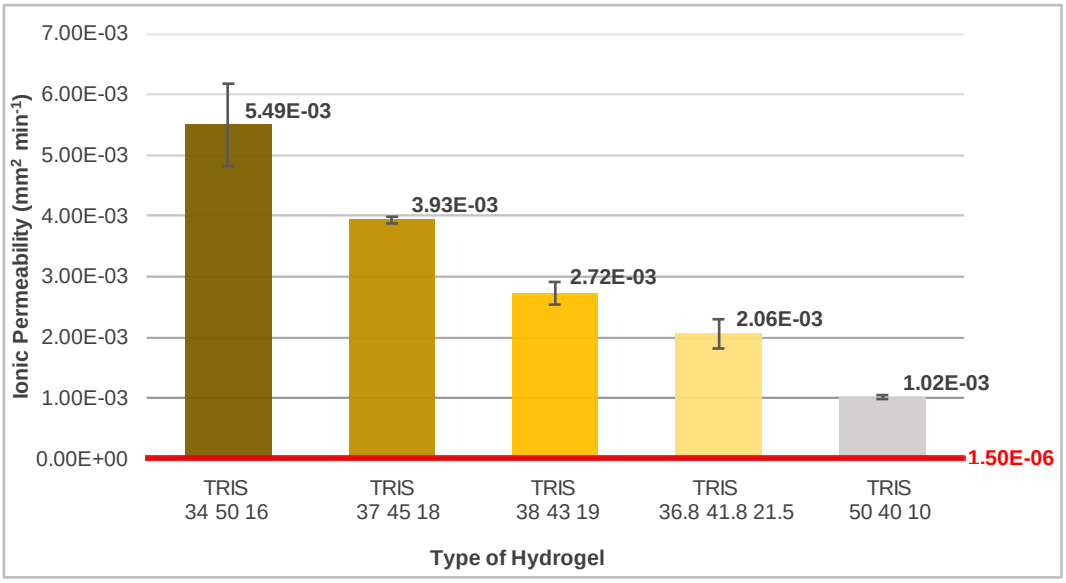


**Figure 33 -** Ionic permeability of the TRIS-based hydrogels. The error bars correspond to the standard deviation.

### 3.2.4 Swelling

Due to the known water absorbance capacity of NVP, it is expected that hydrogels with higher amounts of NVP have higher swelling percentages. The swelling results presented in Figure 34 confirm this expectation. In fact, when the amount of NVP increases, the swelling percentage of the hydrogels also increases. However, this variation is less significant when the percentage of NVP is above 41.8%.

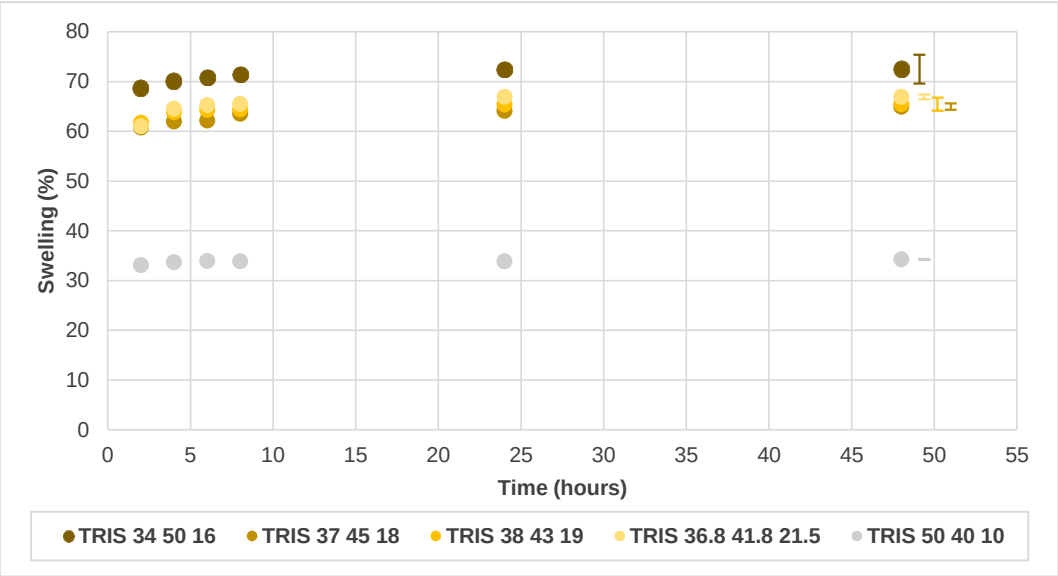


**Figure 34 -** Swelling results of the TRIS-based hydrogels. The error bars correspond to the mean standard deviation.

The results obtained for the TRIS-based hydrogels showed a relationship between the cumulative diclofenac release, ionic permeability and swelling capacity. The increase in the amount of NVP induces an increase in the three parameters aforementioned; however, these variations are not directly proportional. For example, the increase in the cumulative diclofenac release when the amount of NVP increases from 41.8 to 43, corresponds to a negligible variation in the swelling percentage

## 3.3 The Role of the Hydrophobic Materials (TRIS and mPDMS)

The goal here was to compare the effect of two different hydrophobic compounds (TRIS and mPDMS) on the hydrogels' properties and drug release behaviour. In these formulations the amounts of TRIS and mPDMS were inversely changed, keeping constant (≈40%) the total amount of these hydrophobic components. It was added a new material, SiGMA, for the solubilisation of the hydrophilic monomers with the hydrophobic compounds to prevent the phase separation. In Table 7 the composition of the different hydrogels is presented: the red columns refer to the varying amounts of TRIS and mPDMS. It is important to refer that, as in the previous section, it was used a fixed quantity of EGDMA (4.7 mM) and AIBN (6.7 mM) in all formulations. The nomenclature adopted for this type of hydrogels was based on the components of variable composition (TRIS and mPDMS).

**Table 7 –** Compositions, in V/V %, of the different hydrogels by varying the amount of the hydrophobic components (TRIS and mPDMS).

| Material / Name | TRIS | mPDMS | SiGMA | NVP | HEMA |
|---|---|---|---|---|---|
| **mPDMS 36.7** | - | 36.7 | 40 | 5 | 18.3 |
| **TRIS 10 mPDMS 30** | 10 | 30 | 40 | 5 | 15 |
| **TRIS 20 mPDMS 20** | 20 | 20 | 40 | 5 | 15 |

| | | | | | |
|---|---|---|---|---|---|
| **TRIS 30 mPDMS 10** | 30 | 10 | 40 | 5 | 15 |
| **TRIS 35 mPDMS 5** | 35 | 5 | 40 | 5 | 15 |

### 3.3.1 Drug Release

Looking at Figure 35, it is possible to conclude that despite the low differences, with the increase in the amount of mPDMS, the cumulative diclofenac release also increases. Surprisingly, the substitution of TRIS by mPDMS, which is more hydrophobic [101] leads to a higher drug loading and, consequently, drug release. This demonstrates that the behaviour of the hydrogels is not only determined by the hydrophilicity/hydrophobicity of the monomers.

Comparison with data in Figure 31 relative to TRIS-based hydrogels reveals that, more important than the ratio PDMS/TRIS is the use of SiGMA instead of NVP: even with low quantities of mPDMS (5%), the presence of SiGMA in high quantities (40%) decreases significantly the diclofenac release.

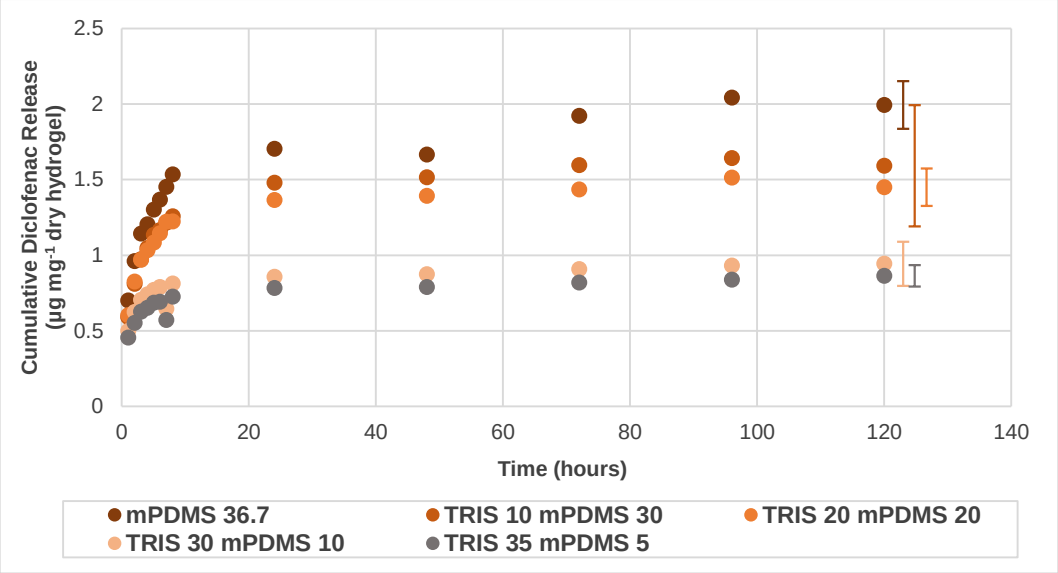


**Figure 35 –** Cumulative diclofenac release of the hydrogels where the amount of the hydrophobic materials (TRIS and mPDMS) was varied. The error bars correspond to the mean standard deviation.

### 3.3.2 Transmittance

Figure 36 shows the transmittance values of the five hydrogels. All of them are above 90%, indicating that they are suitable for the use as CLs.

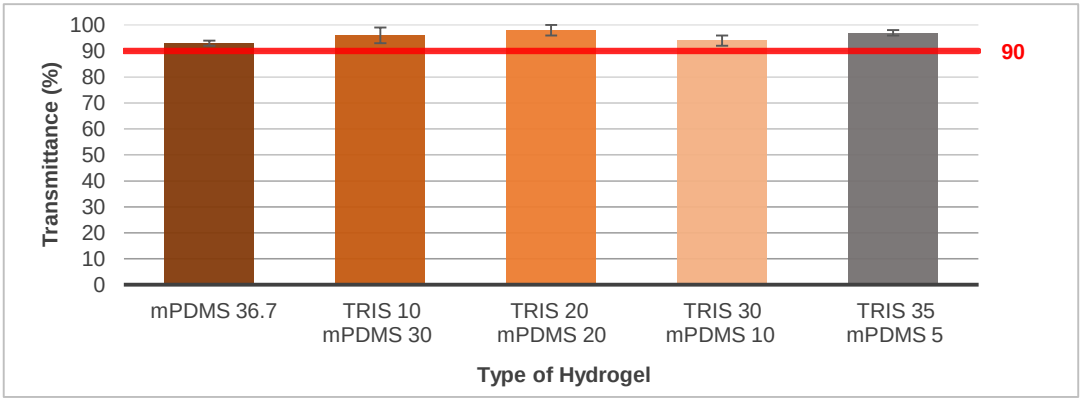


**Figure 36 -** Transmittance of the hydrogels where the amount of the hydrophobic materials (TRIS and mPDMS) was varied. The error bars correspond to the standard deviation.

### 3.3.3 Ionic Permeability

Figure 37 shows a tendency for the decrease of ionic permeability with the decrease in the amount of mPDMS, with the exception of mPDMS 36.7. These results are in accordance with the drug release behaviour because if less drug is loaded and released from the hydrogels, less ions are expected to pass through the hydrogels' matrix. These hydrogels showed a much lower ionic permeability (Figure 37) in comparison with the TRIS-based hydrogels (Figure 33), probably due to the substitution of NVP by SiGMA. Despite being low, these values are all above the minimum accepted value. The error bars in Figure 37, although they seem large, in comparison with the hydrogels above, they are of the same order of magnitude.

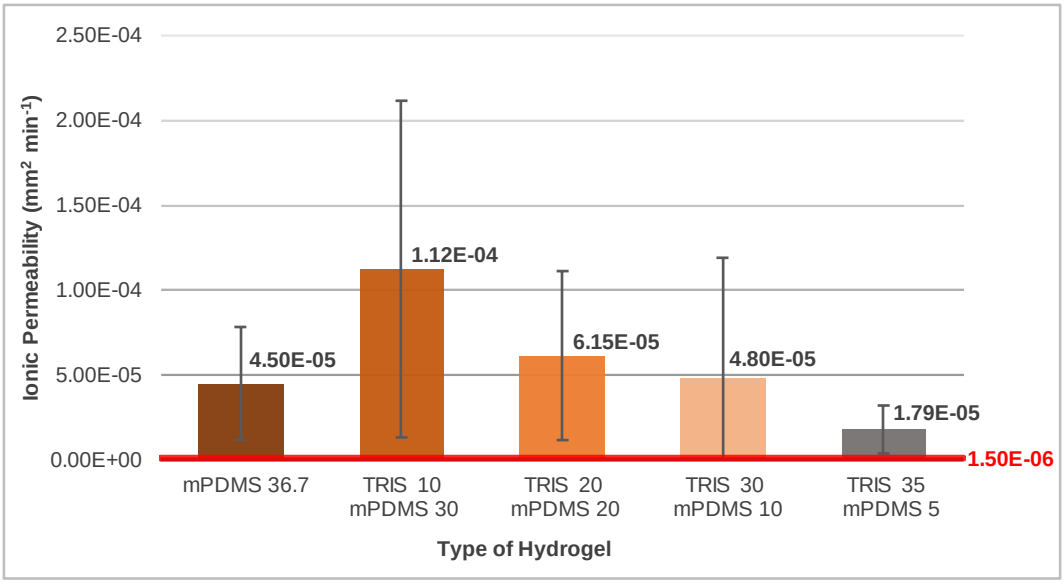


**Figure 37 -** Ionic permeability results of the different hydrogels where the amount of the hydrophobic materials (TRIS and mPDMS) was varied. The error bars correspond to the standard deviation.

### 3.3.4 Swelling

Observing Figure 38, one concludes that swelling decreases with the decrease of the mPDMS amount. The presence of SiGMA, with a significant reduction of the NVP content, compared to the TRIS-based

hydrogels (Figure 34) lead to a decrease in the swelling percentages. Since NVP is a super water absorbent monomer this result is expectable [105].

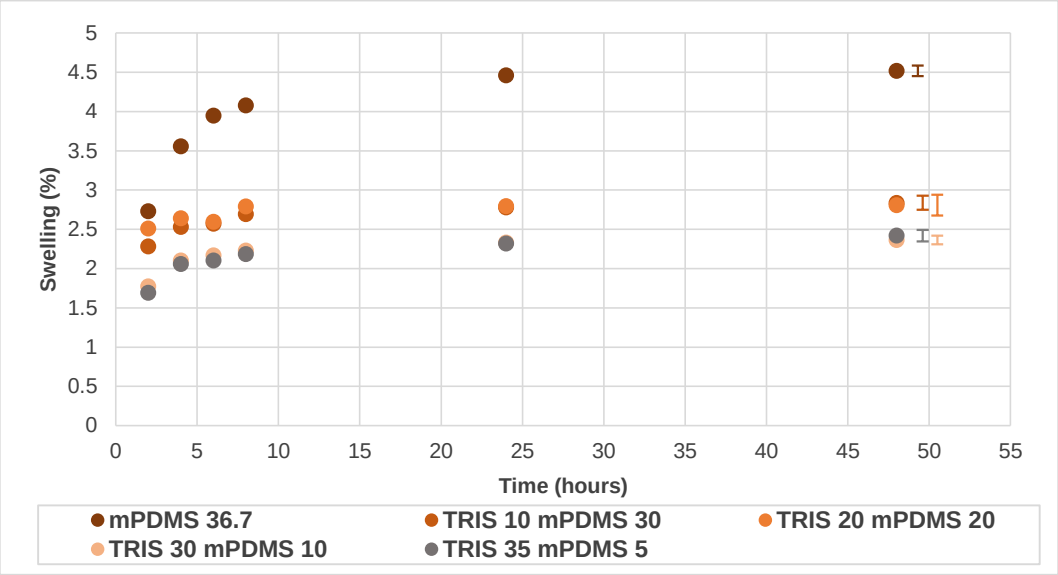


**Figure 38 –** Swelling results of the hydrogels where the amount of the hydrophobic materials (TRIS and mPDMS) was varied. The error bars correspond to the mean standard deviation.

The results obtained in this section prove that a correlation may be established between the amount of mPDMS and cumulative diclofenac release, ionic permeability (except in mPDMS 36.7) and swelling.

## 3.4 The Role of the Hydrophilic Materials (DMA and HEMA)

The aim of the production of the following hydrogels was to study the role of two different hydrophilic compounds: DMA and HEMA. Table 8 shows the hydrogels composition; in one hydrogel half of the amount of NVP was substituted by SiGMA in order to compare the role of these two components. A fixed quantity of EGDMA (4.7 mM) and AIBN (6.7 mM) was used. The nomenclature adopted for this type of hydrogels was based on the materials which the amount was changed.

In this subchapter, the hydrogel DMA 20 will be compared with the TRIS 36.8 41.8 21.5, where the major difference is the substitution of the hydrophilic monomer DMA by HEMA. This comparison can help to understand if this substitution has an impact on the drug release behaviour or other properties of the hydrogels.

**Table 8 –** Compositions, in V/V %, of the hydrogels where mainly the amount of the hydrophilic materials (DMA and HEMA) was varied.

| Material / Name | TRIS | SiGMA | NVP | DMA | HEMA |
|---|---|---|---|---|---|
| **DMA 20** | 40 | - | 40 | 20 | - |
| **SiGMA 20 DMA 20** | 40 | 20 | 20 | 20 | - |
| **DMA 10 HEMA 10** | 40 | - | 40 | 10 | 10 |

### 3.4.1 Drug Release

Observation of Figure 39 shows that, when the amount of DMA decreases, being partially substituted by HEMA, the cumulative diclofenac release also decreases. Also, the substitution of half of NVP by SiGMA in SiGMA 20 DMA 20 decreases approximately three times the cumulative diclofenac release, which may be attributed to the significant reduction in the content of the hydrophilic monomer NVP. Comparison of the hydrogels with composition DMA 20 and TRIS 36.8 41.8 21.5 (Figure 31), shows that the cumulative diclofenac release is much higher in the former, suggesting that DMA might be more hydrophilic than HEMA, which favours drug loading and release. This conclusion is in accordance with the data of Mark [105], who found that polymers prepared with DMA are considered super water absorbent, absorbing several times their weight in water.

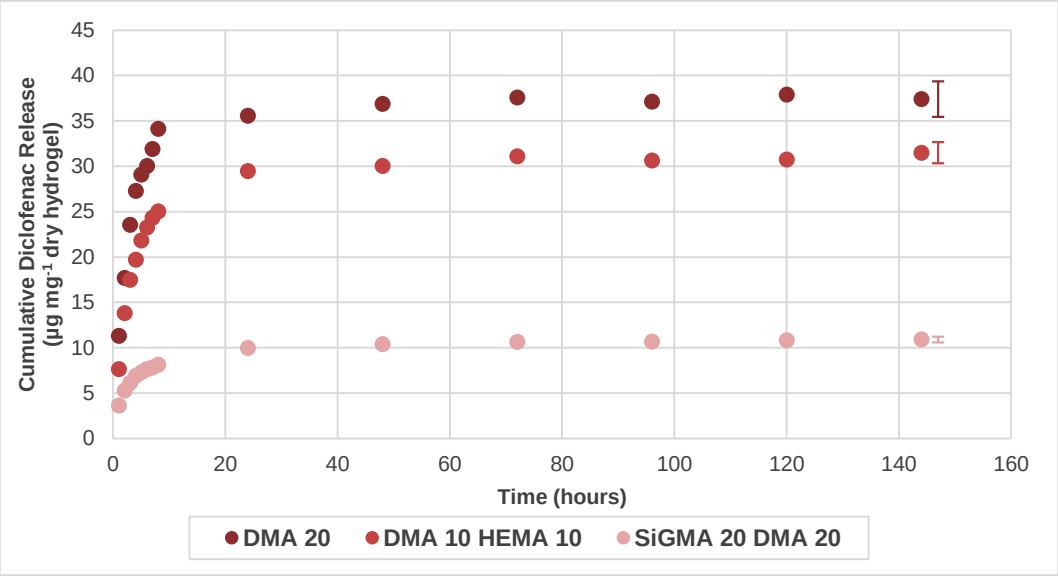


**Figure 39 -** Cumulative diclofenac release of the hydrogels where mainly the amount of the hydrophilic materials (DMA and HEMA) was varied. The error bars correspond to the mean standard deviation.

### 3.4.2 Transmittance

The transmittance for the three hydrogels, shown in Figure 40, is above the minimum accepted value. Another important consideration regarding these hydrogels is that their transmittance percentages are the highest, comparing with the other hydrogels.

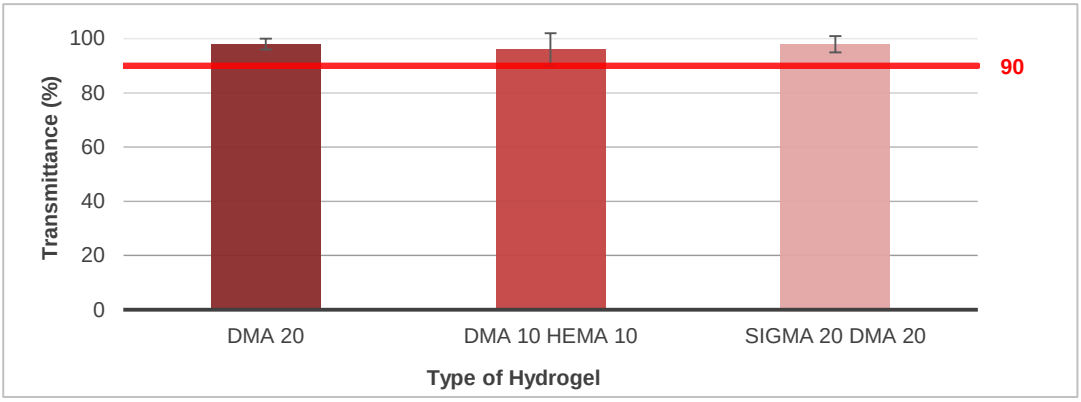


**Figure 40 –** Transmittance of the hydrogels where mainly the amount of the hydrophilic materials (DMA and HEMA) was varied. The error bars correspond to the standard deviation.

### 3.4.3 Ionic Permeability

Analysis of the ionic permeability results obtained for these type of hydrogels (Figure 41) reveal that, the decrease in the amount of DMA from 20% to 10% (V %) leads to a decrease in the $D_{ion}$ values. As expected, the value of the ionic permeability of the DMA 20 hydrogel is higher than that of the hydrogel TRIS 36.8 41.8 21.5 (see Figure 33), since the cumulative diclofenac release is also higher in the former one.

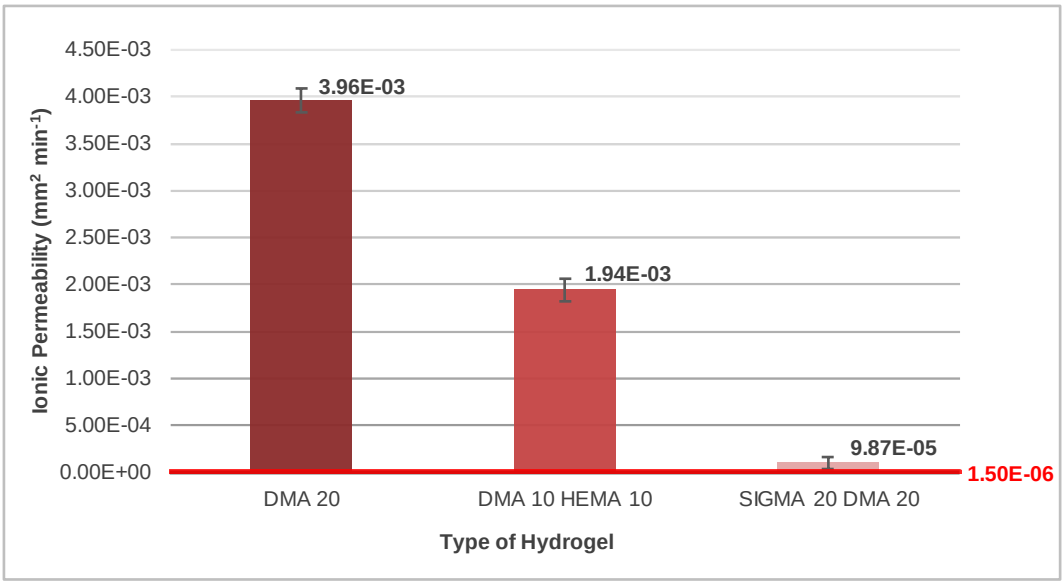


**Figure 41 -** Ionic Permeability of the hydrogels where mainly the amount of the hydrophilic materials (DMA and HEMA) was varied. The error bars correspond to the standard deviation.

### 3.4.4 Swelling

The swelling results presented in Figure 42 show the same tendency as the drug release and ion permeability: the hydrogels with higher amounts of DMA have higher percentages of swelling. The hydrogel DMA 20 after immersion in water almost doubled its weight proving the good capacity of DMA to absorb water. The hydrogel SiGMA 20 DMA 20 has the lowest swelling percentage, showing that the addition of SiGMA leads to a significant decrease in the water absorbed by the hydrogel. Comparison of the DMA 20 with the TRIS 36.8 41.8 21.5 (Figure 34 and Figure 42) confirms that the presence of

DMA is responsible for higher water absorption. This is an important result because when it would be necessary to increase the water content in hydrogels, the use of more hydrophilic monomers, like DMA, can be an option.

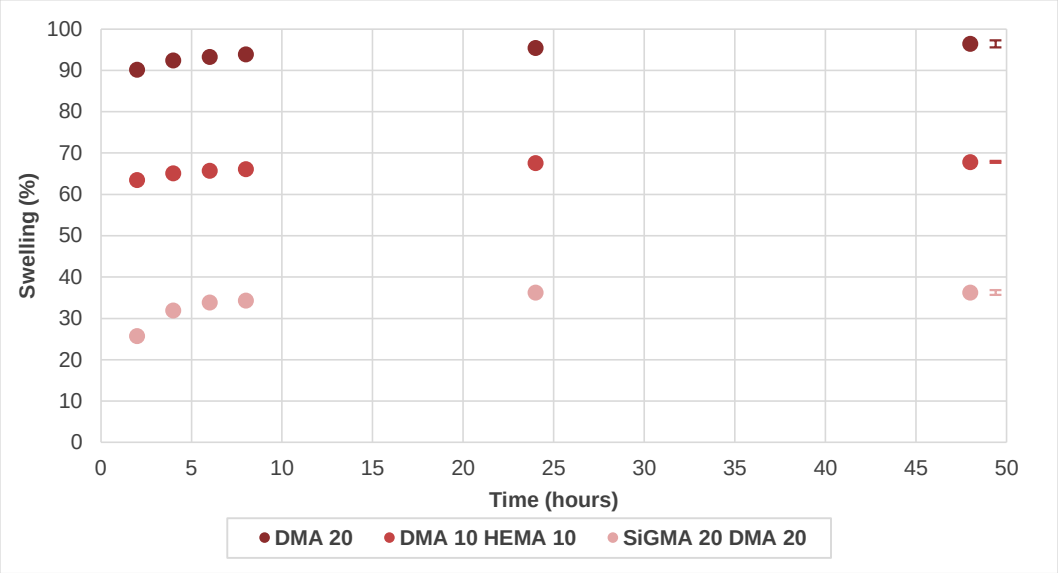


**Figure 42 –** Swelling results of the hydrogels where mainly the amount of the hydrophilic materials (DMA and HEMA) was varied. The error bars correspond to the mean standard deviation.

Again, a positive correlation between the cumulative diclofenac release, ionic permeability and swelling capacity is observed.

## 3.5 mPDMS/DMA-based Hydrogels

The goal in this part of the work was to investigate if hydrogels using mPDMS, as the hydrophobic monomer, and DMA, as the hydrophilic monomer, instead of TRIS and HEMA, have a different behaviour concerning drug release among other properties. As a starting point, a volumetric composition similar to TRIS 36.8 41.8 21.5 was chosen, substituting TRIS by mPDMS and HEMA by DMA. Also, a large part of NVP was replaced by SiGMA, needed to guarantee the solubilisation of the silicone with the hydrophilic monomer, and avoid phase separation. In these hydrogels, fixed quantities of EGDMA (4.7 mM) and AIBN (6.7 mM) were used. The nomenclature adopted for these hydrogels was based in the amounts, in V/V %, used of the respective hydrophobic and hydrophilic monomers (mPDMS and DMA).

**Table 9 –** Compositions, in V/V %, of the hydrogels using mPDMS as the silicone monomer and DMA as the hydrogel monomer.

| Name \ Material | mPDMS | SiGMA | NVP | DMA |
|---|---|---|---|---|
| **mPDMS 36.7 DMA 18.3** | 36.7 | 40 | 5 | 18.3 |
| **mPDMS 36.7 DMA 28.3** | 36.7 | 30 | 5 | 28.3 |

### 3.5.1 Drug Release

Figure 43 shows that the increase in the amount of DMA together with the decrease in the amount of SiGMA lead to a higher cumulative diclofenac release. These results are in accordance with the results above described (section 3.3.1), where it was found that the increase of SiGMA led to a lower cumulative drug release. DMA, being highly hydrophilic, favours the drug release from the hydrogels. Unexpectedly, the cumulative diclofenac release of mPDMS 36.7 DMA 18.3 was approximately the same comparing to the hydrogel mPDMS 36.7 (Figure 35) which has the same composition, except that DMA was substituted by HEMA. In these cases, the differences in the hydrophilicity of DMA and HEMA do not have consequences on the drug release behaviour.

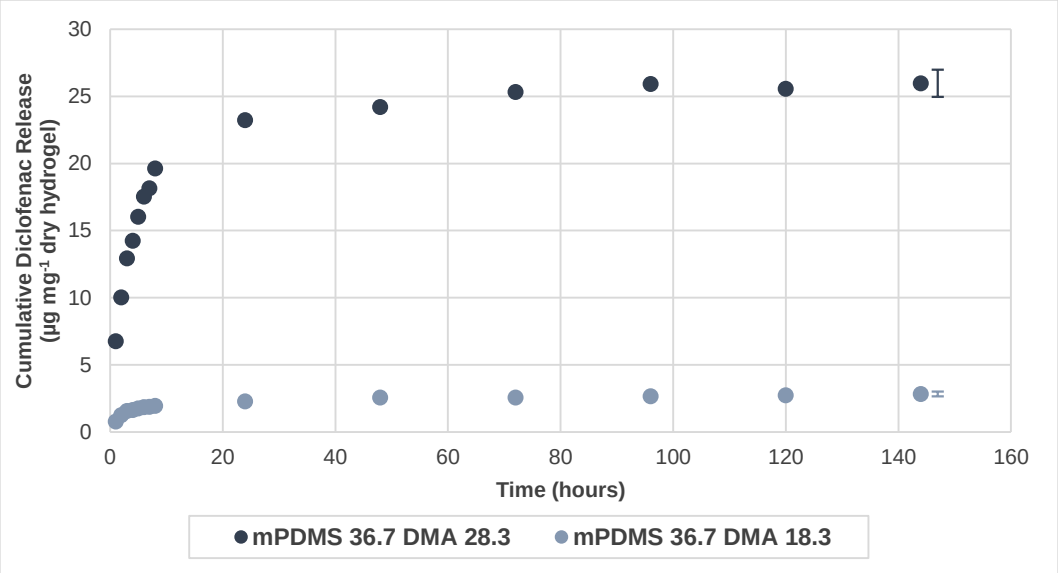


**Figure 43 -** Cumulative diclofenac release of mPDMS/DMA-based hydrogels. The error bars correspond to the mean standard deviation.

### 3.5.2 Transmittance

The transmittance of these two hydrogels was not affected by changing the composition. The two hydrogels presented transmittance percentages above 90%, proving they have the necessary transparency to be used as $CL_s$.

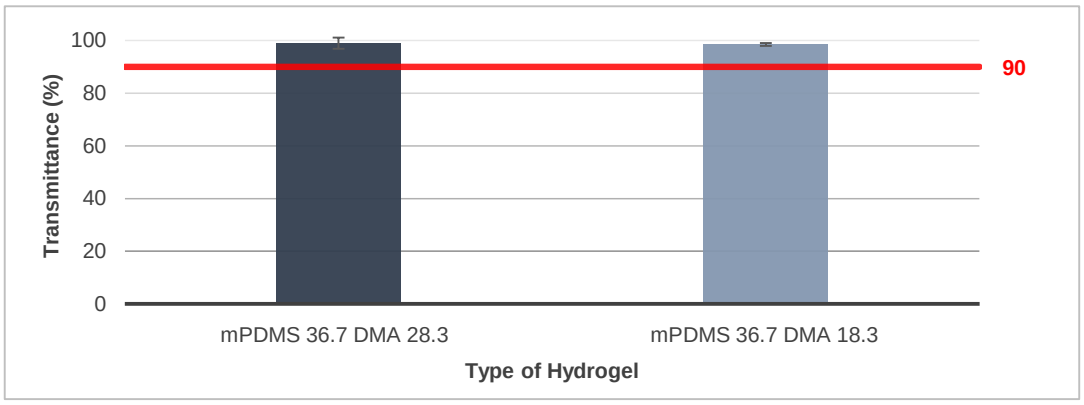


**Figure 44 -** Transmittance of mPDMS/DMA-based hydrogels. The error bars correspond to the standard deviation.

### 3.5.3 Ionic Permeability

The ionic permeability values are in accordance with the drug release tests, being mPDMS 36.7 DMA 28.3 the one with higher $D_{ion}$ (Figure 45), as expected. Also, both hydrogels have ionic permeability above the minimum value which is necessary to promote an adequate on eye movement.

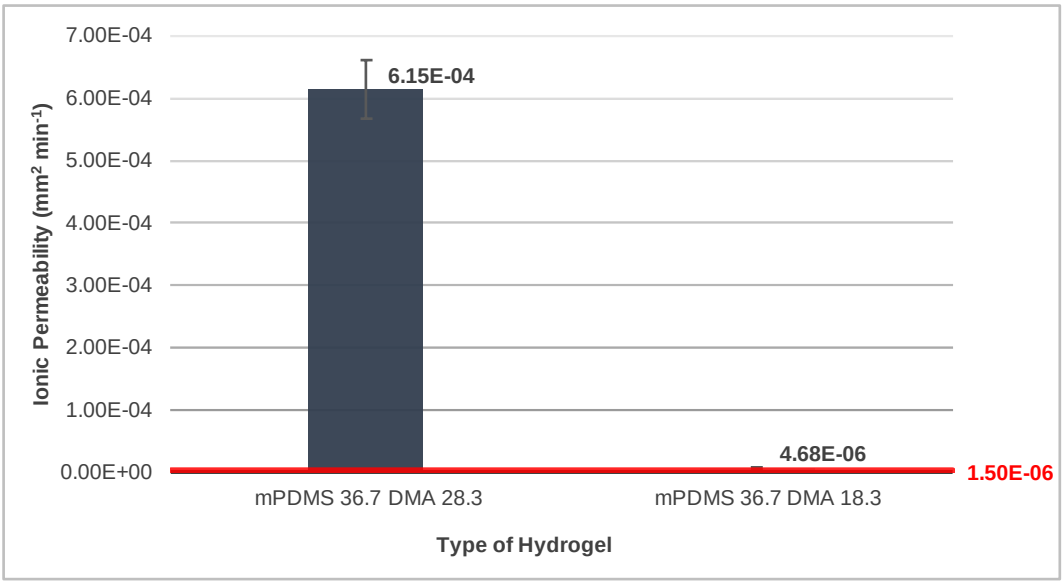


**Figure 45 -** Ionic permeability of mPDMS/DMA-based hydrogels. The error bars correspond to the standard deviation.

### 3.5.4 Swelling

mPDMS 36.7 DMA 28.3 showed a higher swelling percentage than mPDMS 36.7 DMA 18.3 due to the increase in the DMA content and decrease in the SiGMA content (Figure 46). Comparison between the hydrogels mPDMS 36.7 DMA 18.3 and mPDMS 36.7(Figure 38 and Figure 46), reveals a difference in the equilibrium swelling percentages: respectively ≈15% and ≈4.5%. Although, there is no significant difference between the drug release behaviour of these two hydrogels the use of DMA instead of HEMA results in a significant increase on the swelling percentage.

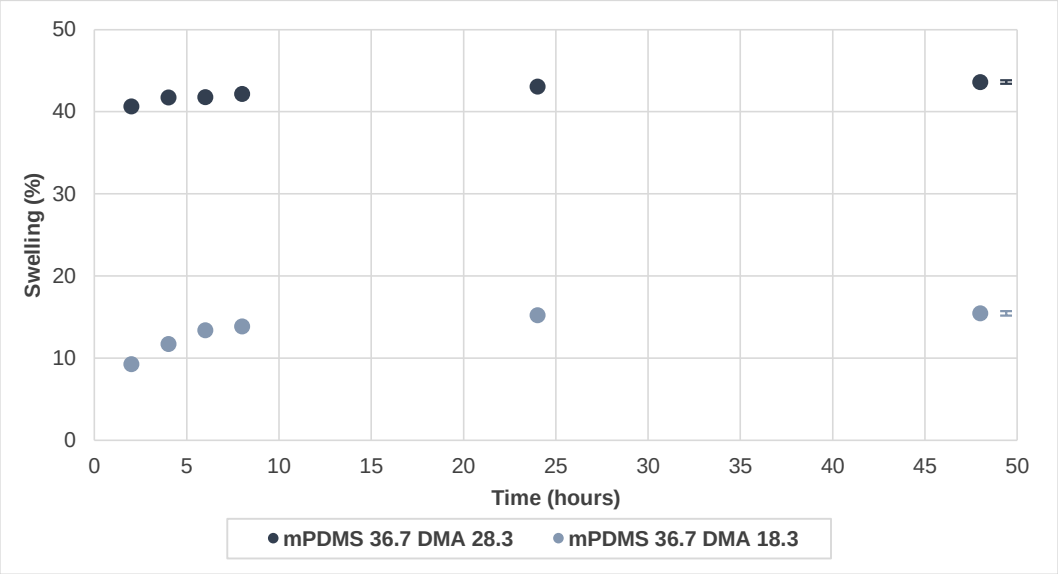


**Figure 46 –** Swelling results of mPDMS/DMA-based hydrogels. The error bars correspond to the mean standard deviation.

## 3.6 Study of Other Properties for the Most Relevant Hydrogels' Types

In this subchapter, it will be presented the results of further characterisation of the hydrogels with the best properties or that revealed a distinct behaviour, among those studied in the last sections. It will be analysed the drug release behaviour using a different drug, dexamethasone, and other properties including: diclofenac release at different loading temperatures, swelling capacity at different temperatures and media, wettability, surface energy, surface morphology, mechanical properties, states of water inside the hydrogels, and pore-size dimensions.

### 3.6.1 Drug Release with Dexamethasone

Further drug release studies were done using dexamethasone, a hydrophobic drug, and three hydrogels: TRIS 36.8 41.8 21.5, mPDMS 36.7, and DMA 20. The choice of these three samples had as objective the evaluation of eventual differences in hydrogels behaviour caused by the use of different hydrophobic (TRIS and mPDMS) and hydrophilic materials (DMA and HEMA). Since the solubility of this drug is quite low in aqueous mediums, two loading conditions were used: NaCl solution with a drug concentration of 0.08 mg $mL^{-1}$ and ethanol solution with a drug concentration of 1 mg $mL^{-1}$. In the mPDMS hydrogel, it was used only the loading with NaCl because, after loading with ethanol, the hydrogel became opaque.

The first conclusion which may be drawn from Figure 47, is that the cumulative dexamethasone release is higher in the hydrogels loaded with ethanol. The hydrogels containing DMA present a higher cumulative dexamethasone release compared with the other types. This result confirms the statement made above that DMA is more hydrophilic than HEMA, leading to a higher drug loading and, consequently, higher cumulative drug release. The mPDMS hydrogel showed a very low cumulative

dexamethasone release (Figure 47). Comparing with the cumulative diclofenac release of TRIS-based hydrogels (see Figure 31), the cumulative dexamethasone release is much lower. This result may have something to do with the fact that dexamethasone is very slightly soluble in aqueous solvents, preventing the loading and release of the drug [101]. The hydrophobic nature of dexamethasone may have also influenced the lower cumulative releases of these hydrogels [101].

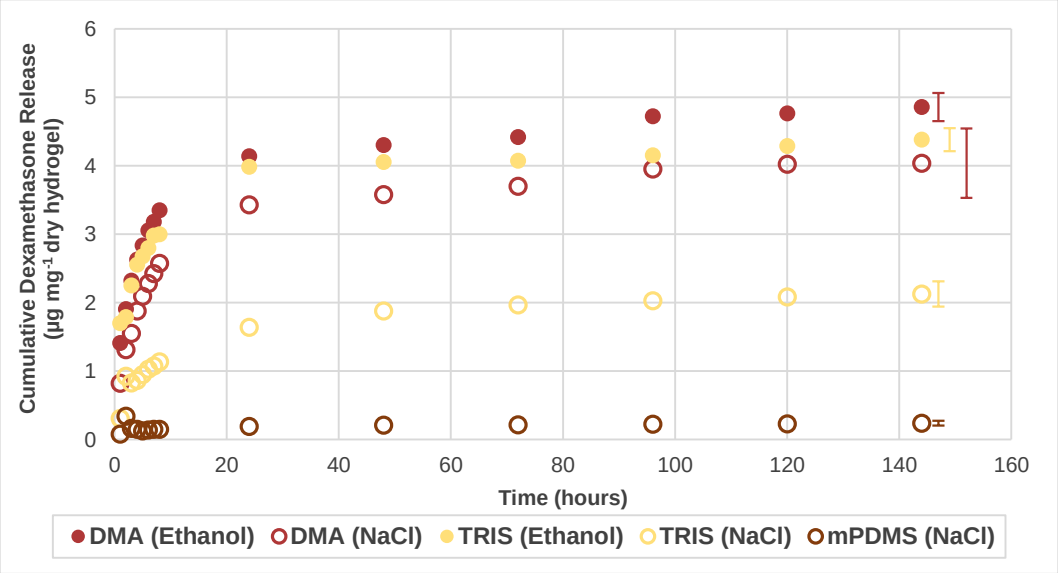


**Figure 47 -** Cumulative dexamethasone release from some hydrogels' types obtained using different loading conditions. The error bars correspond to the mean standard deviation.

### 3.6.2 Effect of the Loading Temperature on Diclofenac Release

To infer if different loading temperatures can induce some alterations in the drug release behaviour, a drug release study was done using diclofenac loaded at 4ºC and 60ºC, and 3 types of hydrogels: TRIS 36.8 41.8 21.5, mPDMS 36.7, and DMA 20.

Observation of Figure 48 reveals that the hydrogels TRIS 36.8 41.8 21.5 and mPDMS 36.7 did not suffer significant alterations in the drug release behaviour when loaded at 4ºC or 60ºC. Contrarily, the hydrogel DMA 20 showed differences between the two loading conditions. The cumulative diclofenac release of DMA 20 loaded at 60ºC reduced to almost half of the value obtained with the DMA 20 loaded at 4ºC. With these results, it is possible to conclude that in general, the increase in the loading temperature does not improve the drug release behaviour of these hydrogels.

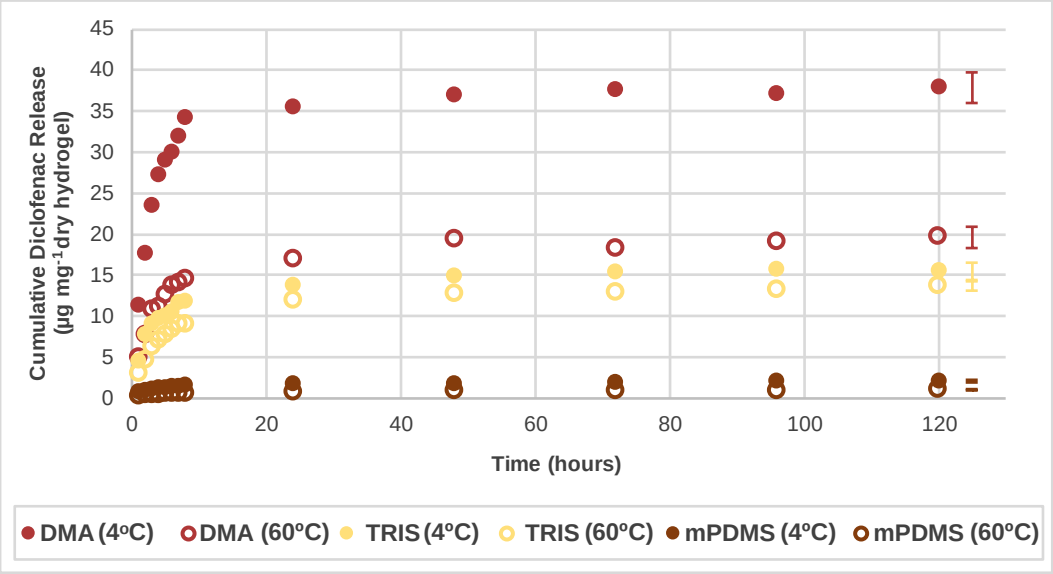


**Figure 48 -** Cumulative diclofenac release of 3 types of hydrogels, loaded at 4ºC and 60ºC. The error bars correspond to the mean standard deviation.

### 3.6.3 Effect of the Temperature and Ionic Strength on Swelling Behaviour

Hydrogels immersed in different types of solutions can present different swelling behaviours. For example, it was proved that hydrogels immersed in ionic solutions, like NaCl, have an increase in their swelling capacities comparatively to that found in water [106]. The possible increase in swelling can be justified by the presence of a higher number of counter-ions in the hydrogel matrix, creating an extra osmotic pressure that swells the hydrogel [106]. At the same time, hydrogels can present structural changes in response to specific stimuli, such as temperature variations [106]. To verify if, in fact, these changes occur in the hydrogels produced in this work, a set of swelling experiments was performed where the hydrogels were immersed in DD water and in a saline solution of NaCl at 4ºC and 60ºC. Three types of hydrogels (TRIS 36.8 41.8 21.5, mPDMS 36.7, DMA 20) were used for the same reasons referred in the section 3.6.1.

Figure 49 shows that, in general no significant differences exist in water and NaCl solution. At the same time, the swelling tests at different temperatures did not lead to differences in the final weight of the hydrogels. The only exception was the hydrogel TRIS 36.8 41.8 21.5, which, at 60ºC, swelled a little bit more immersed in NaCl than in DD water. The results obtained suggest that the swelling of these types of hydrogels is not influenced neither by the temperatures nor by the ionic strength of the immersion solutions.

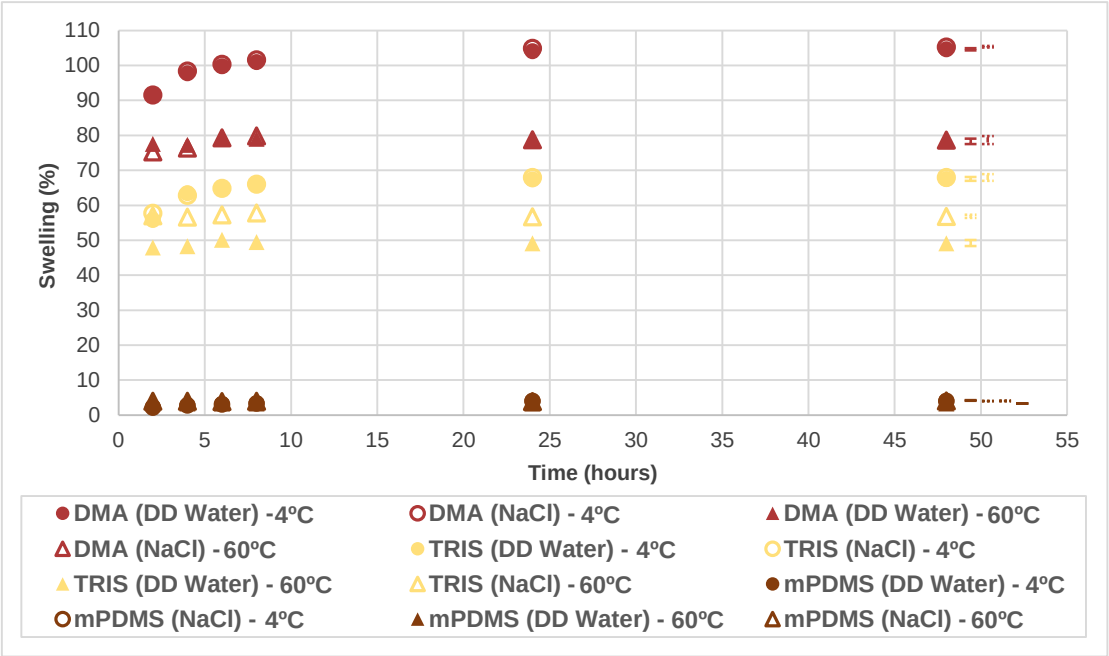


**Figure 49 –** Swelling results, at 4ºC and 60ºC, using DD water and NaCl. The error bars correspond to the mean standard deviation.

### 3.6.4 Wettability

Wettability is an important parameter to evaluate the hydrogels' surface characteristics and their ability to be placed in the eye as a contact lens. For the determination of the wettability, it is usually measured the water contact angle using the captive bubble or sessile drop methods. It is expected to measure distinct contact angles with the two techniques because different substrates are used; water saturated, in the former and dry, in the latter.

In this work, the captive bubble method was used to assess the surface wettability of seven types of hydrogels, in their swollen state: TRIS 34 50 16, TRIS 36.8 41.8 21.5, 8x EGDMA, mPDMS 36.7, TRIS 35 mPDMS 5, DMA 20, and mPDMS 36.7 DMA 28.3. The choice of more hydrogels' types than in the previous tests was due to the need of having a broad range of compositions that allow drawing significant conclusions.

Figure 50 shows no big differences among the contact angles of the different hydrogels. However, some results are inconsistent with the previous studies. Supposedly, DMA 20 should have a more hydrophilic surface than, for example, TRIS 34 50 16 and consequently a lower water contact angle was expected. However, the contact angles obtained are slightly lower for the TRIS-based hydrogels, which have HEMA in its composition that is less hydrophilic. One explanation for these results may have to do with the surface topography of the hydrogels when immersed in water. At the end of this subsection, a general analysis of the effect of the surface roughness on the contact angles will be done. Comparison of the obtained values with the ones of commercial lenses, shows that the contact angle obtained with

DMA 20 (42±4º) is similar to those obtained with lenses of similar compositions (Table 4) such as, Focus NIGHT & DAY® (41.0±7.2º) and $O_2$ OPTIX® (44.3±6.9º) [107].

Other puzzling results are the relatively low contact angles measured on the hydrogels containing mPDMS. Knowing that mPDMS is super hydrophobic, high contact angles on the hydrogels with higher amounts of these material were expected, but the values obtained were: 44±4º for mPDMS 36.7 and 39±3º for PDMS 36.7 DMA 28.3 (Figure 50). In the case of mPDMS 36.7 DMA 28.3, the low contact angle obtained can be explained by the super hydrophilic nature of DMA that offsets the hydrophobic nature of mPDMS. However, the results obtained when compared with the contact angle values of known commercial lenses with similar compositions (Table 4), such as ACUVUE® ADVANCE® (30.5±3.3º) and ACUVUE® OASYS® (32.4±5.5º) [107], are a little above but still acceptable for the use as $CL_s$.

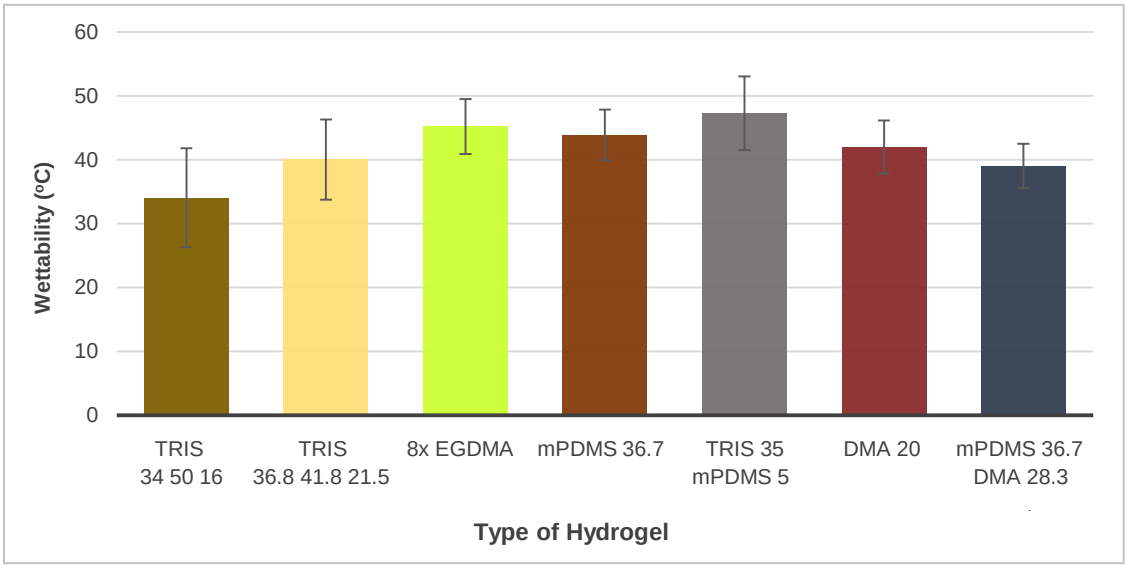


**Figure 50 –** Water contact angles of the different hydrogels obtained using the captive bubble method. The error bars correspond to the standard deviation.

For the determination of the surface energy of the hydrogels, it was necessary to measure the contact angle using the sessile drop method with two liquids: DD water (polar) and diiodomethane (non-polar). Five types of hydrogels were used: TRIS 34 50 16, TRIS 36.8 41.8 21.5, 4x EGDMA, DMA 20 and mPDMS 36.7 DMA 28.3.

Figure 51 shows the contact angle values, for DD water and diiodomethane, of each hydrogel. Looking at the results obtained with DD water, all hydrogels showed contact angles close to 90º. These results lead to the conclusion that these hydrogels are poorly wettable when in their dry state. The hydrogels 4x EGDMA and DMA 20 presented contact angles above 90º. This can be explained by the roughness of the surface (see section 1.2.2.3.5.1), which is considered one of the factors that can influence the wettability of the materials.

According to the models described in section 1.2.2.3.5.1, the heterogeneity and roughness of the surface may affect the contact angle in different ways. The water contact angle values above 90º obtained on relatively hydrophilic surfaces could be justified by the Cassie-Baxter model. A dry and

rough hydrogel is full of depressions and the air entrapped into these depressions makes the contact angle values higher. This model can also explain why the contact angles with captive bubble are lower. When the hydrogel is in its swollen state, the depressions tend to decrease because of the expansion of the hydrogel and consequently less air is entrapped in the surface and lower contact angle values are obtained. Furthermore, in the hydrated state, the polar groups of the hydrogel chains should become exposed to the aqueous phase, leading to lower water contact angles.

Relatively to the contact angles measured with diiodomethane, all hydrogels present similar contact angles values (Figure 51). Comparing with the contact angles obtained by DD water, the ones measured with diiodomethane are lower, confirming the low hydrophilicity of these hydrogels in the dry state.

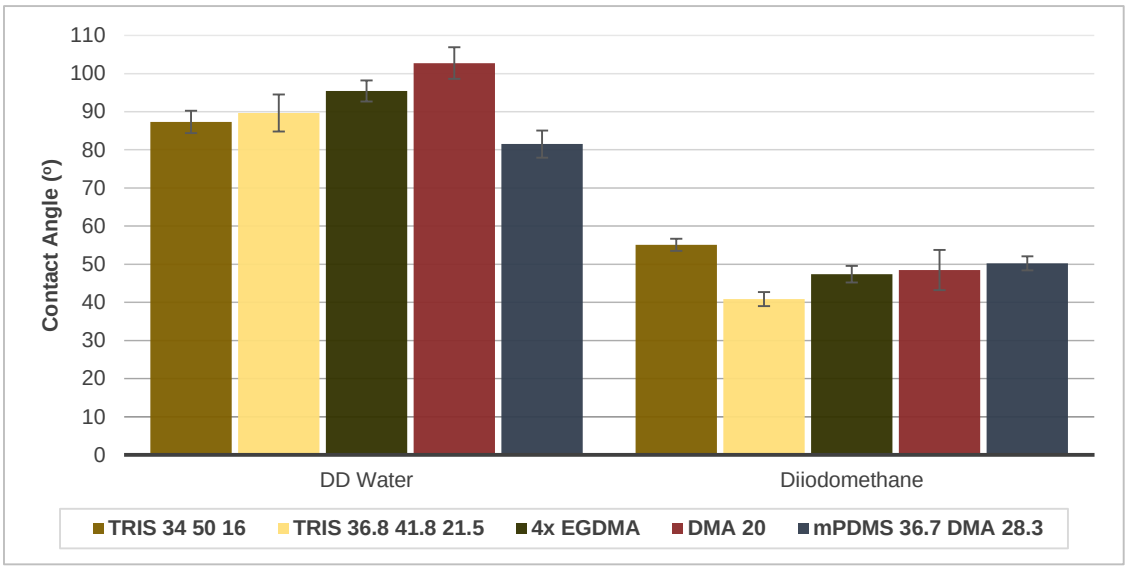


**Figure 51 -** Water and diiodomethane contact angles of the different hydrogels obtained using the sessile drop method. The error bars correspond to the standard deviation.

### 3.6.5 Surface Energy

The determination of the surface energy provides an insight on the surface properties of hydrogels. With the surface energy values it is possible to understand the interactions between the liquid and the solid surface, as well as the nature of the surface (hydrophilic or hydrophobic) [84].

Figure 52 shows the surface energy of the different hydrogels. Each bar is divided into the dispersive and polar components. The calculation of these components was based on the contact angles of DD water and diiodomethane obtained with the sessile drop method. According to Figure 52, the dispersive component is always predominant, being the polar component negligible in the case of DMA 20. These results are consistent with the values of the contact angles shown in Figure 51. Since all hydrogels showed a hydrophobic nature when the contact angle was measured with the sessile drop method, the dispersive component should be higher than the polar component that is related with the hydrophilicity of the surface. Also, in Figure 52, it can be seen that the surface energies obtained are similar in all hydrogels, being the highest value for the hydrogel TRIS 36.8 41.8 21.5. The low values of surface energy, by themselves, indicate that the hydrogels' surface, when in dry state, is poorly wettable.

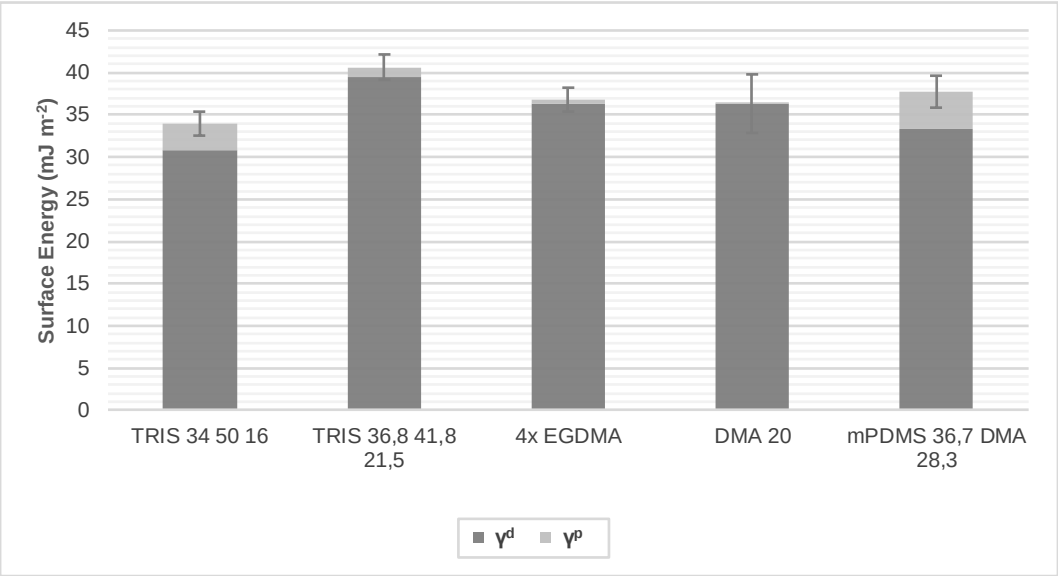


**Figure 52 -** Surface energy of different hydrogels, showing the dispersive ($\gamma^d$) and polar ($\gamma^p$) components. The error bars correspond to the standard deviation.

### 3.6.6 Morphology

The surface analysis of the hydrogels was performed by scanning electron microscopy (SEM). In this subchapter it will be compared different types of hydrogels at x3000 and x10 000 of magnification.

1x EGDMA vs. 8x EGDMA

Figure 53 and Figure 54 show the surface morphology of 1x EGDMA and 8x EGDMA. In general, the hydrogels present a homogeneous surface. 1x EGDMA exhibit some concavities whereas in 8x EGDMA hydrogel it is seen little white protuberances probably due to some debris present on the surface. However, the increase in the amount of the crosslinker does not substantially affect the hydrogels' surface.

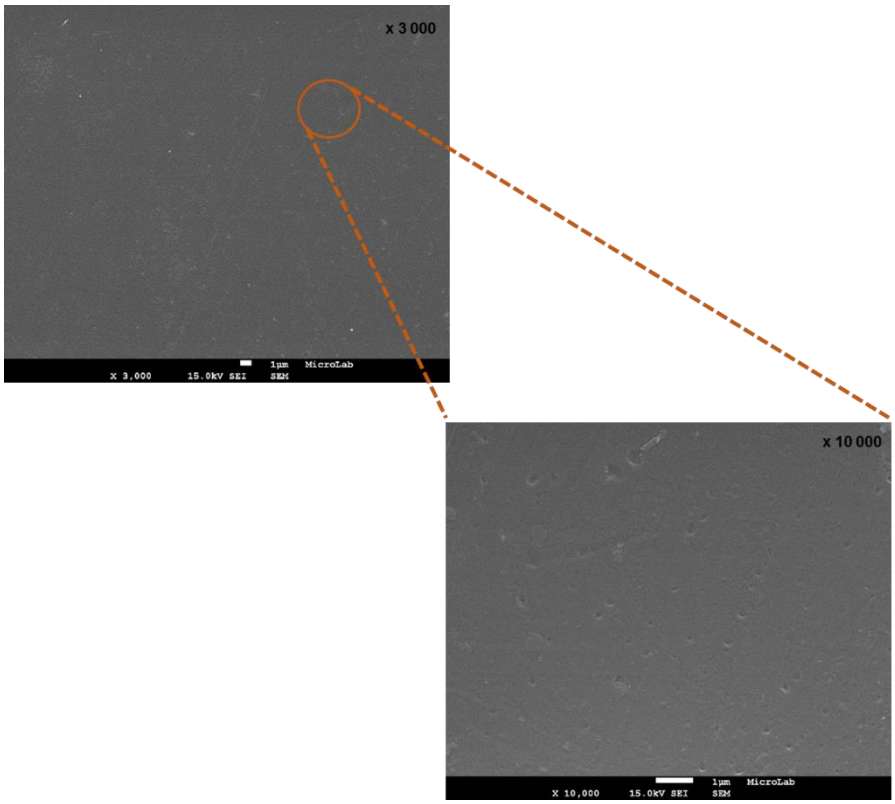


**Figure 53 -** SEM images of the surface of the hydrogel 1x EGDMA.

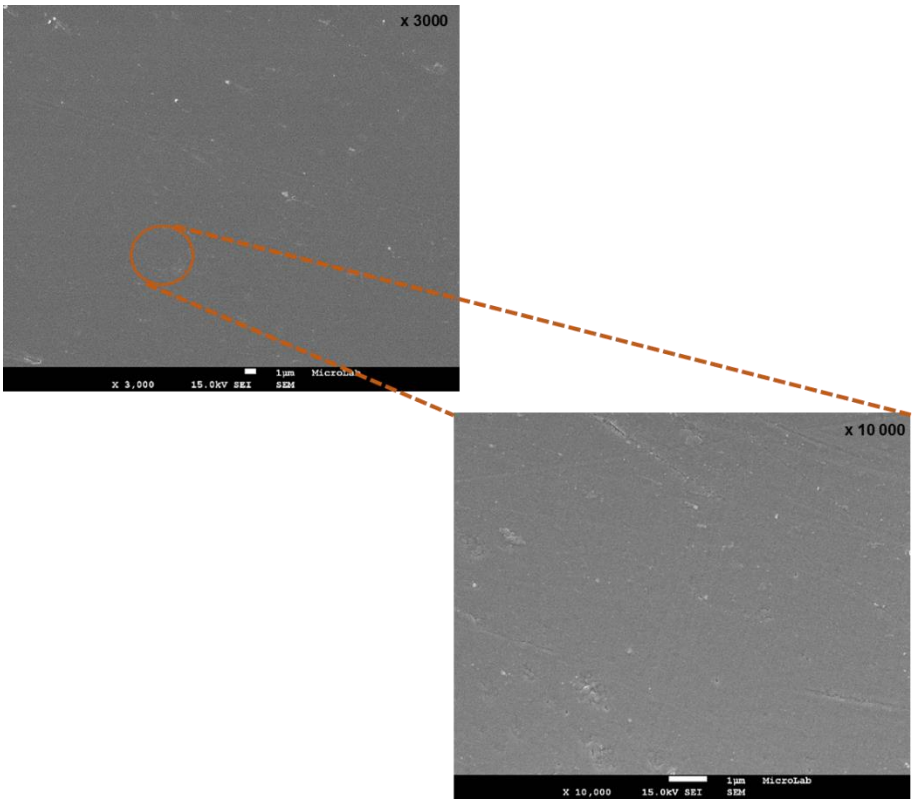


**Figure 54 -** SEM images of the surface of the hydrogel 8x EGDMA.

TRIS 34 50 16 vs. TRIS 36.8 41.8 21.5

Comparing the hydrogel TRIS 36.8 41.8 21.5 (same composition as 1x EGDMA) with TRIS 34 50 16, no big differences are seen (Figure 53 and Figure 55). TRIS 34 50 16 does not present too much features compared to TRIS 36.8 41.8 21.5 and again, these hydrogels showed some debris on the surface. The variation in the amount of TRIS, NVP and HEMA seems does not affect the surface of these hydrogels.

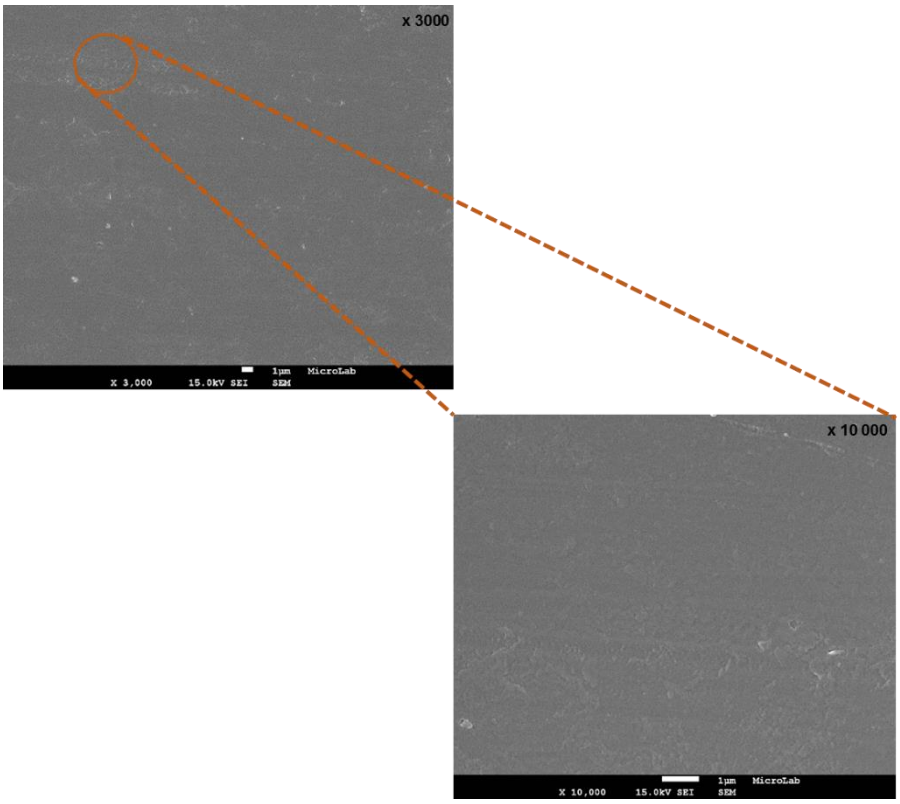


**Figure 55 -** SEM images of the surface of the hydrogel TRIS 34 50 16.

TRIS 36.8 41.8 21.5 vs. DMA 20

Both hydrogels present few debris on the surface, corresponding to the white spots on the images (Figure 53 and Figure 56). Despite the defects of TRIS 36.8 41.8 21.5, no visible changes are seen between the two hydrogels, leading to the conclusion that changing the hydrophilic monomer does not affect the surface morphology.

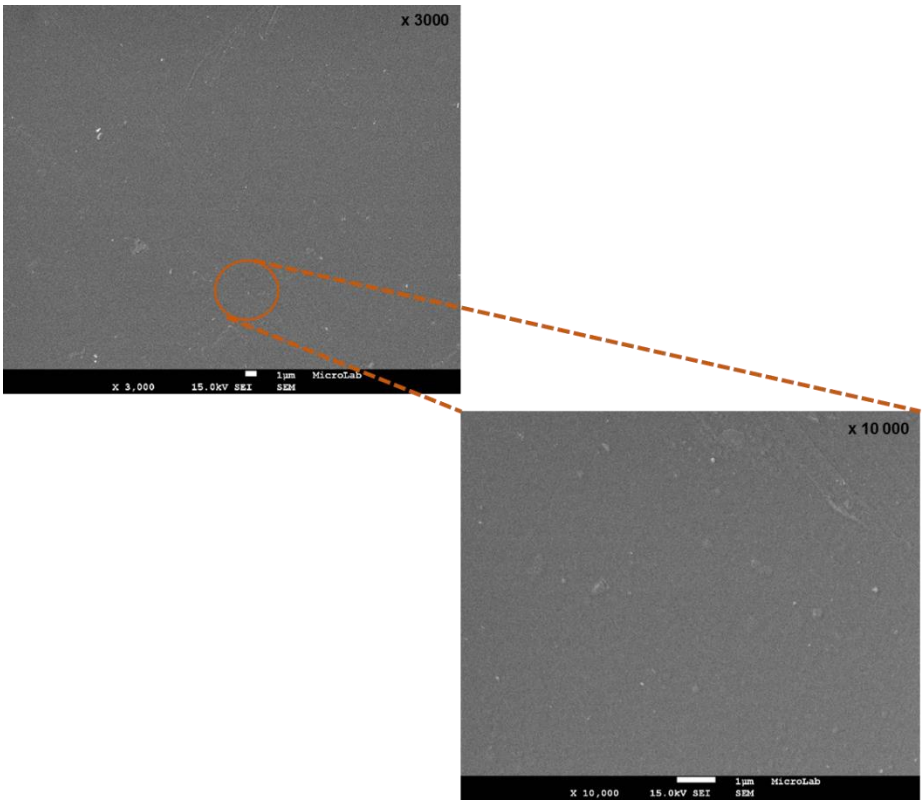


**Figure 56 -** SEM images of the surface of the hydrogel DMA 20.

mPDMS 36.7 vs mPDMS 36.7 DMA 28.3

Observing Figure 57 and Figure 58, differences are seen between the two hydrogels. mPDMS 36.7 shows some stretching marks on the surface, but they should have occurred in any occasional event. Probably, this was due to the detachment of the hydrogel from the glass, after the polymerization reaction. Additionally, at x10 000 of magnification the hydrogel mPDMS 36.7 shows a bacterium on its surface. mPDMS 36.7 DMA 28.3 presents some debris on the surface as well as mPDMS 36.7. Despite the stretching marks of the hydrogel mPDMS 36.7, the use of HEMA or DMA as the hydrophilic monomer did not affect the surface morphology.

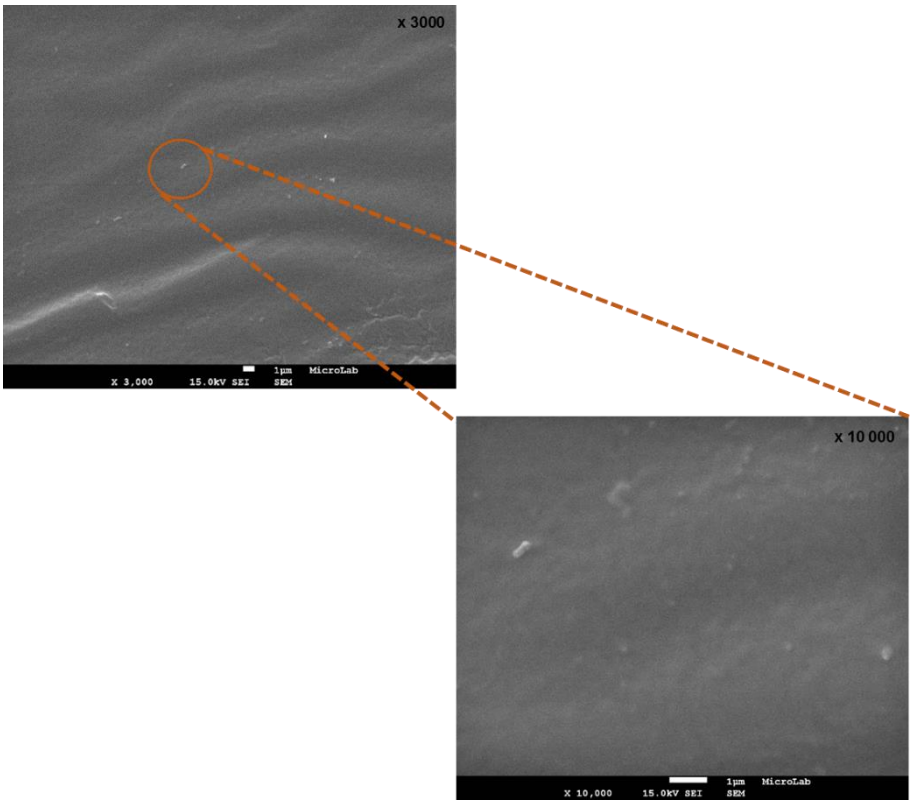


**Figure 57 -** SEM images of the surface of the hydrogel mPDMS 36.7.

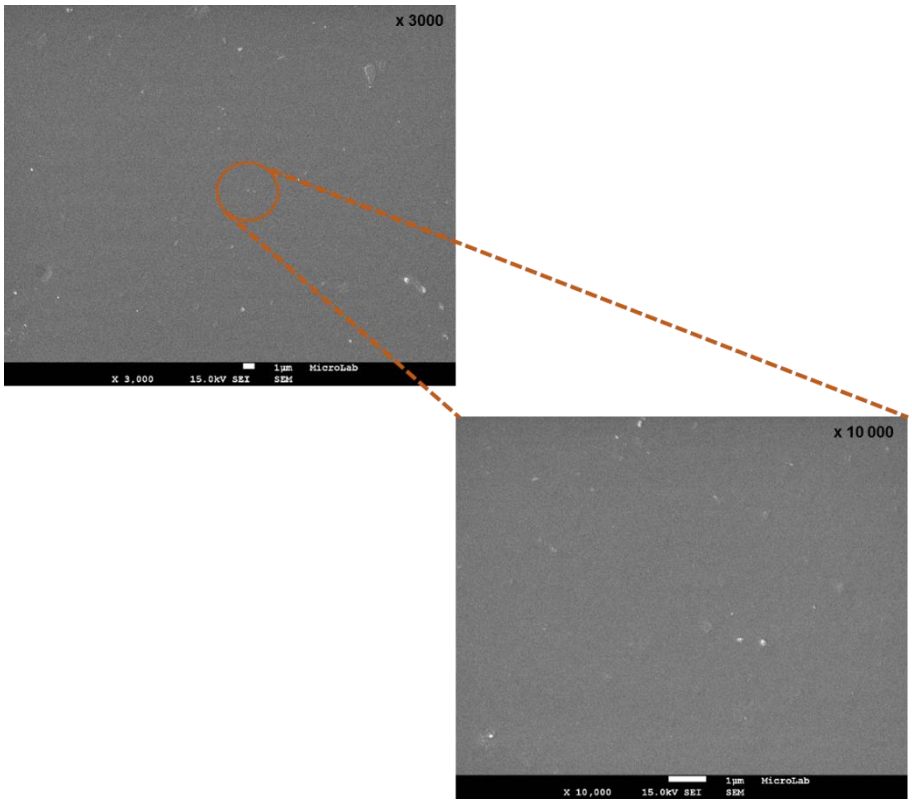


**Figure 58 -** SEM images of the surface of the hydrogel mPDMS 36.7 DMA 28.3.

### 3.6.7 Mechanical Properties

The study of the mechanical properties can give important information about the comfort that the hydrogels can offer when used as $CL_s$ and handling properties. Seven types of hydrogels were studied: TRIS 34 50 16, TRIS 36.8 41.8 21.5, 8x EGDMA, mPDMS 36.7, TRIS 35 mPDMS 5, DMA 20, and mPDMS 36.7 DMA 28.3.

Figure 59 presents the Young's modulus of the different hydrogels tested. As expected, 8x EGDMA presents the highest Young's modulus (7.6E+07 ± 2E+06 Pa) due to the high amount of crosslinker compared with the other hydrogels. High Young's modulus values are not necessarily good features for $CL_s$ because they can lead to discomfort for the wearer. Relatively to the hydrogels containing different hydrophilic materials, the TRIS-based hydrogels have higher Young's modulus than DMA 20. Since DMA 20 is a super water absorber, a relationship between the Young's modulus and the swelling seems to exist: the higher the swelling percentage, the lower the Young's modulus. However, this relationship is not applied to all hydrogels studied. For example, the TRIS-based hydrogels show similar Young's modulus values compared with mPDMS 36.7 and TRIS 35 mPDMS 5, which have much lower swelling percentages. Low swelling capacity should be associated to high Young's modulus: one plausible explanation for the unexpected low values of mPDMS 36.7 and TRIS 35 mPDMS 5 hydrogels may have to do with the presence of SiGMA, which should cause the decrease in the Young's modulus.

The hydrogel mPDMS 36.7 DMA 28.3 showed the lowest Young's modulus (Figure 59). This result confirms the statements made in the previous subchapters that although this hydrogel has a super hydrophobic silicone monomer in its composition, the hydrophilic material (DMA) can offset the hydrophobic part, increasing the water content and consequently decreasing the Young's modulus.

The values obtained in these mechanical studies are similar to those reported for commercial lenses. For example, the Young's modulus obtained for DMA 20 was 1.04E+06 ± 5E+04 Pa (Figure 59), which compares with the values of 1.5E+06 Pa for Focus NIGHT & DAY® (Lotrafilcon A) and 1.0E+06 Pa for $O_2$ OPTIX® (Lotrafilcon B) (see Table 4). For the commercial lenses with mPDMS in their composition, the Young's modulus are 7.2E+05 Pa for ACUVUE® OASYS® and 4.3E+05 Pa for ACUVUE® ADVANCE® (see Table 4), which are identical with the mPDMS 36.7 DMA 28.3 (4.4E+05 ± 6E+04 Pa).

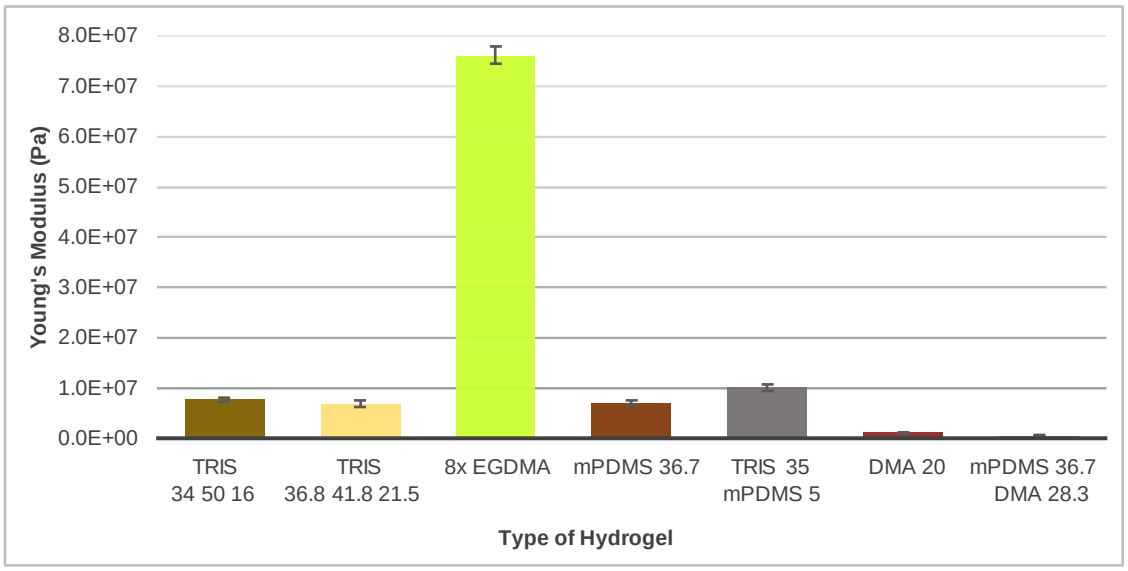


**Figure 59 -** Young's modulus of the different hydrogels. The error bars correspond to the standard deviation.

Besides the Young's modulus, the average tension at break and elongation at break are important parameters to define the hydrogels behaviour. According to Billmeyer studies [108], a polymer can be: soft (low Young's modulus) and tough (high elongation at break); hard (high Young's modulus) and brittle (low elongation at break) or hard and at the same time strong (high tension at break).

Analysis of Figure 60 shows that the hydrogel 8x EGDMA presents the highest value of tension at break (5E+06 ± 1E+06 Pa). It is a plausible result since the higher degree of crosslinking shall require a higher tension to break this hydrogel, comparing with the others. According to Billmeyer, the hydrogel 8x EGDMA is considered hard and strong due to its high Young's modulus and tension at break. The hydrogel DMA 20 shows a low value of tension at break, which is expectable since this hydrogel may be considered a soft material and consequently demands lower amounts of tension to be broken. Comparison of Figure 59 and Figure 60, reveals that a relationship between Young's modulus and tension at break exists: higher Young's modulus correspond to higher tensions at break of the hydrogels.

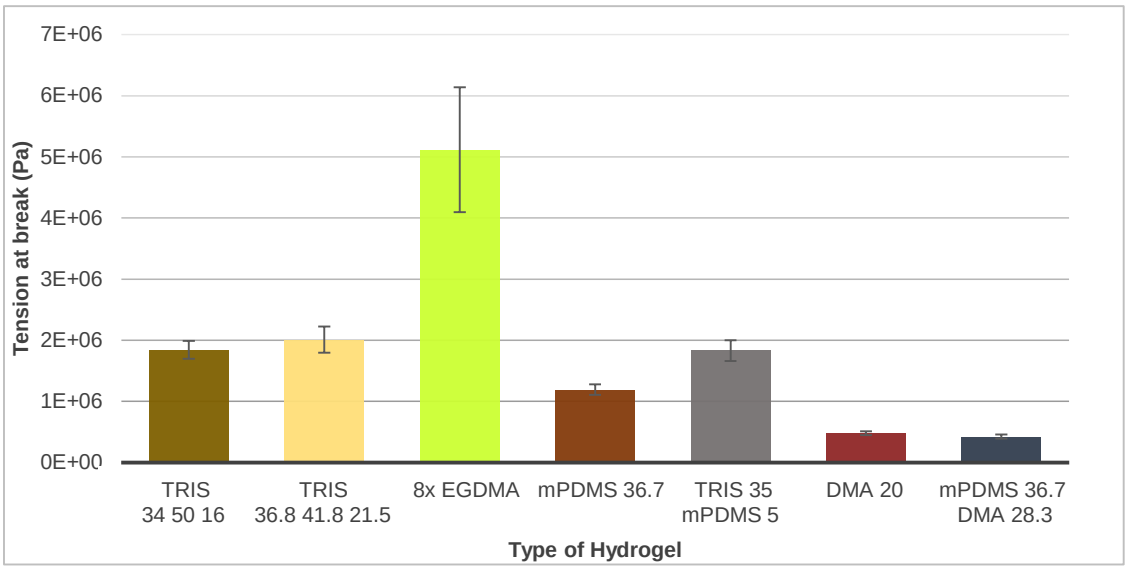


**Figure 60 -** Tension at break of the different hydrogels. The error bars correspond to the standard deviation.

Figure 61 presents the elongation at break of each hydrogel. The hydrogel mPDMS 36.7 DMA 28.3 shows the highest value of elongation at break (2.8±0.7). This result proves that, although this hydrogel has low Young's modulus, it can be tough. However, DMA 20, which also presents a low value of Young's modulus, showed a significantly lower value for elongation at break compared with mPDMS 36.7 DMA 28.3. This result leads to the conclusion that DMA 20 is not as tough as mPDMS 36.7 DMA 28.3. As expected, the 8x EGDMA hydrogel presents the lowest elongation at break value (0.09±0.05), proving that this material is brittle despite being strong.

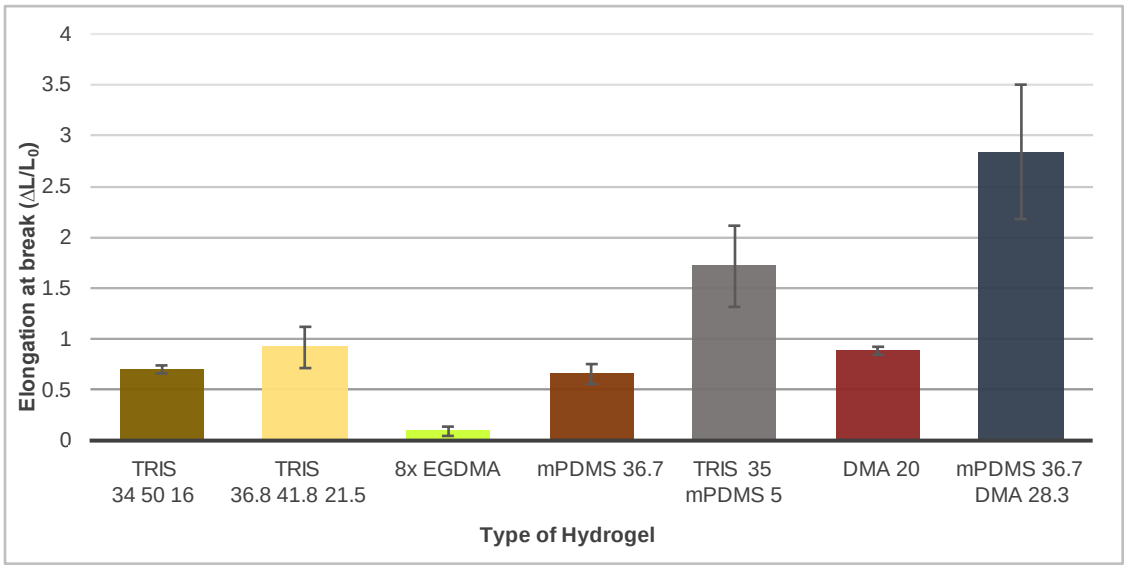


**Figure 61 -** Elongation ($\Delta L/L_0$) at break of the different hydrogels. The error bars correspond to the standard deviation.

The study of the toughness is important to confirm the mechanical features that were previously assigned to the hydrogels. Also, this parameter allows to infer how much energy is necessary to cause the failure of the hydrogel. Observing Figure 62, the hydrogel 8x EGDMA shows one of the lowest values of toughness (3E+05 ± 2E+05 J $m^{-3}$). It is an expectable result because a strong material like 8x EGDMA

needs less energy to break, contrarily to, for example, TRIS 36.8 41.8 21.5 that needs more energy to break looking to the Young's modulus obtained.

The only outlier present in Figure 62 is TRIS 35 mPDMS 5 hydrogel that shows the highest value of toughness (2.7E+06±7.5E+05 J $m^{-3}$).

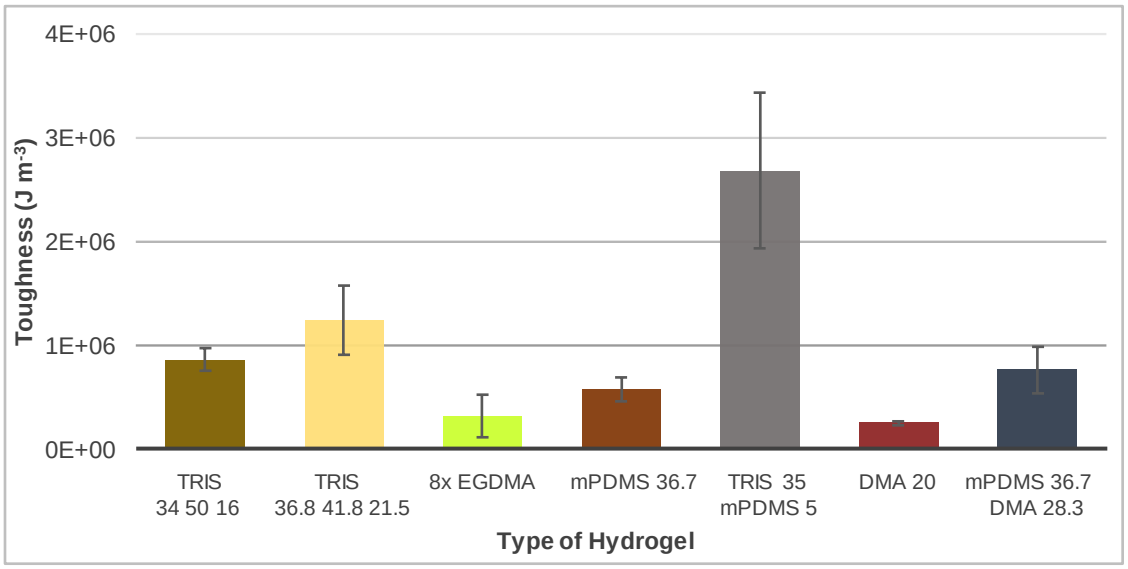


**Figure 62 -** Toughness of the different hydrogels. The error bars correspond to the standard deviation.

### 3.6.8 Water States in Hydrogels

As seen above, the hydrogels' behaviour is strongly dependent on the amount of water in their inside. Also, the states of the water in the hydrogels is of extreme importance. For this study, five types of hydrogels were analysed by DSC: TRIS 34 50 16, TRIS 36.8 41.8 21.5, 4x EGDMA, DMA 20, and mPDMS 36.7 DMA 28.3. Although, tests have been attempted for other hydrogels, e.g. hydrogels where the amount of the hydrophobic compounds was changed and the 8x EGDMA hydrogel, and due to their low swelling percentages, it was not possible to detect the peaks of water using that technique.

As shown in Figures 63-67, for all hydrogels studied two peaks were observed in the thermograms corresponding to free and loosely bound water in three independent tests. Generally, no significant changes were found between the measurements, for each type of hydrogel. In each heating cycle, the first peak observed (order from left to right) was from the loosely bound water at temperatures below 0ºC. The second peak, related to the free water, was detected at temperatures around 0ºC.

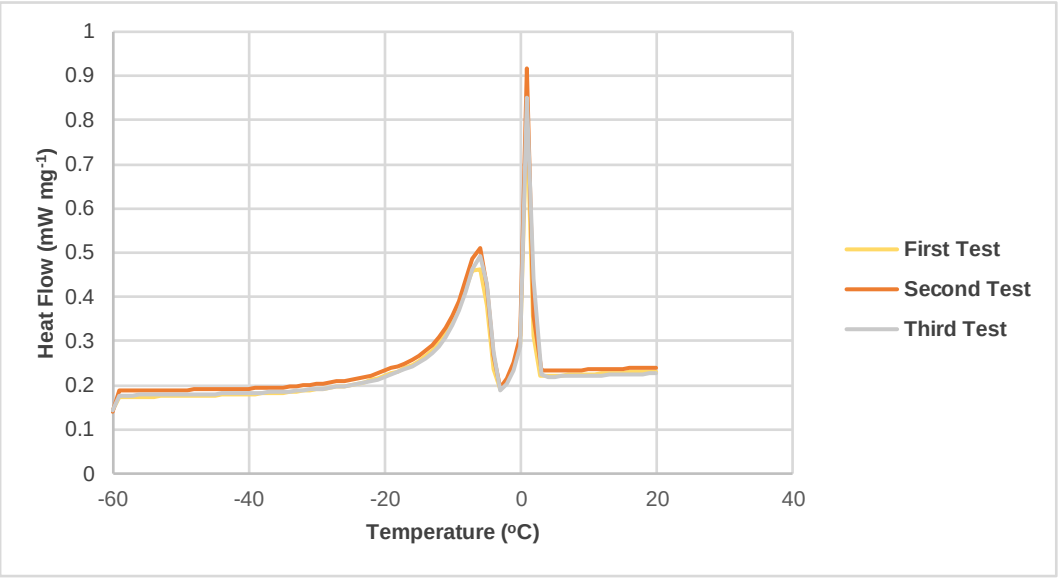


**Figure 63 -** Thermograms of the three measurements made for the TRIS 34 50 16 hydrogel.

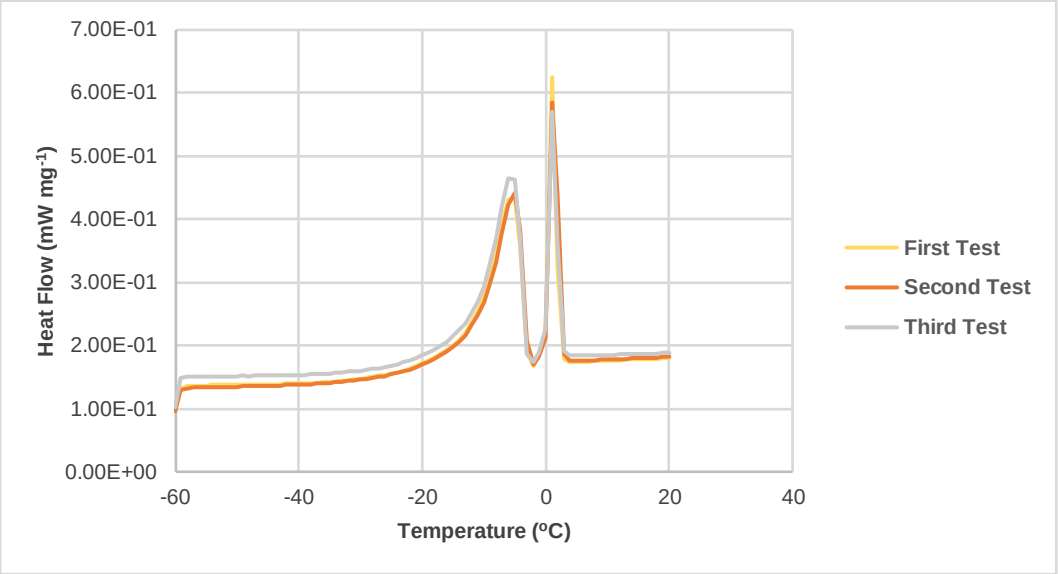


**Figure 64 -** Thermograms of the three measurements made for the TRIS 36.8 41.8 21.5 hydrogel.

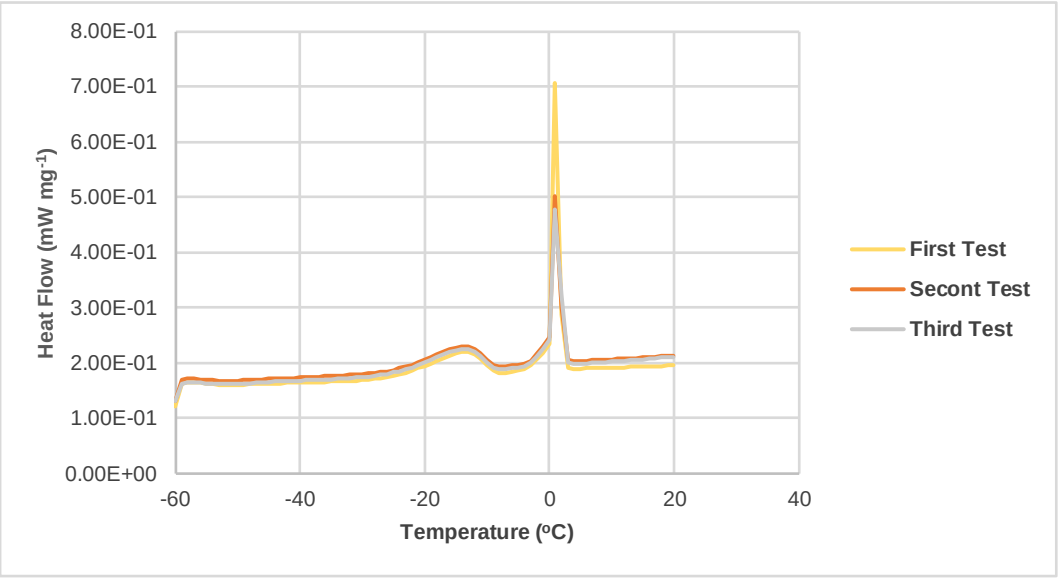


**Figure 65 –** Thermograms of the three measurements made for the 4x EGDMA hydrogel.

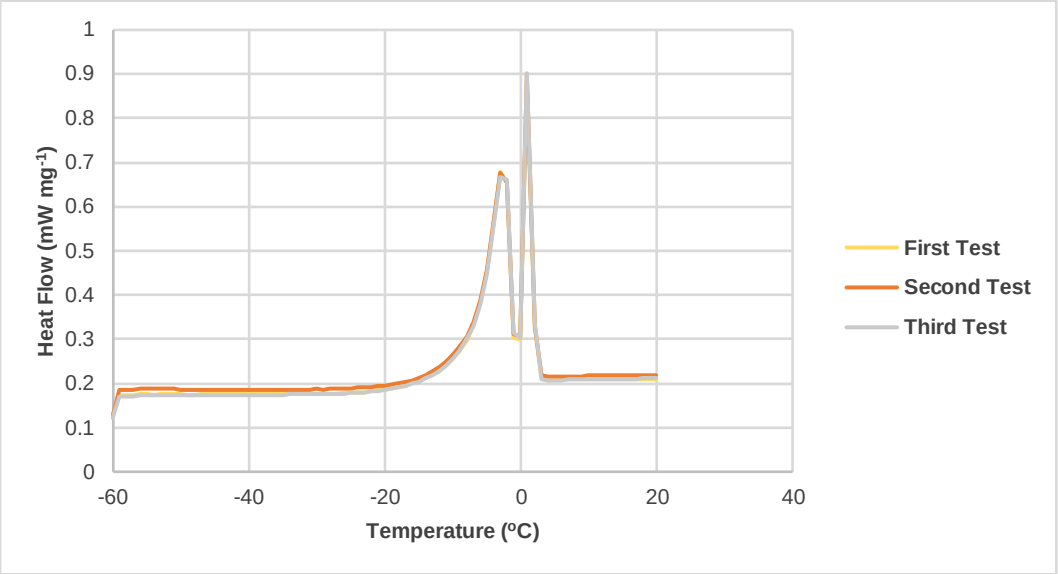


**Figure 66 -** Thermograms of the three measurements made for the DMA 20 hydrogel.

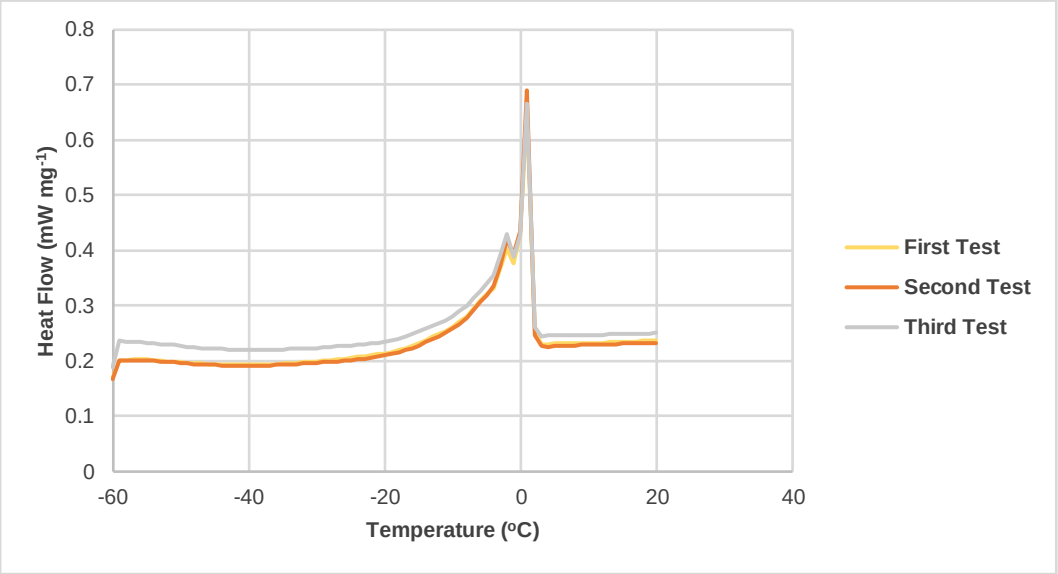


**Figure 67 -** Thermograms of the three measurements made for the mPDMS 36.7 DMA 28.3 hydrogel.

With the help of the software *Proteus Thermal Analysis*, it was possible to determine the enthalpy of fusion of the water contained in the samples analysed (Table 10) through the integration of the peaks together or separately, using well-defined intervals (between the onset and the end of the peaks). In some cases, it was necessary to make the integration of the two peaks together because in certain samples, the two peaks were not well-defined to be measured separately (Figure 66 and Figure 67). In Table 10, it is presented the enthalpy of fusion of water in J $g^{-1}$. The values obtained are an average of the three measurements made for each hydrogel.

**Table 10 -** Enthalpy of fusion of water calculated for each hydrogel analysed and its respective swelling capacity.

| Hydrogel Type | Enthalpy of fusion of water, $\Delta H_f$, (J $g^{-1}$) | Swelling Capacity (%) |
|---|---|---|
| 4x EGDMA | 29±2 | 39.0±0.2 |
| mPDMS 36.7 DMA 28.3 | 59±2 | 43.6±0.2 |
| TRIS 36.8 41.8 21.5 | 76±3 | 66.9±0.5 |
| TRIS 34 50 16 | 89±3 | 73±3 |
| DMA 20 | 96±1 | 96.4±0.8 |

Observing the Table 10, it is seen a relationship between the swelling capacity and the enthalpy of fusion of water of the hydrogels: the lower the swelling capacity the lower the enthalpy of fusion of water.

The amount of free and loosely bound water was then calculated by dividing the enthalpy of fusion measured for the known enthalpy of fusion of bulk water (333.6 J $g^{-1}$) [70]. The amount of the tightly bound water was then calculated, subtracting the amounts of free and loosely bound water from the total water content in the hydrogel. Figure 68 presents the equilibrium water content and the percentages of the

three states of water in each hydrogel. In the last two hydrogels (DMA 20 and mPDMS 36.7 DMA 28.3), the percentages of the free and loosely bound water are presented together because, as it was said above, the determination in of the enthalpy of fusion of these type of waters was not possible because the peaks were not separated.

The percentage of free and loosely bound water is higher than the percentage of the tightly bound water except in TRIS 36.8 41.8 21.5 and 4x EGDMA hydrogels. In the case of the hydrogel TRIS 36.8 41.8 21.5, the percentages of free + loosely bound water is almost the same as the tightly bound water (within the error), so it will be considered in the group where the portion of free and loosely bound water is higher. The fact that the 4x EGDMA showed higher values of tightly bound water in their matrix than free and loosely bound water makes sense because the hydrogels with higher amounts of crosslinker, tend to have their mesh tighter and therefore the space for the free and loosely bound water is reduced. Thus, the percentage of tightly bound water, that is the water strongly bound to the hydrogels' pore walls, is higher.

The results obtained lead to the conclusion that the amount of crosslinker strongly influences the states of water in hydrogels.

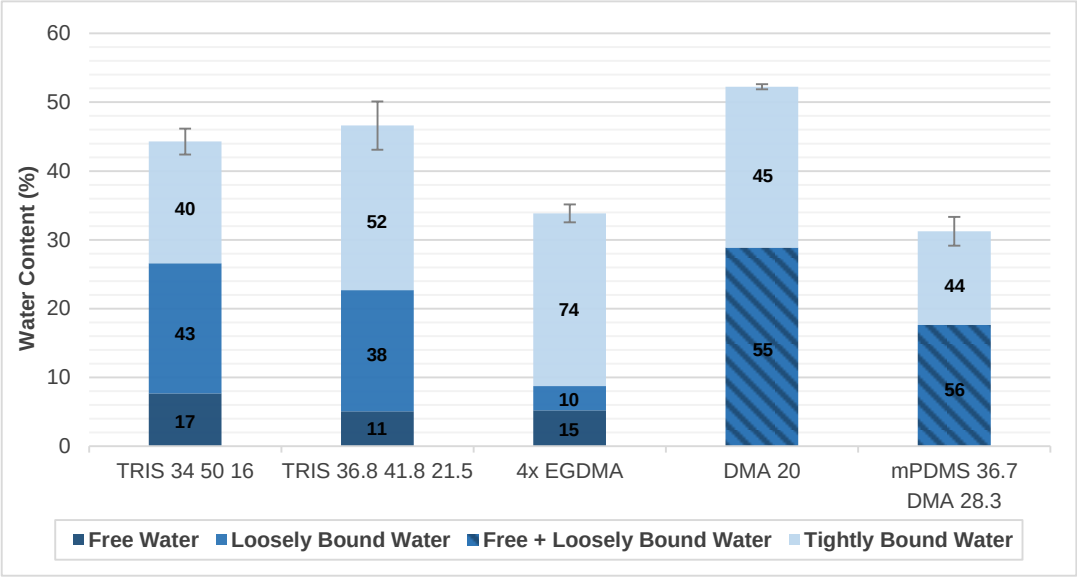


**Figure 68 -** Equilibrium water content and the relative portions of the different water states presented in each hydrogel. The error bars correspond to the standard deviation.

### 3.6.9 Thermoporometry

Thermoporometry allows the determination of the pore-size dimensions of the hydrogels. From the thermograms shown in the Figures 63-67, the pore size dimensions were determined using the methods proposed by Brun et al. [75] and Landry [73] which were described in section 1.2.2.3.4.1.

Figure 69 presents the pore-size dimensions of the five hydrogels studied using the two methods referred above. The values obtained for the pore-size dimensions with Landry's method are always lower than the Brun's method; however, the pore-size tendency was not altered. The hydrogel 4x EGDMA shows the lowest values of pore dimensions. It was an expectable result because hydrogels

with higher amounts of crosslinker have their mesh tighter and so the pore-size dimensions are small. The mPDMS 36.7 DMA 28.3 shows the highest pore-size dimensions.

The pore-size dimensions can be related to the drug release behaviour of the hydrogels. It is expected that hydrogels with higher pore-size dimensions have a higher capacity of loading and release of drugs. The hydrogels with larger pore-size dimensions (DMA 20 and mPDMS 36.7 DMA 28.3) are the ones with higher cumulative diclofenac release (Figure 39 and Figure 43). On the other hand, the hydrogel 4x EGDMA with the smallest pore-size has lower cumulative diclofenac release (Figure 26) compared with DMA 20 and mPDMS 36.7 DMA 28.3 hydrogels.

The pore-size dimensions can be also related with the states of the water in hydrogels. Hydrogels with lower pore-size dimensions tend to have less space for the free and loosely bound water, being the tightly bound water the dominant one. This affirmation can be confirmed observing the Figure 68, where the 4x EGDMA has the higher amount of tightly bound water and smaller pore-size dimensions. On the other hand, the DMA 20 hydrogel presents one of the highest pore-size dimensions and consequently higher amounts of free and loosely bound water compared with tightly bound water.

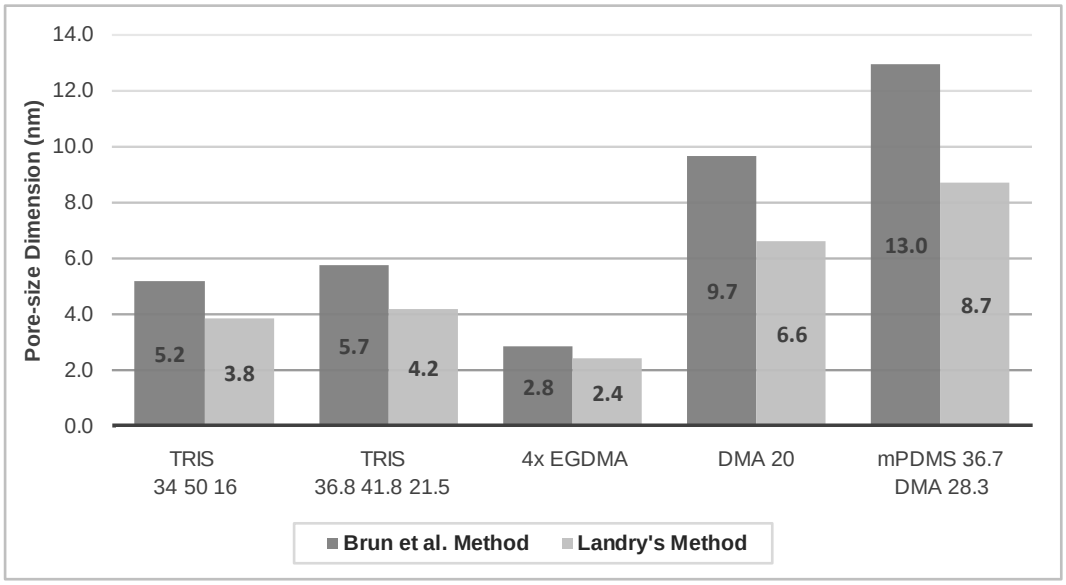


**Figure 69 -** Pore-size dimensions of the different hydrogels.

## 3.7 Release Profiles Vs Therapeutic Windows

To predict whether or not the studied hydrogels can efficiently deliver the drug above the therapeutic window when used as contact lenses in real conditions, the therapeutic windows of diclofenac and dexamethasone that are already in the market in the form of eye drops were determined. Using the release data of each hydrogel, it was calculated the average amount of drug that is released from the hydrogel per hour and compared to the therapeutic windows to see how long they can deliver effectively the drug in the eye.

Currently, diclofenac is administrated through eye drops (1 mg $mL^{-1}$, Voltaren®) to treat a variety of complications. It is frequently used for post-surgery of ocular problems (1 drop 3 times per day) or for the relief of ocular pain and photophobia (1 drop every 4 hours or every 6 hours) [109]. On the other hand,

dexamethasone is usually delivered through a 1 mg $mL^{-1}$ of solution (Ronic®) to treat affections in general. In more severe acute affections, it is frequently applied 1 drop each hour (considering that the patient applies during 16 hours and the other 8 hours he is asleep), whereas in acute affections it is applied 1 drop 3-6 times per day [110].

Considering that only 5% of the portion administered into the eye is absorbed by the cornea [8] and that the eye drop volume is 33 µL [111], the posology for each drug is:

- 4.95-8.25 µg per day for diclofenac;
- 4.95-28.05 µg per day for dexamethasone.

So, the therapeutic needs of the cornea are about: 0.21-0.34 µg per hour for diclofenac, and 0.21-1.2 µg per hour for dexamethasone. Another important parameter is the limit of toxicity, which for both drugs shall be above the concentration of the eye drops. These lower and upper limits define the so-called therapeutic window.

In the present cases, the concentrations measured experimentally are quite below the upper limits previously referred. Since the samples used in the experiments have dry weights between 20-30 mg, and commercial contact lenses are usually bellow 20 mg, toxicity shall not be a problem.

From the drug release profiles (µg $mg^{-1}$ dry hydrogel) obtained for each hydrogel, the average mass of drug released at each hour by a contact lens of 20 mg (dry weight) was estimated through the use of the software *TableCurve 2D 5.0*: an equation was fit to the cumulative release curve and then the derivative was calculated. Annex A.1 present the drug release rate (in µg $h^{-1}$) as a function of time for each type of hydrogel. The figures also show the lower limit of the therapeutic windows (correspondent to the values previously referred for the therapeutic needs of the cornea).

Table 11 and Table 12 show the number of hours during which diclofenac and dexamethasone concentrations in the lacrimal fluid, after release from the hydrogels, shall remain between the limits of the therapeutic window.

**Table 11 –** Number of hours during which the hydrogels delivered diclofenac within the therapeutic window.

| Hydrogel Type | Time (hours) |
|---|---|
| **1x EGDMA** | 70 |
| **2x EGDMA** | 46 |
| **4x EGDMA** | 48 |
| **8x EGDMA** | 20 |
| **TRIS 34 50 16** | 36 |
| **TRIS 37 45 16** | 35 |
| **TRIS 38 43 19** | 67 |

| | |
|---|---|
| **TRIS 36.8 41.8 21.5** | 70 |
| **TRIS 50 40 10** | 25 |
| **mPDMS 36.7** | 19 |
| **TRIS 10 mPDMS 30** | 16 |
| **TRIS 20 mPDMS 20** | 14 |
| **TRIS 30 mPDMS 10** | 6 |
| **TRIS 35 mPDMS 5** | 6 |
| **DMA 20** | 41 |
| **DMA 10 HEMA 10** | 42 |
| **SiGMA 20 HEMA 20** | 49 |
| **mPDMS 36.7 DMA 18.3** | 27 |
| **mPDMS 36.7 DMA 28.3** | 38 |

**Table 12 -** Hours that the respective hydrogels delivered dexamethasone within therapeutic window. In brackets the respective type of loading solution is shown.

| Hydrogel Type | Time (hours) |
|---|---|
| **TRIS 36.8 41.8 21.5 (Ethanol)** | 29 |
| **TRIS 36.8 41.8 21.5 (NaCl)** | 40 |
| **DMA 20 (Ethanol)** | 35 |
| **DMA 20 (NaCl)** | 36 |
| **mPDMS 36.7 (NaCl)** | 2 |

Observing the Figures in the Annex A.1, the released masses per hour decrease with time as expected, because the release rates from the hydrogels are diffusion controlled [112]. An ideal contact lens should release drug within the therapeutic window all the time; however, the hydrogels studied in this work cannot sustain the desired release rates at all times.

Observing Table 11, it is possible to conclude that all hydrogels can deliver efficiently diclofenac within the therapeutic window for at least 6 hours. The hydrogel TRIS 36.8 41.8 21.5 (same composition as 1x EGDMA) was considered the best hydrogel, delivering diclofenac within the therapeutic window for 70 hours. TRIS 30 mPDMS 10 and TRIS 35 mPDMS 5 hydrogels showed the lowest number of hours within the therapeutic window.

Table 12 shows that TRIS 36.8 41.8 21.5 (NaCl) can deliver dexamethasone in the eye for 40 hours. mPDMS 36.7 (NaCl) showed the lowest time within the therapeutic window, only 2 hours. This result has to do with the nature of the hydrogel and the drug that, probably, prevented the loading and the subsequent release of dexamethasone. The high hydrophobic nature of this hydrogel together with the hydrophobic nature of dexamethasone could be the cause of the low efficiency of this type of hydrogel.

These results prove that TRIS 36.8 41.8 21.5, probably, has the best composition to be used as a contact lens for therapeutic purposes.

## 3.8 Global Discussion

In this work, hydrogels of different compositions were prepared and characterised in order to find optimised formulations which combine good drug release profiles with adequate characteristics as contact lens materials.

First of all, by taking into account that the requirements for an adequate contact lens material demand the presence of both hydrophilic and hydrophobic components, it was attempted several combinations of HEMA and DMA, as hydrophilic monomers, with TRIS and mPDMS, as hydrophobic ones. DMA is more hydrophilic than HEMA leading to a greater capacity of water absorption, while mPDMS was more hydrophobic than TRIS. Thus, combination of mPDMS with DMA leads to a compensation of effects. Moreover, the addition of NVP and/or SiGMA, highly hydrophilic and amphiphilic monomers respectively, was also determinant for the swelling behaviour.

In relation to the drug release behaviour, it was concluded that the increase in the amount of crosslinker present in the hydrogels decreases the quantity of diclofenac released. 8x EGDMA showed a decrease of almost tenfold compared to 1x EGDMA hydrogel. Also, the drug release behaviour proved to be influenced by the type of monomers present in the hydrogels. DMA 20 showed the highest cumulative diclofenac release due to the presence of DMA, which is considered a super water absorbent. The substitution of TRIS by mPDMS leads to higher swelling, drug loading and, consequently, drug release which was unexpected since mPDMS is more hydrophobic than TRIS. Comparison of the additives NVP and SiGMA shows that the presence of the former increases considerably the drug release probably due to its high hydrophilicity. The results obtained with the other drug tested in this work (dexamethasone) suggest that the hydrophobic nature of dexamethasone and its low solubility in aqueous solutions were the key factors for the low cumulative releases obtained with all hydrogels.

The wettability of the hydrogels depends on the type of method used to measure the water contact angles. Dry hydrogels measured with the sessile method were hydrophobic, while hydrated samples were hydrophilic. The most unexpected result was that the hydrophilicity/hydrophobicity of the hydrogels could not be directly correlated with the hydrophilicity/hydrophobicity of their components, but should be mostly determined by the morphology/topography of the surfaces. Unfortunately, this could not be confirmed by the SEM analysis which did not reveal significant differences among the hydrogels.

The surface energies of the hydrogels were not much dependent on the composition and varied within a narrow range (34-41 mJ $m^{-2}$).

The mechanical properties of the hydrogels were found to depend sharply on the amount of crosslinker: the hydrogel 8x EGDMA presented the largest Young's modulus and the lowest value of toughness. The hydrogels containing DMA have the lowest Young's modulus, but the values of toughness depended on all the monomers present.

Relatively to the water states in the hydrogels, it was observed that they vary with the amount of crosslinker, amount of hydrophilic monomers and also with the pore-size dimensions. The increase in the crosslinker leads to smaller pore-size dimensions, which in turn leads to higher amount of tightly bound water in the hydrogel, such as in the hydrogel 4x EGDMA. The increase of the hydrophilicity of the hydrogel's monomers leads to larger pore-size dimensions and consequently higher amount of free and loosely bound water, as shown by the hydrogel DMA 20. Also, a direct relationship between the cumulative drug released and the pore-size dimensions was found (larger pore-size dimensions lead to a higher cumulative drug release); DMA 20 and mPDMS 36.7 DMA 28.3 showed the largest pore-size dimensions and high cumulative diclofenac release.

Looking at the therapeutic purposes of these hydrogels, it was concluded that diclofenac or dexamethasone released from all hydrogels never reached the limits of toxicity for both drugs. The hydrogel TRIS 36.8 41.8 21.5 was considered the best hydrogel, delivering diclofenac and dexamethasone within the therapeutic window for 70 and 40 hours, respectively.

Analysing all the results obtained during this work, it is possible to draw some conclusions about the materials to be used as well as the relative amounts of each of them. DMA showed to be an excellent hydrophilic monomer capable of increasing the drug release while keeping the adequate mechanical properties, ionic permeability and transmittance. Moreover, the replacement of NVP by SiGMA seems not to be a good alternative, since it decreases the water content of the hydrogels and, consequently, decreases the drug release, ionic permeability and compromises the mechanical properties of the hydrogels. Another aspect that is necessary to take into account is the quantity of the crosslinker because, in high amounts, it can compromise not only the drug release behaviour but also the hydrogels' properties.

# 4 Conclusions and Future Work

## 4.1 Conclusions

The main goal of the present master thesis was to understand how the changes of the composition of the hydrogels, can induce modifications in their drug release behaviour and their physical properties. Nineteen different hydrogels were produced which were grouped in 5 sets. In each set a specific effect was evaluated, as follows;

- The influence of varying the amount of the crosslinker in hydrogels based on TRIS/NVP/HEMA;
- The effect of varying the percentage of the components in hydrogels based on TRIS/NVP/HEMA;
- The effect of interchanging the hydrophobic materials mPDMS and TRIS, frequently used as the silicone monomers in commercial lenses;
- The effect of interchanging the hydrophilic monomers DMA and HEMA, frequently used in commercial lenses;
- The effect of using both mPDMS and DMA as the silicone and hydrophilic materials respectively, instead of TRIS and HEMA.

Concerning the influence of the amount of crosslinker, it was observed that the increase in the amount of crosslinker led to a decrease in the cumulative diclofenac release, ionic permeability and swelling percentage. This result was expectable because a large amount of crosslinker makes the hydrogels' mesh tighter, which decreases the capacity of these hydrogels to absorb water and hampers the drug loading and release. Also, the increase in the amount of crosslinker affects the mechanical properties of hydrogels. The hydrogel 8x EGDMA showed a Young´s modulus of 7.6E+07 Pa ± 2E+06 Pa, about an order of magnitude above than the hydrogel where the normal amount of EGDMA was added (1x EGDMA). That hydrogel also showed the lowest value of elongation at break proving that, despite being strong is brittle. In conclusion, the increase in the amount of crosslinker in hydrogels could bring comfort issues for the $CL_s$ wearers.

Relatively to the hydrogels where the amounts of TRIS, NVP and HEMA were varied, it was observed that a minimum amount of NVP (40%, V/V %) was necessary in order to avoid the opacity of the hydrogels. With the increase in the amount of NVP, the cumulative diclofenac release, ionic permeability and swelling also increase, more evidently for the latter property. Again, this result was expectable because NVP is known to increase the water content of the $CL_s$ formulations. The hydrogels TRIS 34 50 16 and TRIS 36.8 41.8 21.5 showed Young's modulus a little above the values reported for commercial lenses. However, analysis of the elongation at break of these hydrogels shows that they have some resistance.

The hydrogels where the hydrophobic compound TRIS was substituted by mPDMS showed a higher cumulative diclofenac release. mPDMS 36.7 and TRIS 35 mPDMS 5 showed similar Young's modulus values compared with TRIS-based hydrogels, which have higher percentage of swelling and

consequently should have lower values of Young's modulus. At the same time, these hydrogels showed similar values of elongation at break compared with TRIS-based hydrogels.

The results obtained with TRIS-based hydrogels where the hydrophilic monomer HEMA was substituted by DMA, led to the conclusion that DMA is more hydrophilic than HEMA, leading to an increase in the swelling capacity. The cumulative diclofenac release and ionic permeability also increased in the majority of the cases. In these hydrogels, it was also used SiGMA for the solubilisation of the silicone monomer with the hydrophilic monomer. The hydrogel SiGMA 20 DMA 20 showed the lowest cumulative diclofenac release and swelling percentage proving that the addition of SiGMA leads to a significant decrease in the water absorbed by the hydrogel. The hydrogels with higher amount of DMA and lower amount of SiGMA showed lower Young's modulus and higher elongation at break. The Young's modulus obtained for DMA 20 is similar to the values reported for commercial lenses with similar compositions (Focus NIGHT & DAY® and $O_2$ OPTIX™). Overall, the adequate properties obtained especially with DMA 20 suggest that this hydrogel could be a good candidate for the use as a contact lens material.

The theory that DMA is more hydrophilic than HEMA is confirmed when comparing mPDMS 36.7 DMA 18.3 with mPDMS 36.7 (containing HEMA instead of DMA): although the drug release was similar it was observed a higher swelling percentage in the former. The Young's modulus value of mPDMS 36.7 DMA 28.3 is similar to the values reported for two known commercial lenses containing the same silicone material, ACUVUE® OASYS® and ACUVUE® ADVANCE®. Despite the low Young's modulus of mPDMS 36.7 DMA 28.3, this hydrogel showed the highest elongation at break, showing the toughness of the material. Due to the similarities with commercial lenses and other good characteristics, this type of hydrogel could be used for therapeutic contact lenses.

The release of dexamethasone was also evaluated. Lower amounts of drug were released from the hydrogels compared with diclofenac. Two possible explanations for this result could be the low solubility of this drug in aqueous mediums and its hydrophobic nature, which hampers the drug loading and release.

In the last part of the work, a more detailed characterization of the most promising formulations was done, being evaluated several other properties. In relation to the wettability, all hydrated hydrogels showed a hydrophilic surface (contact angles obtained with the captive bubble method around 40º). Wettability measurements carried out on the dry hydrogels allowed to estimate its surface energy. The low surface energy values and the predominance of the dispersive component, proved the lower hydrophilicity of the hydrogels in the dry state. This characteristic, which was observed even when a high percentage of hydrophilic monomers was present, may be attributed to the surface roughness of the dry hydrogels, according to the Cassie-Baxter model.

The pore-size dimensions of hydrogels can be related with the states of water inside their matrix: higher pore-size dimensions lead to higher quantities of free and loosely bound water. Another interesting result was obtained with 8x EGDMA that demonstrated that the increase in the amount of crosslinker increases the amount of tightly bound water due to the reduced pore-size dimensions compared with the other hydrogels.

Finally, the efficiency of the drug delivery of the hydrogels was assessed through the comparison of the concentration of the drugs released with the therapeutic windows of two commercially available ophthalmic drugs, Voltaren® (diclofenac) and Ronic® (dexamethasone). All hydrogels can efficiently deliver diclofenac and dexamethasone within the therapeutic window, being the hydrogel TRIS 36.8 41.8 21.5 the most efficient for the two drugs tested, with 70 hours and 40 hours of release, respectively.

Taking into account the drug release behaviours and all the properties studied throughout this work, it is possible to point out some hydrogels that have potential to be used as new drug carriers to the eye. The chosen hydrogels include: TRIS 34 50 16, TRIS 36.8 41.8 21.5, DMA 20, and mPDMS 36.7 DMA 28.3. However, most important than proposing alternative formulations was the attempt to better understand the role that each component of the hydrogel formulation plays in the hydrogel properties. Significant differences in the drug release behaviour as well as the water content and pore-size dimensions were observed due to the different contributions of the hydrophilic and hydrophobic materials.

## 4.2 Future Work

Throughout this work, a variety of hydrogels' formulations were studied in order to understand the role of each component on the performance of these materials as therapeutic $CL_s$.

Some important properties were assessed but, more properties should be studied, such as oxygen permeability and surface roughness. The oxygen permeability is an important parameter to ensure an adequate level of oxygenation of the eye and the surface roughness is also important because it affects the user's comfort.

Regarding the drug release, other drugs should be tested to have a more representative sampling of the behaviour of the hydrogels to different drugs. Since in this work it was tested anti-inflammatory drugs, it could be interesting to study drugs intended to treat other eye problems. These drugs could be, for example, ciprofloxacin (an antibiotic for eye infections treatment), ketotifen fumarate (an antihistamine for allergic conjunctivitis treatment) and timolol (a beta blocker for glaucoma treatment). Also, strategies to increase the drug loading and to improve the drug release kinetics, such as incorporating agents that interact with the drugs, should be attempted.

From the acquired knowledge, it would be easier now to design a more systematic investigation where the relative amounts of the most interesting components (TRIS, DMA, NVP) were changed. This does not preclude the test of other materials commonly associated to commercial $CL_s$, namely methacrylic acid (MAA), methyl methacrylate (MMA) and poly(vinylpyrrolidone) (PVP).

Finally, in vivo tests should be performed to confirm the adequacy of the best hydrogels as therapeutic contact lens materials.

# 5 Bibliography


1. Cholkar, K., Dasari, S. R. & Pal, D. in *Ocular Transporters and Receptors: Their Role in Drug Delivery* 1–36 (Woodhead Publishing Limited, 2013). doi:10.1533/9781908818317.1

2. Zhu, J., Zhang, E. & Del Rio-Tsonis, K. in *eLS* (John Wiley & Sons, Ltd, 2012).

3. Seeley, R. R., Stephens, T. D. & Tate, P. in *Anatomy & Physiology* 521–542 (McGraw-Hill, 2008).

4. Alvarez-Lorenzo, C., Hiratani, H. & Concheiro, A. Contact Lenses for Drug Delivery. *Am. J. Drug Deliv.* **4,** 131–151 (2006).

5. Patel, A., Cholkar, K., Agrahari, V. & Mitra, A. K. Ocular drug delivery systems: An overview. *World J Pharmacol.* **2,** 47–64 (2013).

6. Gaudana, R., Ananthula, H. K., Parenky, A. & Mitra, A. K. Ocular Drug Delivery. *AAPS J.* **12,** 348–360 (2010).

7. Hsu, K.-H., Gause, S. & Chauhan, A. Review of ophthalmic drug delivery by contact lenses. *J. Drug Deliv.* **24,** 123–135 (2014).

8. Guzman-Aranguez, A., Colligris, B. & Pintor, J. Contact Lenses: Promising Devices for Ocular Drug Delivery. *J. Ocul. Pharmacol. Ther.* **00,** 1–12 (2012).

9. White, C. J., Tieppo, A. & Byrne, M. E. Controlled drug release from contact lenses: a comprehensive review from 1965-present. *J. Drug Deliv. Sci. Technol.* **21,** 369–384 (2011).

10. Chauhan, A. Ophthalmic Drug Delivery Through Contact Lenses. *Contact Lens Spectr.* **27,** 23–29 (2012).

11. Bajpai, A. K., Shukla, S. K., Bhanu, S. & Kankane, S. Responsive polymers in controlled drug delivery. *Prog. Polym. Sci.* **33,** 1088–1118 (2008).

12. White, C. J. & Byrne, M. E. Molecularly imprinted therapeutic contact lenses. *Expert Opin. Drug Deliv.* (2010).

13. Costa, V. P. *et al.* Development of therapeutic contact lenses using a supercritical solvent impregnation method. *J. Supercrit. Fluids* **52,** 306–316 (2010).

14. Peng, C.-C., Kim, J. & Chauhan, A. Extended delivery of hydrophilic drugs from silicone-hydrogel contact lenses containing vitamin E diffusion barriers. *Biomaterials* **31,** 4032–47 (2010).

15. Kumar, A. & Jha, G. Drug delivery through soft contact lenses: An introduction. *Chronicles Young Sci.* **2,** 3 (2011).

16. Bengani, L. C., Hsu, K.-H., Gause, S. & Chauhan, A. Contact lenses as a platform for ocular drug delivery. *Expert Opin. Drug Deliv.* **10,** 1483–96 (2013).

17. Karlgard, C. C. S., Jones, L. W. & Moresoli, C. Ciprofloxacin interaction with silicon-based and conventional hydrogel contact lenses. *Eye Contact Lens* **29,** 83–9 (2003).

18. Garhwal, R. *et al.* Sustained ocular delivery of ciprofloxacin using nanospheres and conventional contact lens materials. *Invest. Ophthalmol. Vis. Sci.* **53,** 1341–52 (2012).

19. Kim, M. J. *et al.* Optimal concentration of human epidermal growth factor (hEGF) for epithelial healing in experimental corneal alkali wounds. *Curr. Eye Res.* **22,** 272–9 (2001).

20. Razmjoo, H. *et al.* Comparative Study of Two Silicone Hydrogel Contact Lenses used as Bandage Contact Lenses after Photorefractive Keratectomy. *Int. J. Prev. Med.* **3,** 718–22 (2012).

21. Corren, J. in *Middleton's Allergy Essentials* 205–224 (2016).

22. Tieppo, A. *et al.* Sustained in vivo release from imprinted therapeutic contact lenses. *J. Control. Release* **157,** 391–7 (2012).

23. Maulvi, F. A., Soni, T. G. & Shah, D. O. Extended release of hyaluronic acid from hydrogel

contact lenses for dry eye syndrome. *J. Biomater. Sci. Polym. Ed.* **26,** 1035–50 (2015).

24. Hsu, K.-H., Carbia, B. E., Plummer, C. & Chauhan, A. Dual drug delivery from vitamin E loaded contact lenses for glaucoma therapy. *Eur. J. Pharm. Biopharm.* **94,** 312–21 (2015).

25. Peng, C.-C., Burke, M. T., Carbia, B. E., Plummer, C. & Chauhan, A. Extended drug delivery by contact lenses for glaucoma therapy. *J. Control. Release* **162,** 152–8 (2012).

26. Saraiya, N. V & Goldstein, D. A. Dexamethasone for ocular inflammation. *Expert Opin. Pharmacother.* **12,** 1127–31 (2011).

27. Cho, H., Wolf, K. J. & Wolf, E. J. Management of ocular inflammation and pain following cataract surgery: focus on bromfenac ophthalmic solution. *Clin. Ophthalmol.* **3,** 199–210 (2009).

28. O'Brien, T. P. Emerging guidelines for use of NSAID therapy to optimize cataract surgery patient care. *Curr. Med. Res. Opin.* **21,** 1131–7 (2005).

29. Pubchem. Diclofenac Sodium. Available at: https://pubchem.ncbi.nlm.nih.gov/compound/5018304#section=Top. (Accessed: 24th April 2016)

30. Diclofenac Sodium Salt. Available at: http://www.sigmaaldrich.com/catalog/product/sigma/d174?lang=pt&region=PT. (Accessed: 24th April 2016)

31. Pubchem. Dexamethasone. Available at: https://pubchem.ncbi.nlm.nih.gov/compound/5743#section=Top. (Accessed: 24th April 2016)

32. Dexamethasone. Available at: http://www.sigmaaldrich.com/catalog/product/sigma/d1756?lang=pt&region=PT. (Accessed: 24th April 2016)

33. Sánchez Ferreiro, A. V. & Muñoz Bellido, L. Evolution and history of contact lenses. *Arch. la Soc. Española Oftalmol. (English Ed.* **87,** 265–266 (2012).

34. Schifrin, L. G. & Rich, W. J. in *The Contact Lens Industry Structure, Competition, and Public Policy* 9–12 (1984).

35. Contacts, 1800. Da Vinci to Disposable: A History of Contact Lenses. (2014). Available at: http://www.1800contacts.com/connect/articles/da-vinci-disposable-history-contact-lenses#vinci.

36. Chirila, T. *Biomaterials and Regenerative Medicine in Ophthalmology*. (Woodhead Publishing Limited and CRC Press LLC, 2010).

37. FDA. U.S. Food and Drug Administration. *Types of Contact Lenses* (2015). Available at: http://www.fda.gov/MedicalDevices/ProductsandMedicalProcedures/HomeHealthandConsumer/ConsumerProducts/ContactLenses/ucm062319.htm#rgp.

38. Boyd, K. & Pagan-Duran, B. American Academy of Ophthalmology. *Contact Lens Types* (2016). Available at: http://www.aao.org/salud-ocular/consejos/contact-lens-types.

39. The European Contact Lens Forum (ECLF). *Today's Truth about Contact Lenses*. (2009).

40. EUROMCONTACT a.i.s.b.l. *A Comparison of European Soft Contact Lens and Lens Care Markets in 2014*. (2015).

41. Dumbleton, K. The Physical and Clinical Characteristics of Silicone Hydrogel Lenses: How They Work? *Silicone Hydrogels* (2002). Available at: http://www.siliconehydrogels.org/editorials/previous_editorials_kathryn.asp. (Accessed: 19th October 2015)

42. Tranoudis, I. & Efron, N. Tensile properties of soft contact lens materials. *Cont. Lens Anterior Eye* **27,** 177–91 (2004).

43. Efron, N. & Maldonado-Codina, C. Development of Contact Lenses from a Biomaterial Point of View – Materials, Manufacture, and Clinical Application. *Comprehensive Biomaterials* (2011).

44. Jones, L. & Tighe, B. Silicone Hydrogel Contact Lens Materials Update - Part 1. *Silicone Hydrogels* (2004). Available at: http://www.siliconehydrogels.org/editorials/index_july.asp.

45. Stapleton, F., Stretton, S., Papas, E., Skotnitsky, C. & Sweeney, D. F. Silicone Hydrogel Contact Lenses and the Ocular Surface. *Ocul. Surf.* **4,** 24–43 (2006).

46. Chou, B. The Evolution of Silicone Hydrogel Lenses. *Contact Lens Spectr.* (2008).

47. Nicolson, P. C. & Vogt, J. Soft contact lens polymers: an evolution. *Biomaterials* **22,** 3273–3283 (2001).

48. Garrett, Q. & Milthorpe, B. K. Human serum albumin adsorption on hydrogel contact lenses in vitro. *Invest. Ophthalmol. Vis. Sci.* **37,** 2594–2602 (1996).

49. Bohnert, J. L., Horbett, T. A., Ratner, B. D. & Royce, F. H. Adsorption of proteins from artificial tear solutions to contact lens materials. *Invest. Ophthalmol. Vis. Sci.* **29,** 362–373 (1988).

50. Garrett, Q., Laycock, B. & Garrett, R. W. Hydrogel lens monomer constituents modulate protein sorption. *Invest. Ophthalmol. Vis. Sci.* **41,** 1687–95 (2000).

51. Ademović, Z., Marić, S., Kingshott, P. & Iličković, Z. Hydrogel from Polyacrylic Acid for Reduction of Bioadhesion on Silicone Contact Lenses. *Contemporary Materials* **1,** 95–100 (2014).

52. Tighe, B. Trends and Developments in Silicone Hydrogel Materials. *Silicone Hydrogels* (2006). Available at: http://www.siliconehydrogels.org/editorials/sep_06.asp. (Accessed: 2nd May 2016)

53. Kim, J., Conway, A. & Chauhan, A. Extended delivery of ophthalmic drugs by silicone hydrogel contact lenses. *Biomaterials* **29,** 2259–69 (2008).

54. 3-[Tris(trimethylsiloxy)silyl]propyl methacrylate (TRIS). Available at: http://www.sigmaaldrich.com/catalog/product/aldrich/446130?lang=pt&region=PT. (Accessed: 7th May 2016)

55. 2-Hydroxyethyl methacrylate (HEMA). Available at: http://www.sigmaaldrich.com/catalog/product/aldrich/525464?lang=pt&region=PT. (Accessed: 2nd May 2016)

56. N,N-Dimethylacrylamide (DMA). Available at: http://www.sigmaaldrich.com/catalog/product/aldrich/274135?lang=pt&region=PT. (Accessed: 7th May 2016)

57. 1-Vinyl-2-pyrrolidinone (NVP). Available at: http://www.sigmaaldrich.com/catalog/product/sial/95060?lang=pt&region=PT. (Accessed: 2nd May 2016)

58. Gelest. Monomethacryloxypropyl terminated Polydimethylsiloxane. Available at: http://shop.gelest.com/Product.aspx?catnum=MCR-M22&Index=0&TotalCount=1. (Accessed: 10th May 2016)

59. Sweeney, D., Fonn, D. & Evans, K. Silicone Hydrogels: The Evolution of a Revolution. *Contact Lens Spectr.* (2006).

60. Pérez-Ortíz, N., Navarro-Villoslada, F., Orellana, G. & Moreno-Jiménez, F. Determination of the oxygen permeability (Dk) of contact lenses with a fiber-optic luminescent sensor system. *Sensors Actuators B Chem.* **126,** 394–399 (2007).

61. Brennan, N. A., Coles, M.-L. C. & Ang, J. H.-B. An evaluation of silicone-hydrogel lenses worn on a daily wear basis. *Clin. Exp. Optom.* **89,** 18–25 (2006).

62. Lira, M. *et al.* Changes in UV-visible transmittance of silicone-hydrogel contact lenses induced by wear. *Optom. Vis. Sci.* **86,** 332–9 (2009).

63. Peng, C.-C. & Chauhan, A. Ion transport in silicone hydrogel contact lenses. *J. Memb. Sci.* **399-400,** 95–105 (2012).

64. Paradiso, P. *et al.* Comparison of two hydrogel formulations for drug release in ophthalmic

lenses. *J. Biomed. Mater. Res. B. Appl. Biomater.* **102,** 1170–80 (2014).

65. Nicolson, P. C. *et al.* Extended wear ophthalmic lens. (1998).

66. Zhu, J. & Marchant, R. E. Design properties of hydrogel tissue-engineering scaffolds. *Expert Rev. Med. Devices* **8,** 607–26 (2011).

67. Ganji, F., Farahani, S. V. & Vasheghani-Farahani, E. Theoretical Description of Hydrogel Swelling: A Review. *Iran. Polym. J.* **19,** 375–398 (2010).

68. Cursaru, B., Stanescu, P. O. & Teodorescu, M. The states of water in hydrogels synthesized from diepoxy-terminated poly(ethylene glycol)s and aliphatic polyamines. *UPB Sci. Bull. Ser. B Chem. Mater. Sci.* **72,** 99–114 (2010).

69. Tranoudis, I. & Efron, N. Water properties of soft contact lens materials. *Cont. Lens Anterior Eye* **27,** 193–208 (2004).

70. Zauer, M., Kretzschmar, J., Großmann, L., Pfriem, A. & Wagenführ, A. Analysis of the pore-size distribution and fiber saturation point of native and thermally modified wood using differential scanning calorimetry. *Wood Sci. Technol.* **48,** 177–193 (2013).

71. Watson, H. Understanding the differential scanning calorimetry of PCMs. *Pure Temp* (2014). Available at: http://www.puretemp.com/stories/dsc.

72. Park, S., Venditti, R., Jameel, H. & Pawlak, J. Changes in pore size distribution during the drying of cellulose fibers as measured by differential scanning calorimetry. *Carbohydr. Polym.* **66,** 97–103 (2006).

73. Landry, M. R. Thermoporometry by differential scanning calorimetry: experimental considerations and applications. *Thermochim. Acta* **433,** 27–50 (2005).

74. Wulff, M. Pore size determination by thermoporometry using acetonitrile. *Thermochim. Acta* **419,** 291–294 (2004).

75. Brun, M., Lallemand, A., Quinson, J.-F. & Eyraud, C. A new method for the simultaneous determination of the size and shape of pores: the thermoporometry. *Thermochim. Acta* **21,** 59–88 (1977).

76. Read, M. L., Morgan, P. B. & Maldonado-Codina, C. Measurement errors related to contact angle analysis of hydrogel and silicone hydrogel contact lenses. *J. Biomed. Mater. Res. B. Appl. Biomater.* **91,** 662–8 (2009).

77. Keir, N. & Jones, L. Wettability and silicone hydrogel lenses: a review. *Eye Contact Lens* **39,** 100–8 (2013).

78. Lin, M. C. & Svitova, T. F. Contact lenses wettability in vitro: effect of surface-active ingredients. *Optom. Vis. Sci.* **87,** 440–7 (2010).

79. Menzies, K. L. & Jones, L. The impact of contact angle on the biocompatibility of biomaterials. *Optom. Vis. Sci.* **87,** 387–99 (2010).

80. Holly, F. J. & Refojo, M. F. Wettability of hydrogels. I. Poly (2-hydroxyethyl methacrylate). *J. Biomed. Mater. Res.* **9,** 315–26 (1975).

81. Shin, S. *et al.* Bio-Inspired Extreme Wetting Surfaces for Biomedical Applications. *Materials (Basel).* **9,** 116 (2016).

82. Wang, Y. *et al.* Interfacial Structures, Surface Tensions, and Contact Angles of Diiodomethane on Fluorinated Polymers. *J. Phys. Chem. C* **118,** 10143–10152 (2014).

83. Whyman, G., Bormashenko, E. & Stei, T. The rigorous derivation of Young, Cassie–Baxter and Wenzel equations and the analysis of the contact angle hysteresis phenomenon. *Chem. Phys. Lett.* **450,** 355–359 (2008).

84. Campbell, D., Carnell, S. M. & Eden, R. J. Applicability of contact angle techniques used in the analysis of contact lenses, part 1: comparative methodologies. *Eye Contact Lens* **39,** 254–62

(2013).

85. Correia, N. T., Ramos, J. J. M., Saramago, B. J. V. & Calado, J. C. G. Estimation of the Surface Tension of a Solid: Application to a Liquid Crystalline Polymer. *J. Colloid Interface Sci.* **189,** 361–369 (1997).

86. Fowkes, F. M. Attractive Forces at Interfaces. *Ind. Eng. Chem.* **56,** 40–52 (1964).

87. Adão, Saramago & Fernandes. Estimation of the Surface Properties of Styrene-Acrylonitrile Random Copolymers from Contact Angle Measurements. *J. Colloid Interface Sci.* **217,** 94–106 (1999).

88. Guryca, V., Hobzová, R., Prádný, M., Sirc, J. & Michálek, J. Surface morphology of contact lenses probed with microscopy techniques. *Cont. Lens Anterior Eye* **30,** 215–22 (2007).

89. Swapp, S. Scanning Electron Microscopy (SEM). *Geochemical Instrumentation and Analysis* Available at: http://serc.carleton.edu/research_education/geochemsheets/techniques/SEM.html. (Accessed: 11th May 2016)

90. Kato, M. Theoretical analysis of scanning electron microscopes with plural detectors as an application field of photometric stereo. *MVA* 183–186 (1992).

91. Liu, F., Wu, J., Chen, K. & Xue, D. Morphology Study by Using Scanning Electron Microscopy. *Microsc. Sci. Technol. Appl. Educ.* 1781–1792 (2010).

92. Laboratories, S. How SEM Works. Available at: http://www.seallabs.com/how-sem-works.html. (Accessed: 11th May 2016)

93. French, K. Contact lens material properties Part 2 - Mechanical behaviour and modulus. *Contact Lens Mon.* **230,** 29–34 (2005).

94. French, K. Why is modulus important? *Silicone Hydrogels* (2007). Available at: http://www.siliconehydrogels.org/editorials/oct_07.asp.

95. Teo, T. J., Yang, G. & Chen, I.-M. in *Handbook of Manufacturing Engineering and Technology* 1–63 (Springer London, 2014).

96. Rosenfield, M., Logan, N. & Edwards, K. H. in *Optometry: Science, Techniques and Clinical Management* 335–356 (Elsevier Health Sciences, 2009).

97. Szczotka-Flynn, L. Looking at Silicone Hydrogels Across Generations. (2008). Available at: http://www.optometricmanagement.com/articleviewer.aspx?articleid=101727. (Accessed: 17th October 2015)

98. Yañez, F., Concheiro, A. & Alvarez-Lorenzo, C. Macromolecule release and smoothness of semi-interpenetrating PVP-pHEMA networks for comfortable soft contact lenses. *Eur. J. Pharm. Biopharm. Off. J. Arbeitsgemeinschaft für Pharm. Verfahrenstechnik e.V* **69,** 1094–103 (2008).

99. Vendra, V. K., Wu, L. & Krishnan, S. Polymer Thin Films for Biomedical Applications. *Nanotechnologies Life Sci.* (2011).

100. Vazquez, R., Nogueira, R., Orfão, M., Mata, J. L. & Saramago, B. Stability of triglyceride liquid films on hydrophilic and hydrophobic glasses. *J. Colloid Interface Sci.* **299,** 274–82 (2006).

101. Guidi, G. Silicone Hydrogels and their use as Ophthalmic Drug Delivery Systems. (McMaster University, Canada, 2013).

102. Lahooti, S., Rio, O. Del, Neumann, A. W. & Cheng, P. Axisymmetric drop shape analysis. *Applied Surface Thermodynamics* (1996).

103. Akhtar, M. F., Ranjha, N. M. & Hanif, M. Effect of ethylene glycol dimethacrylate on swelling and on metformin hydrochloride release behavior of chemically crosslinked pH-sensitive acrylic acid-polyvinyl alcohol hydrogel. *Daru* **23,** 41 (2015).

104. Singh, B., Chauhan, G. S., Kumar, S. & Chauhan, N. Synthesis, characterization and swelling

responses of pH sensitive psyllium and polyacrylamide based hydrogels for the use in drug delivery (I). *Carbohydr. Polym.* **67,** 190–200 (2007).

105. Herman F. Mark. in *Encyclopedia of Polymer Science and Technology, Concise* 557–562 (2013).

106. Okay, O. in *Hydrogel Sensors and Actuators* (ed. G. Gerlach and K.-F. Arndt) 1–14 (Springer Series on Chemical Sensors and Biosensors, 2009).

107. Maldonado-Codina, C. & Morgan, P. B. In vitro water wettability of silicone hydrogel contact lenses determined using the sessile drop and captive bubble techniques. *J. Biomed. Mater. Res. A* **83,** 496–502 (2007).

108. Billmeyer, J. F. in *Textbook of polymer science* (ed. Billmeyer, J. F.) 229–257 (1984).

109. Infarmed. Folheto Informativo: Voltaren 1 mg/ml Colírio. 4 (2011). Available at: http://www.infarmed.pt/infomed/download_ficheiro.php?med_id=9289&tipo_doc=fi.

110. Infarmed. Folheto Informativo: Ronic 1 mg/ml colírio. 5 (2011). Available at: http://www.infarmed.pt/infomed/download_ficheiro.php?med_id=5403&tipo_doc=fi.

111. German, E., Hurst, M. & Wood, D. Reliability of drop size from multi-dose eye drop bottles: is it cause for concern? *Eye* **13,** 93–100 (1999).

112. Paradiso, P., Serro, A. P., Saramago, B., Colaço, R. & Chauhan, A. Controlled Release of Antibiotics From Vitamin E-Loaded Silicone-Hydrogel Contact Lenses. *J. Pharm. Sci.* **105,** 1164–72 (2016).

# Annex A.1

Therapeutic windows analysis for all hydrogels' formulations

**Diclofenac Release**

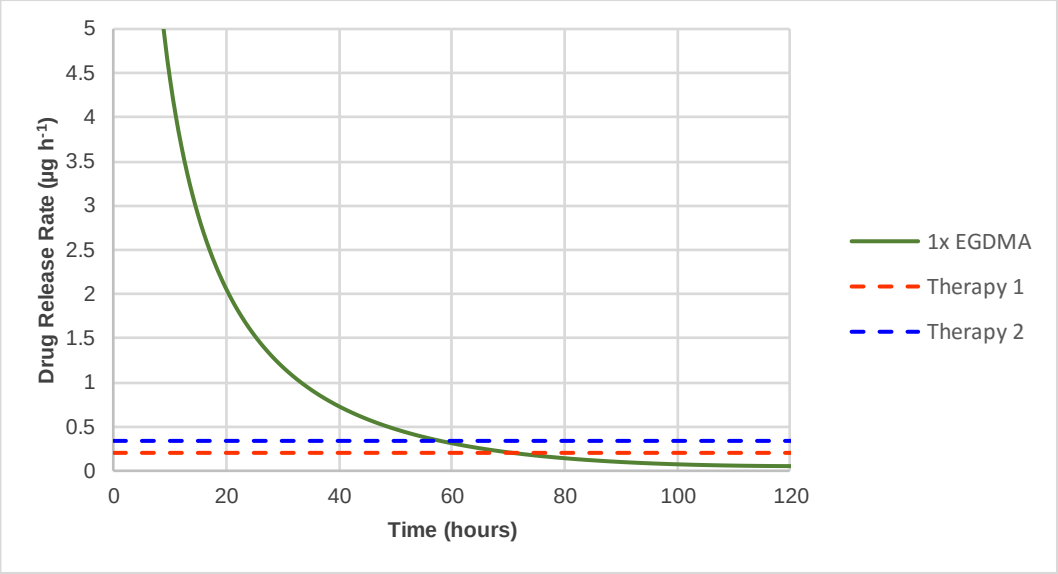


**Figure 1 -** Hourly average release rate for 1x EGDMA hydrogel. Drug release rates of Voltaren® are reported by the dashed lines (therapy 1 – minimum posology; therapy 2 – maximum posology).

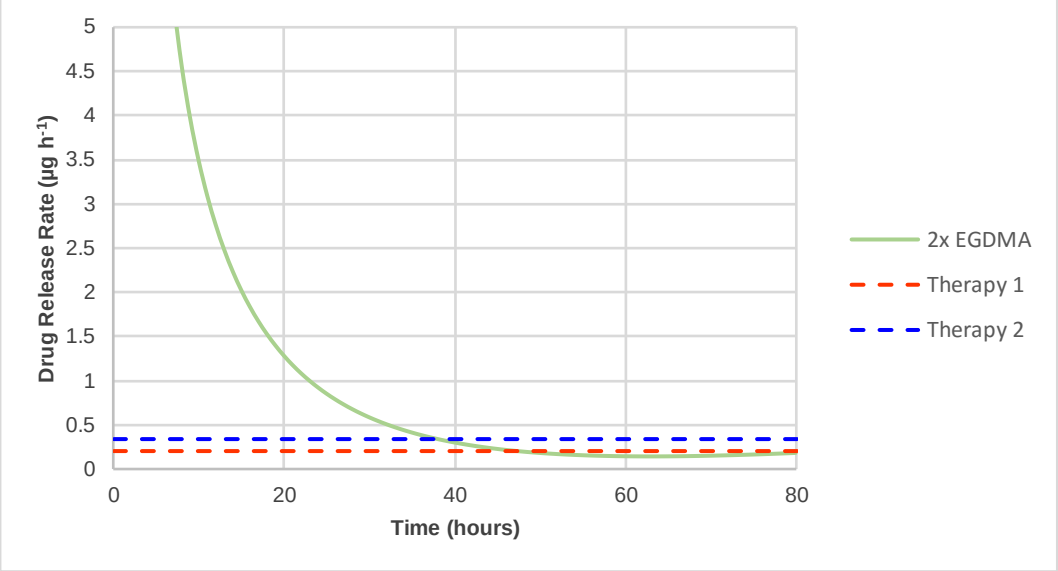


**Figure 2 -** Hourly average release rate for 2x EGDMA hydrogel. Drug release rates of Voltaren® are reported by the dashed lines (therapy 1 – minimum posology; therapy 2 – maximum posology).

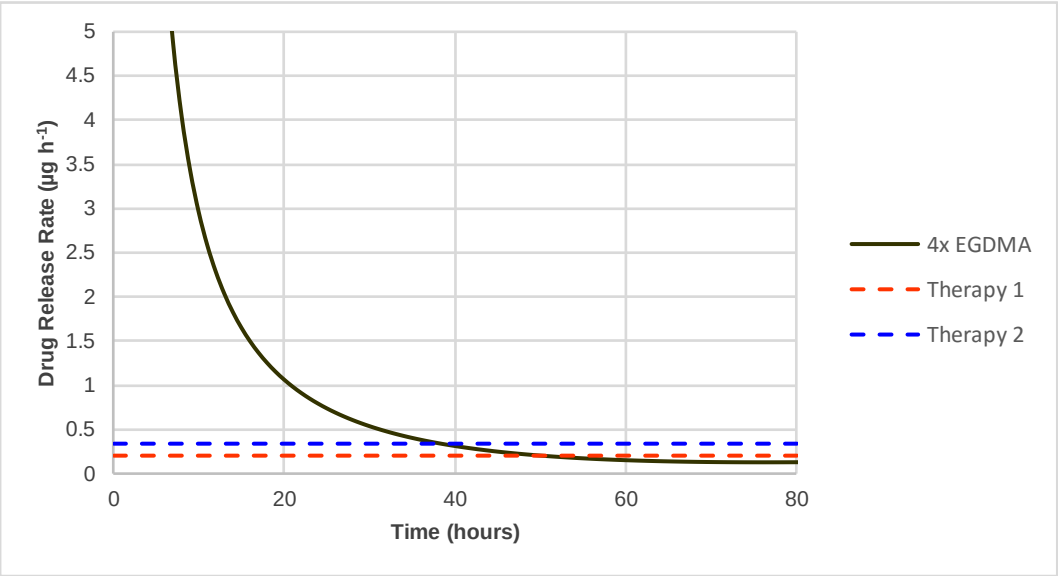


**Figure 3 -** Hourly average release rate for 4x EGDMA hydrogel. Drug release rates of Voltaren® are reported by the dashed lines (therapy 1 – minimum posology; therapy 2 – maximum posology).

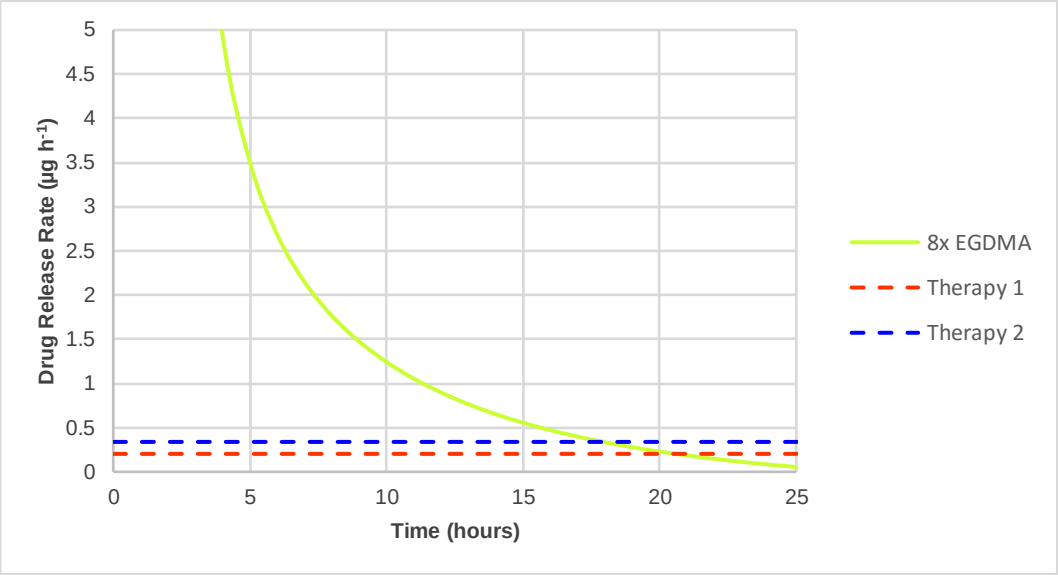


**Figure 4 -** Hourly average release rate for 8x EGDMA hydrogel. Drug release rates of Voltaren® are reported by the dashed lines (therapy 1 – minimum posology; therapy 2 – maximum posology).

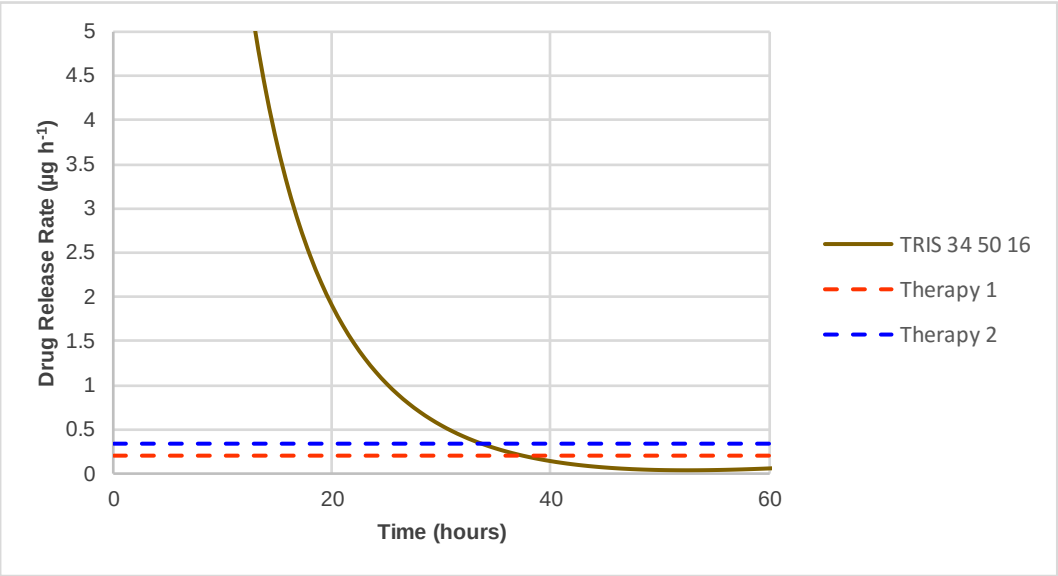


**Figure 5 -** Hourly average release rate for TRIS 34 50 16 hydrogel. Drug release rates of Voltaren® are reported by the dashed lines (therapy 1 – minimum posology; therapy 2 – maximum posology).

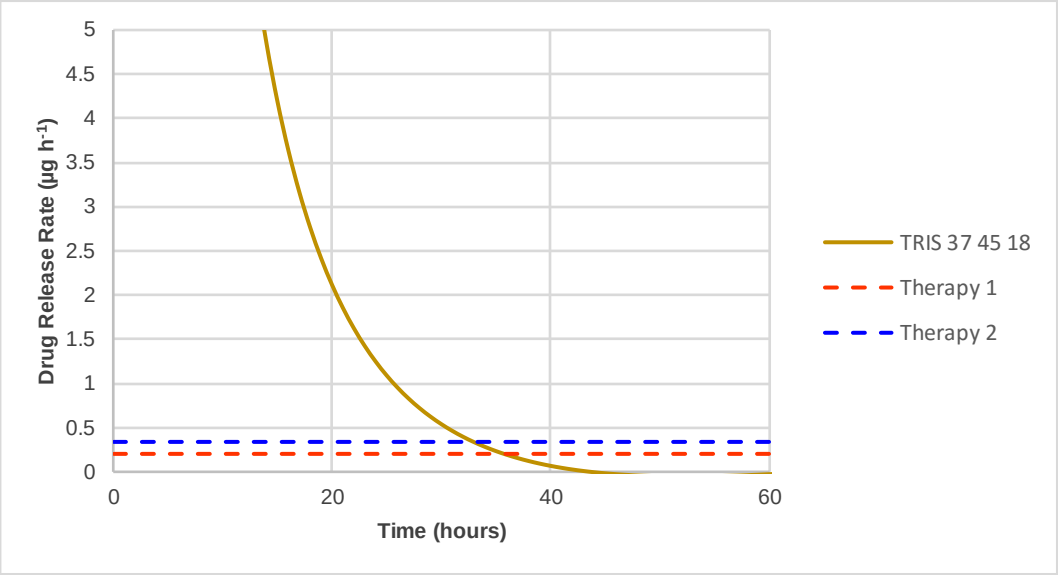


**Figure 6 -** Hourly average release rate for TRIS 37 45 18 hydrogel. Drug release rates of Voltaren® are reported by the dashed lines (therapy 1 – minimum posology; therapy 2 – maximum posology).

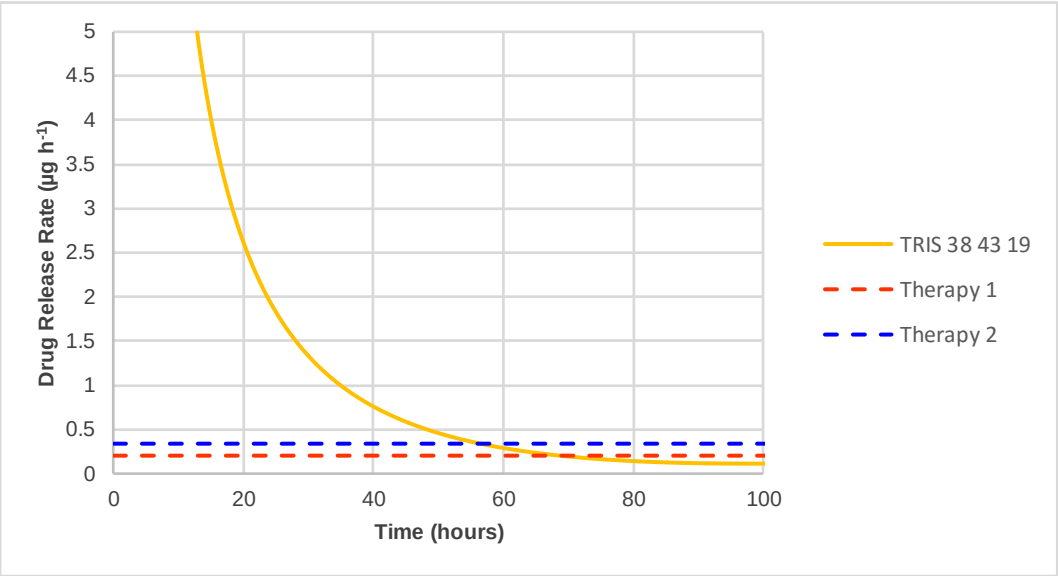


**Figure 7 -** Hourly average release rate for TRIS 38 43 19 hydrogel. Drug release rates of Voltaren® are reported by the dashed lines (therapy 1 – minimum posology; therapy 2 – maximum posology).

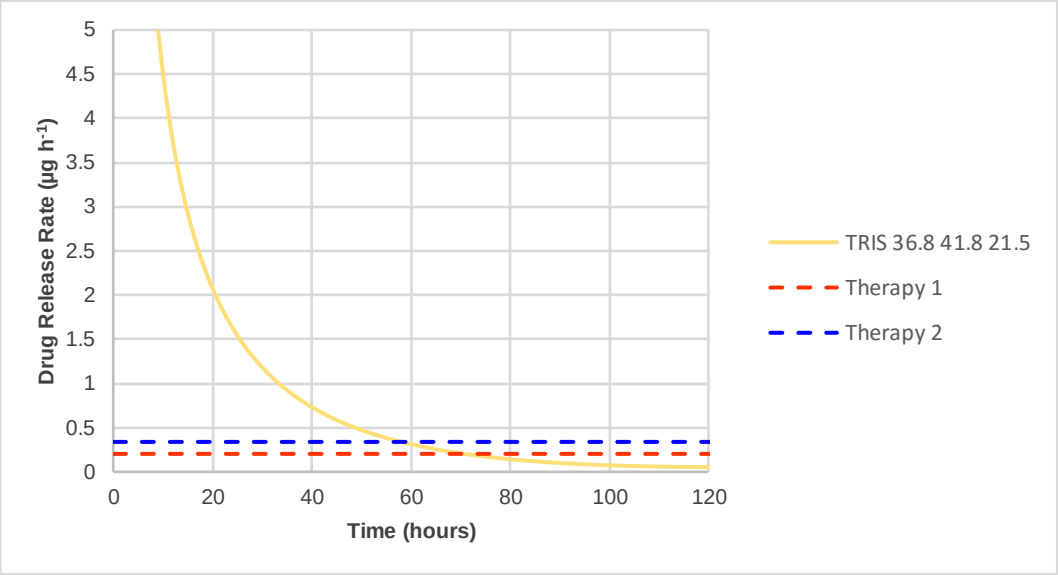


**Figure 8 -** Hourly average release rate for TRIS 36.8 41.8 21.5 hydrogel. Drug release rates of Voltaren® are reported by the dashed lines (therapy 1 – minimum posology; therapy 2 – maximum posology).

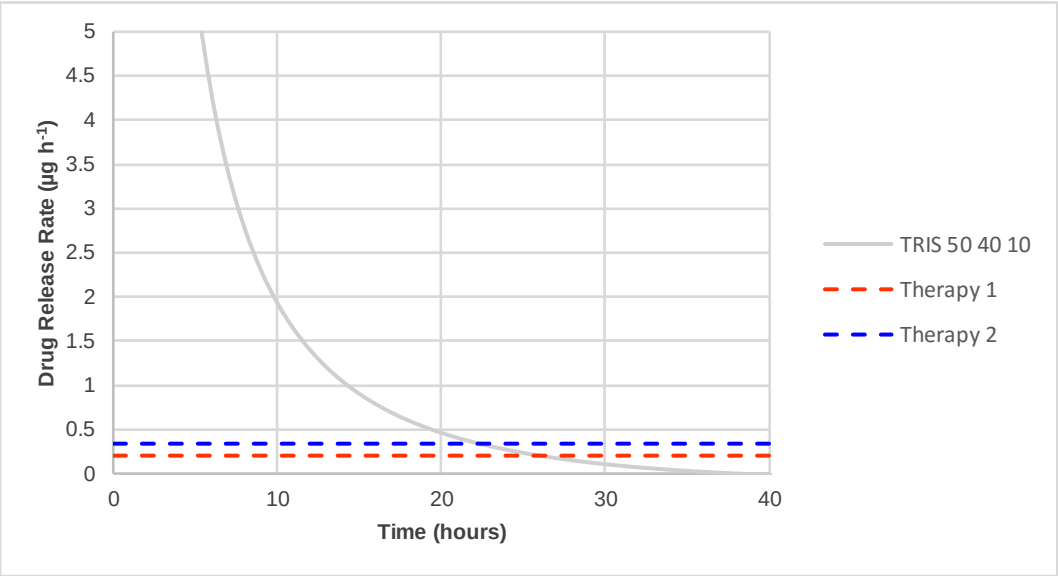


**Figure 9 -** Hourly average release rate for TRIS 50 40 10 hydrogel. Drug release rates of Voltaren® are reported by the dashed lines (therapy 1 – minimum posology; therapy 2 – maximum posology).

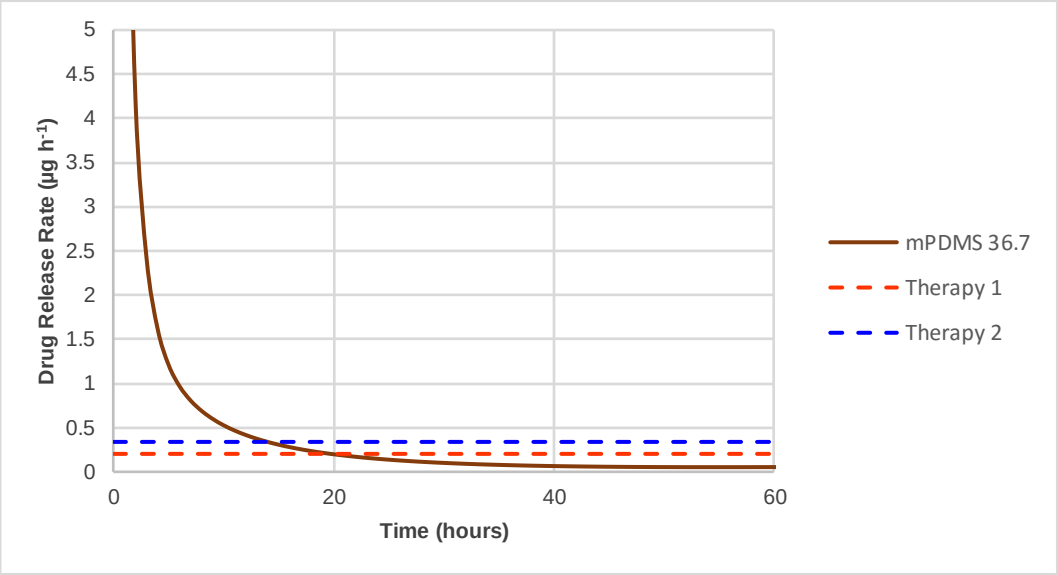


**Figure 10 -** Hourly average release rate for mPDMS 36.7 hydrogel. Drug release rates of Voltaren® are reported by the dashed lines (therapy 1 – minimum posology; therapy 2 – maximum posology).

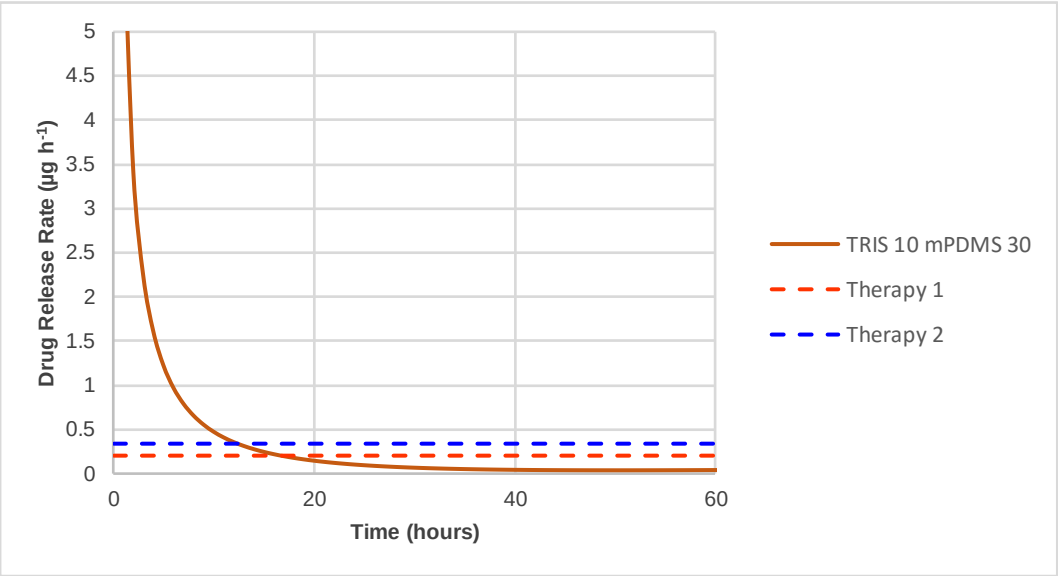


**Figure 11 -** Hourly average release rate for TRIS 10 mPDMS 30 hydrogel. Drug release rates of Voltaren® are reported by the dashed lines (therapy 1 – minimum posology; therapy 2 – maximum posology).

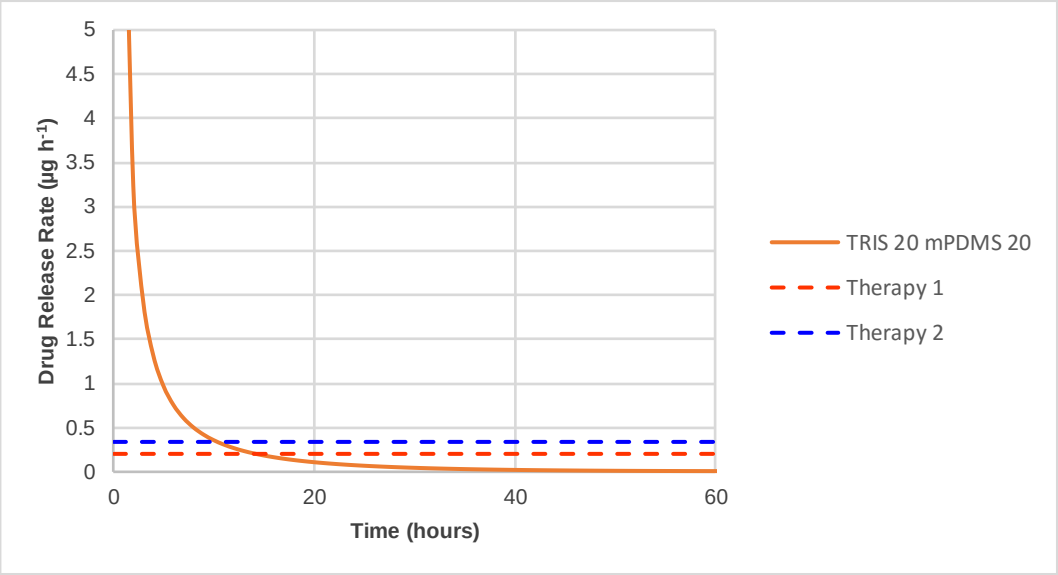


**Figure 12 -** Hourly average release rate for TRIS 20 mPDMS 20 hydrogel. Drug release rates of Voltaren® are reported by the dashed lines (therapy 1 – minimum posology; therapy 2 – maximum posology).

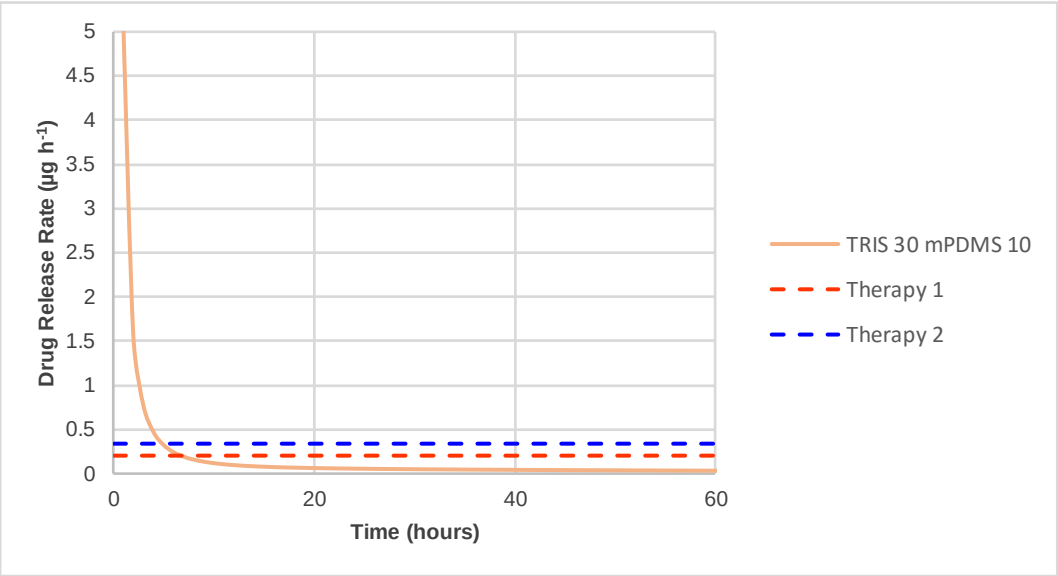


**Figure 13 -** Hourly average release rate for TRIS 30 mPDMS 10 hydrogel. Drug release rates of Voltaren® are reported by the dashed lines (therapy 1 – minimum posology; therapy 2 – maximum posology).

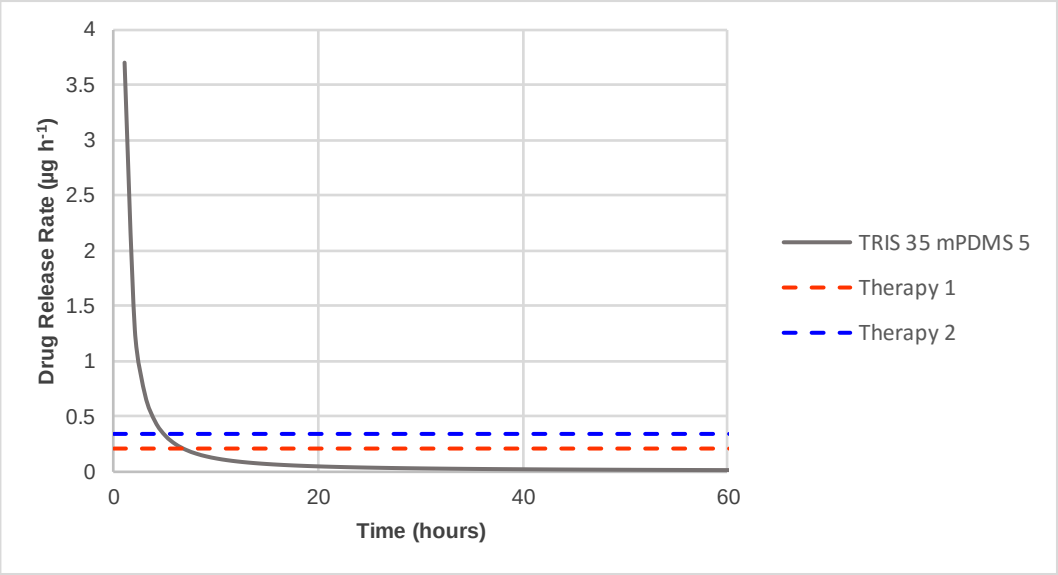


**Figure 14 -** Hourly average release rate for TRIS 35 mPDMS 5 hydrogel. Drug release rates of Voltaren® are reported by the dashed lines (therapy 1 – minimum posology; therapy 2 – maximum posology).

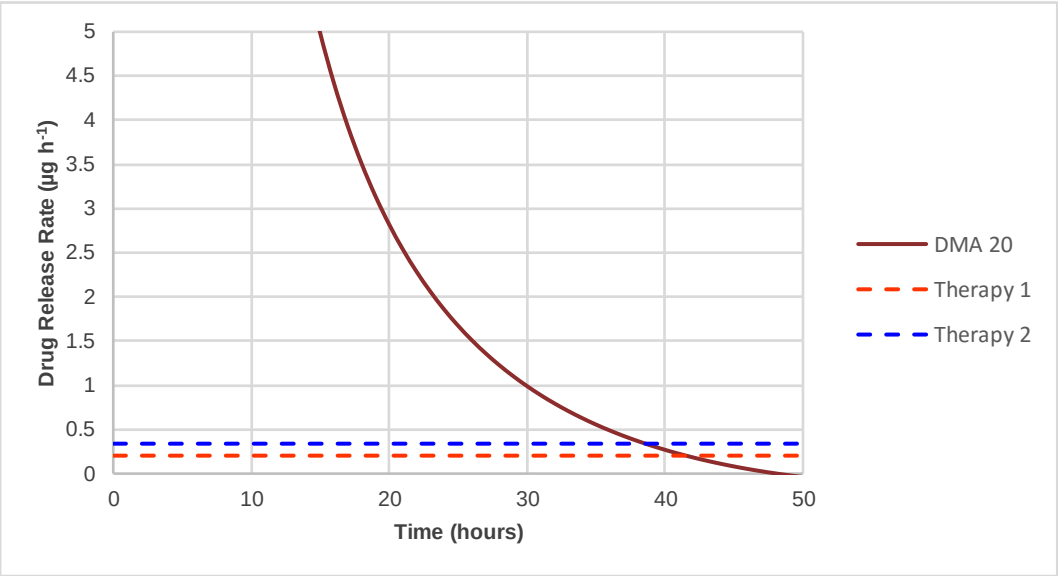


**Figure 15 -** Hourly average release rate for DMA 20 hydrogel. Drug release rates of Voltaren® are reported by the dashed lines (therapy 1 – minimum posology; therapy 2 – maximum posology).

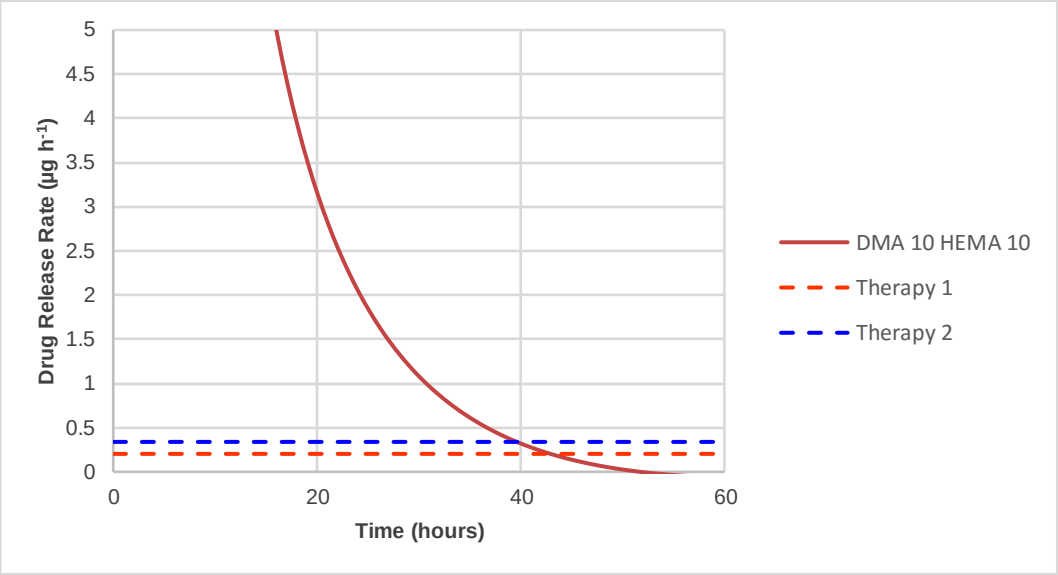


**Figure 16 -** Hourly average release rate for DMA 10 HEMA 10 hydrogel. Drug release rates of Voltaren® are reported by the dashed lines (therapy 1 – minimum posology; therapy 2 – maximum posology).

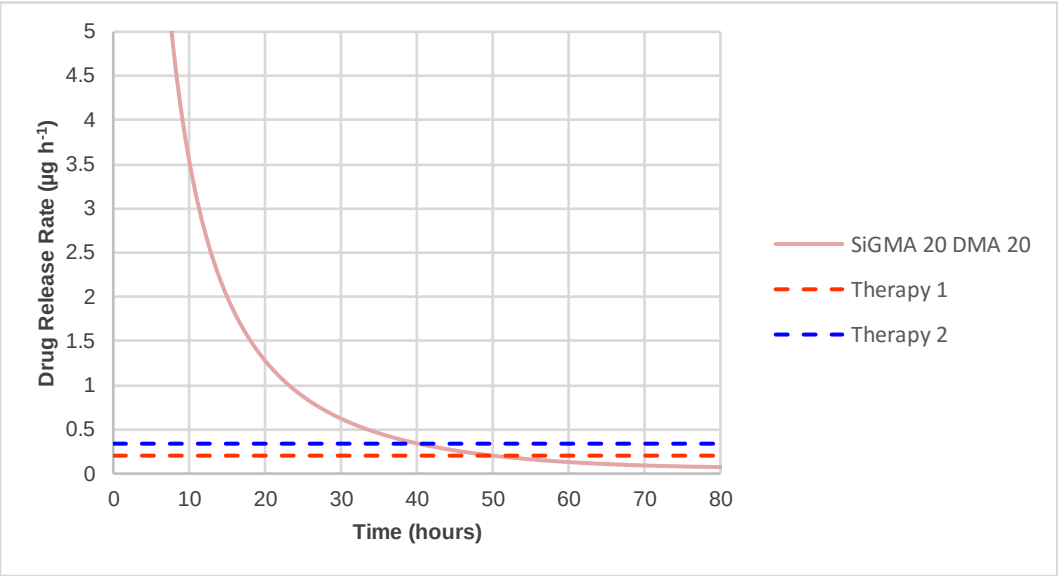


**Figure 17 -** Hourly average release rate for SiGMA 20 DMA 20 hydrogel. Drug release rates of Voltaren® are reported by the dashed lines (therapy 1 – minimum posology; therapy 2 – maximum posology).

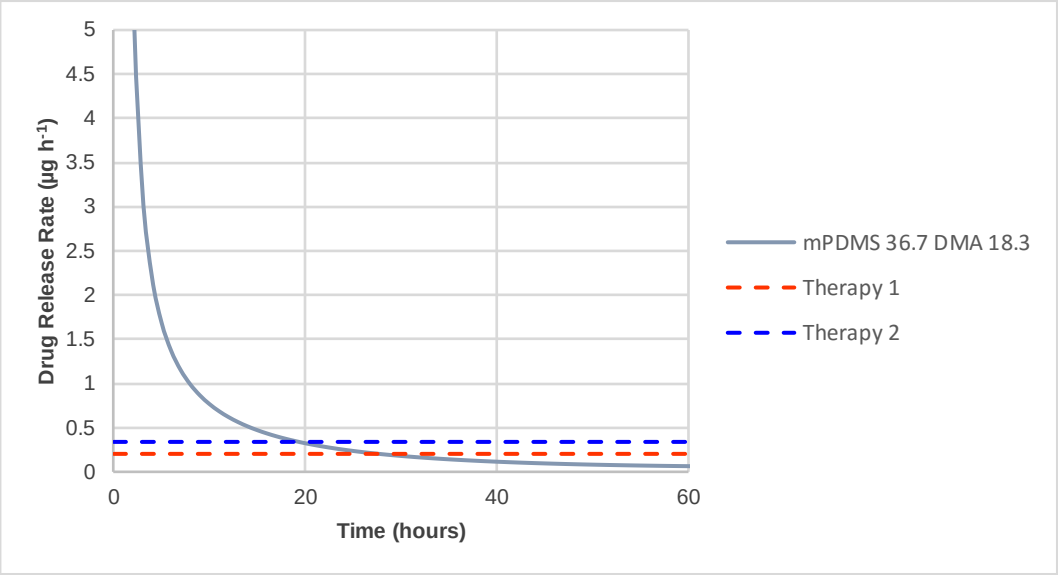


**Figure 18 -** Hourly average release rate for mPDMS 36.7 DMA 18.3 hydrogel. Drug release rates of Voltaren® are reported by the dashed lines (therapy 1 – minimum posology; therapy 2 – maximum posology).

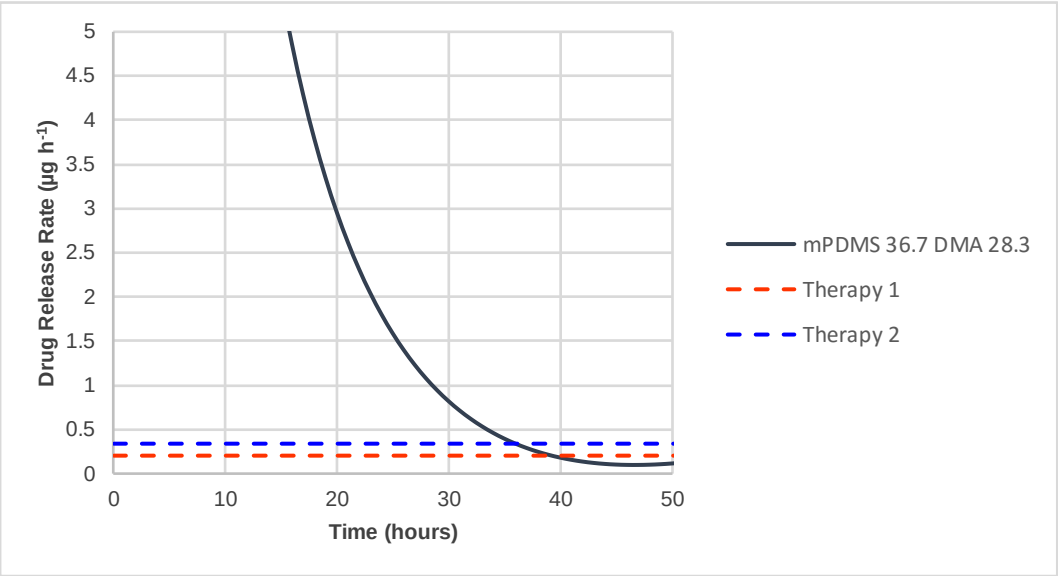


**Figure 19 -** Hourly average release rate for mPDMS 36.7 DMA 28.3 hydrogel. Drug release rates of Voltaren® are reported by the dashed lines (therapy 1 – minimum posology; therapy 2 – maximum posology).

## Dexamethasone Release

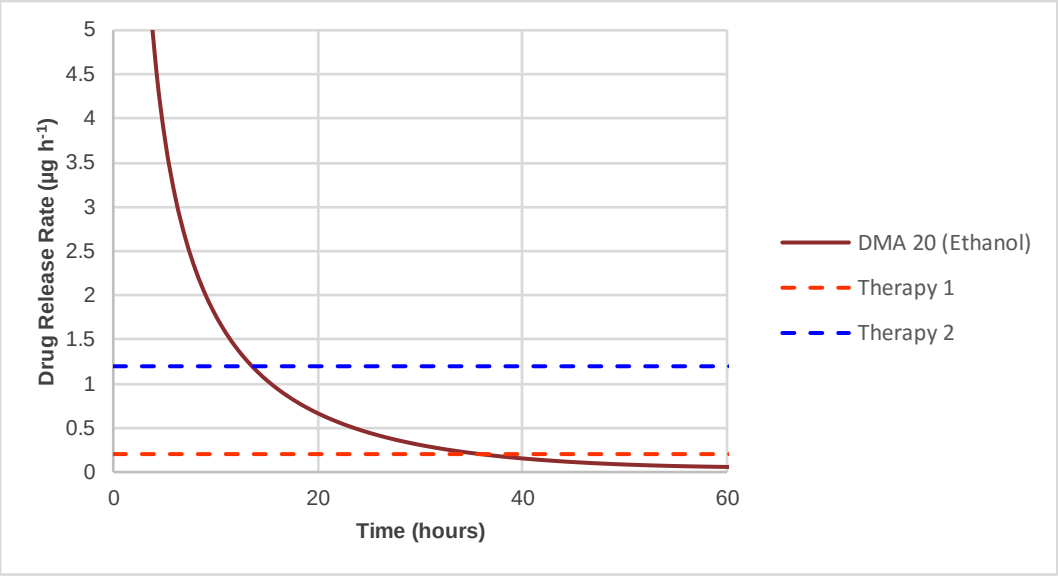


**Figure 20 -** Hourly average release rate for DMA 20 hydrogel. Drug release rates of Ronic® are reported by the dashed lines (therapy 1 – minimum posology; therapy 2 – maximum posology). In brackets the respective type of loading solution is shown.

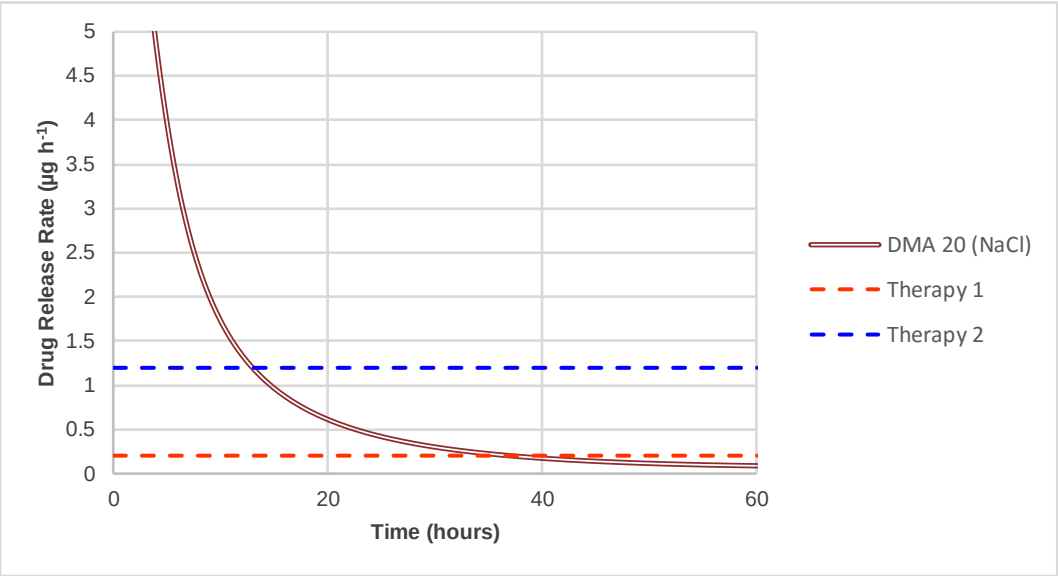


**Figure 21 -** Hourly average release rate for DMA 20 hydrogel. Drug release rates of Ronic® are reported by the dashed lines (therapy 1 – minimum posology; therapy 2 – maximum posology). In brackets the respective type of loading solution is shown.

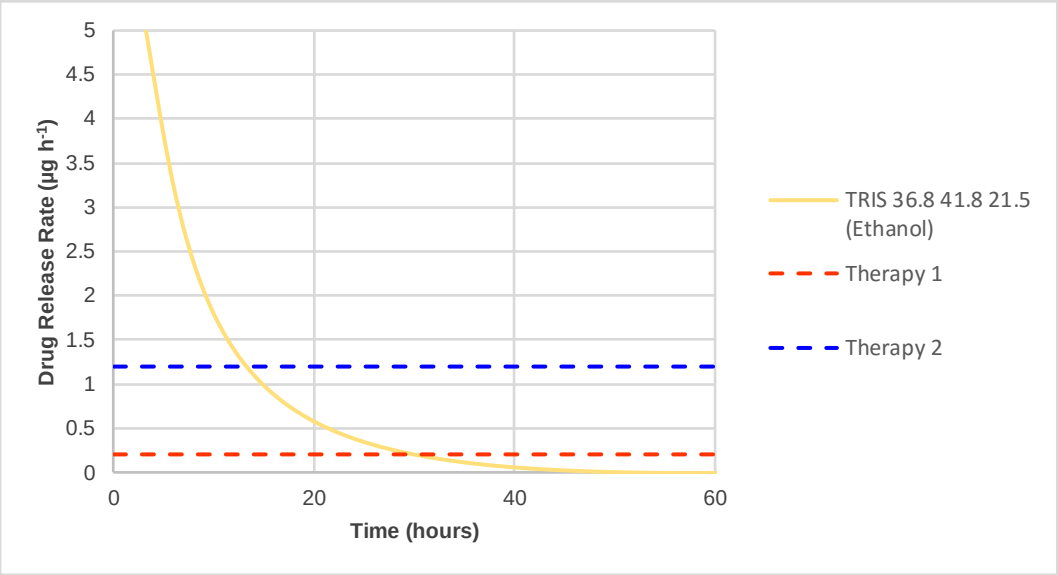


**Figure 22 -** Hourly average release rate for TRIS 36.8 41.8 21.5 hydrogel. Drug release rates of Ronic® are reported by the dashed lines (therapy 1 – minimum posology; therapy 2 – maximum posology). In brackets the respective type of loading solution is shown.

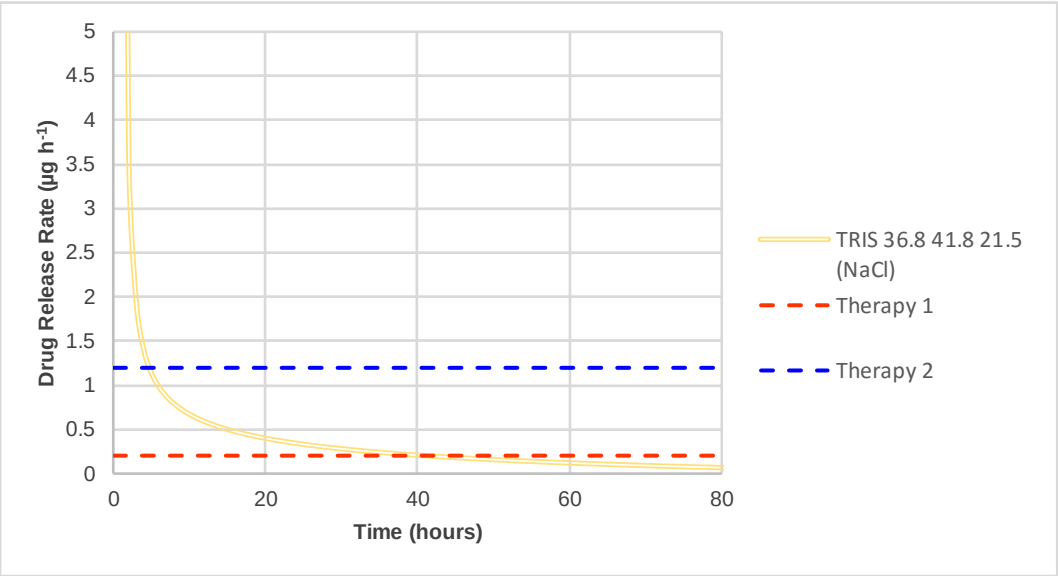


**Figure 23 -** Hourly average release rate for TRIS 36.8 41.8 21.5 hydrogel. Drug release rates of Ronic® are reported by the dashed lines (therapy 1 – minimum posology; therapy 2 – maximum posology). In brackets the respective type of loading solution is shown.

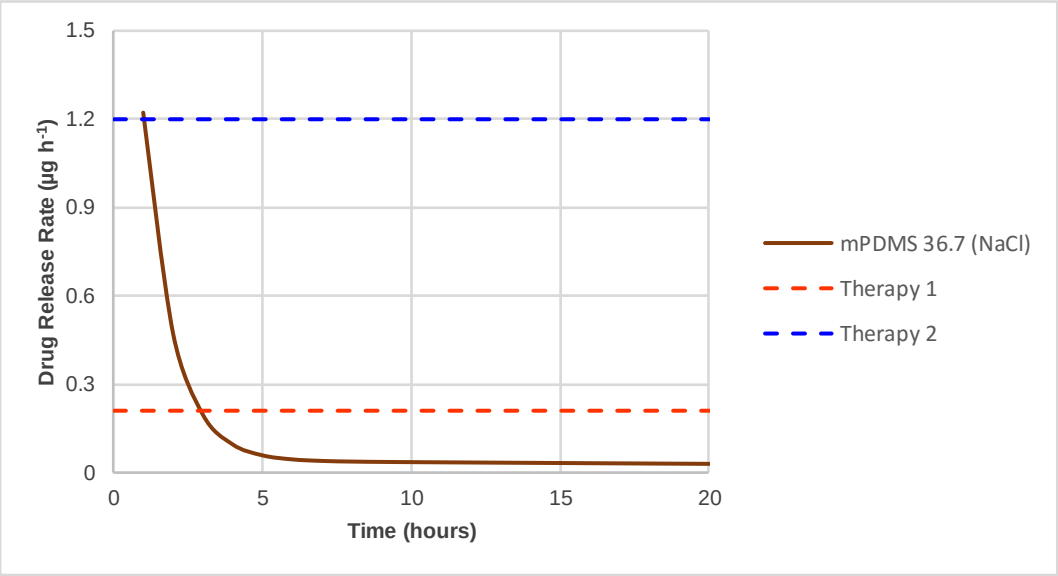


**Figure 24 -** Hourly average release rate for mPDMS 36.7 hydrogel. Drug release rates of Ronic® are reported by the dashed lines (therapy 1 – minimum posology; therapy 2 – maximum posology). In brackets the respective type of loading solution is shown.